

The Role of Meiotic Genes in Regulating Somatic Aging in *C. elegans*

by

Julia Alison Loose

B.S., Susquehanna University, 2016

Submitted to the Graduate Faculty of the
School of Medicine in partial fulfillment
of the requirements for the degree of
Doctor of Philosophy

University of Pittsburgh

2022

UNIVERSITY OF PITTSBURGH

SCHOOL OF MEDICINE

This dissertation was presented

by

Julia Alison Loose

It was defended on

February 18, 2022

and approved by

Dr. Kara Bernstein, Associate Professor, Department of Microbiology and Molecular Genetics

Dr. Matthew Nicotra, Assistant Professor, Departments of Surgery and Immunology

Dr. Kyle Orwig, Professor, Department of Obstetrics, Gynecology and Reproductive Sciences

Dr. Judith Yanowitz, Associate Professor, Department of Obstetrics, Gynecology and
Reproductive Sciences

Dissertation Director: Dr. Arjumand Ghazi, Associate Professor, Department of Pediatrics

Copyright © by Julia Alison Loose

2022

The Role of Meiotic Genes in Regulating Somatic Aging in *C. elegans*

Julia Alison Loose, PhD.

University of Pittsburgh, 2022

Reproduction and longevity have a complex relationship due to the resources needed for procreation and somatic maintenance of an aging organism. There is evidence in many species that reproduction can be harmful to the health of the organism and detrimental for longevity. However, there is also evidence to suggest that reproduction can be advantageous beyond the evolutionary benefit of species propagation, and can improve maternal health and longevity. Many of these studies, especially in human populations, are strictly correlative and there is a lack of understanding of causation and mechanisms. We were interested in determining if the health of the germ line has a causative role in the overall health and aging of an organism. *C. elegans* have proven to be a powerful model system to study the biology of aging and reproduction. Here we utilized these strengths of *C. elegans*, to explore the relationship between germ line integrity and longevity. We discovered that multiple mutations in the germline-specific process of meiosis shorten the lifespan in *C. elegans*. In detailed analysis of three meiotic genes, HTP-3, a component of the synaptonemal complex, SPO-11, an enzyme functioning during double-strand break formation along with DSB-2, revealed that this lifespan shortening is also accompanied with accelerated aging and impaired healthspan of the animal. We found that these meiotic mutants shared their transcriptomic profiles with older *C. elegans* and the transcriptomes of aging human tissues, underscoring the role of these genes in controlling aging. Through mechanistic explorations, we identified somatic protein aggregation as a potential downstream target through which SPO-11 and HTP-3 impact aging. These results demonstrate that the integrity of the germ

line has a causative role in the maintenance of somatic aging and broaden our understanding of the relationship between reproduction and longevity.

Table of Contents

Preface.....	xiv
1.0 Introduction.....	1
1.1 Classical theories of aging.....	1
1.1.1 The Disposable Soma Theory of Aging.....	3
1.2 The relationship between reproduction and aging.....	4
1.2.1 Antagonistic and beneficial relationships between reproduction and longevity	4
1.2.2 Impact of the timing of reproduction on aging	6
1.2.3 Impact of mating and pregnancy on aging	7
1.2.4 Effects of aging on fertility: reproductive aging across species	8
1.3 Using <i>C. elegans</i> as a model to study aging and reproduction	12
1.3.1 Using <i>C. elegans</i> as a model system to study aging	12
1.3.2 Longevity pathways discovered and studied in <i>C. elegans</i>	14
1.3.3 Investigating healthspan using <i>C. elegans</i>.....	17
1.3.4 Using <i>C. elegans</i> to study reproduction.....	20
1.3.5 Germline signals impact aging.....	25
1.3.6 Molecular mechanisms linking somatic health and reproductive aging.....	28
2.0 Meiotic dysfunction shortens lifespan and diminishes healthspan.....	30
2.1 Introduction	30
2.2 Results.....	33
2.2.1 Mutations in all aspects of meiosis impact lifespan.....	33

2.2.2 Germline-specific inactivation of meiotic genes shortens lifespan	37
2.2.3 Mutations in meiosis impact healthspan	42
2.2.4 Mutations in meiosis impact protein homeostasis.....	47
2.3 Discussion	53
2.3.1 Mutations in meiosis impact lifespan	54
2.3.2 Knockdown of <i>dsb-2</i> , <i>htp-3</i> and <i>spo-11</i> in the germ line for the entirety of the animal's life decreases lifespan	55
2.3.3 Mutations in meiosis have variable impacts on healthspan and protein homeostasis	57
2.3.4 Mutations in <i>dsb-2</i> , <i>htp-3</i> , and <i>spo-11</i> impact the status of protein homeostasis	57
2.4 Methods	59
2.4.1 <i>C. elegans</i> strains and culture	59
2.4.2 Lifespans	60
2.4.3 Thrashing assay	60
2.4.4 Pumping assay	61
2.4.5 Learning	62
2.4.6 Aggregation assay	63
2.4.7 Pathogen stress assays	63
2.4.8 qPCR	64
2.4.9 <i>unc-52</i> paralysis assay.....	64
2.4.10 Generation of <i>dsb-2</i> RNAi clone	65
3.0 Meiotic mutants exhibit prematurely-aging transcriptional profiles	66

3.1 Introduction	66
3.2 Results.....	68
3.2.1 The meiotic mutants share significant fractions of their transcriptomes	68
3.2.2 Genes differentially regulated in <i>htp-3</i> and <i>spo-11</i> mutants share similarities with <i>C. elegans</i> aging.....	72
3.2.3 Genes differentially regulated in <i>htp-3</i> and <i>spo-11</i> mutants share similarities with genes differentially regulated in human aging.....	75
3.3 Discussion	78
3.3.1 Differences between <i>spo-11</i>, <i>dsb-2</i>, and <i>htp-3</i> mutant transcriptomes	78
3.3.2 Gene expression changes from meiosis mutations are widespread in different tissues.....	79
3.3.3 Similarities between human aging transcriptomes and <i>spo-11</i> or <i>htp-3</i> mutant transcriptomes	80
3.4 Methods	81
3.4.1 <i>C. elegans</i> strains and culture	81
3.4.2 RNA Seq.....	82
3.4.3 Transcriptome analysis.....	82
4.0 Molecular mechanisms underlying meiotic control of aging	84
4.1 Introduction	84
4.2 Results.....	86
4.2.1 Germline-to-soma signaling in meiotic mutants does not require coelomocyte endocytosis	86
4.2.2 Wnt signaling does not impact the lifespan of <i>spo-11</i> or <i>htp-3</i> mutants.....	87

4.2.3	Genes commonly upregulated in meiosis mutants impact lifespan	88
4.2.4	Protein homeostasis genes are differentially regulated in <i>spo-11</i> and <i>htp-3</i> mutants and overexpression of <i>rpn-6.1</i> rescues <i>spo-11</i> mutant lifespan	90
4.3	Discussion	92
4.3.1	Wnt signaling does not affect lifespan in meiosis mutants	92
4.3.2	<i>irlid-53</i> and Y19D10A.5 knockdown increase lifespan	93
4.3.3	Overexpression of RPN-6.1 extends <i>spo-11</i> lifespan	94
4.4	Methods	95
4.4.1	<i>C. elegans</i> strains and culture	95
4.4.2	Lifespans	95
4.4.3	Generation of <i>irlid-53</i> RNAi clone	96
5.0	Auxin treatment increases lifespan in <i>C. elegans</i>	97
5.1	Introduction	97
5.2	Results.....	99
5.2.1	Auxin exposure beginning during development or beginning during adulthood extends lifespan	99
5.2.2	Strains facilitating AID-mediated germline depletion are long-lived	103
5.3	Discussion	105
5.4	Methods	107
5.4.1	<i>Caenorhabditis elegans</i> maintenance	107
5.4.2	Lifespan assays	108
6.0	General Discussion.....	109
6.1	Short lived mutants with reduced fertility	109

6.2 Why do mutations in different meiotic genes have different impacts on aging? ..	110
6.3 Are there sex specific differences in how meiotic gene mutations impact aging?	111
6.4 How is meiotic disruption signaled to the soma to impact aging?	112
6.5 Using basic research to understand complex relationships	114
7.0 Other Contributions	118
7.1 Transcription elongation factor, TCER-1 impacts longevity, stress resistance and healthspan	118
7.2 The functional impact of TCER-1 splicing on stress response and healthspan....	120
7.3 Tissue specific immune regulation through NHR-49	121
Appendix Supplementary Data	122
Bibliography	134

List of Tables

Table 1: Apoptosis, DNA breaks, and fertility phenotype of meiotic mutants with shortened lifespan	35
Table 2: Genes upregulated in <i>spo-11</i>, <i>dsb-2</i>, and <i>htp-3</i> mutants	89
Table 3: Lifespans of animals exposed to auxin	102
Table 4: Shared genes in ANM genetic variants and our study	117
Appendix Table 1: Lifespans of all meiosis mutants	122
Appendix Table 2: Germline specific RNAi lifespans for meiosis gene knockdown	123
Appendix Table 3: Lifespan of AID strains.....	124
Appendix Table 4: Lifespan of meiosis mutants in germline-less background.....	125
Appendix Table 5: Thrashing rate of meiosis mutants	126
Appendix Table 6: Pumping rate of meiosis mutants over time	127
Appendix Table 7: Learning index of meiosis mutants with age.....	128
Appendix Table 8: Survival of <i>dsb-2</i> mutants upon exposure to PA14	128
Appendix Table 9: Aggregation of PAB-1 in meiosis mutant.....	129
Appendix Table 10: Paralysis of <i>unc-52</i> animals with meiosis genes knocked down.....	130
Appendix Table 11: Knockdown of <i>cup-4</i> in <i>spo-11</i> mutants	130
Appendix Table 12: Wnt ligand knockdown in <i>spo-11</i> and <i>htp-3</i> mutants	131
Appendix Table 13: Knockdown of upregulated genes in <i>dsb-2</i>, <i>htp-3</i>, and <i>spo-11</i> mutants	132
Appendix Table 14: Lifespans of RPN-6.1, CCT-2, or CCT-8 overexpression strains with <i>spo-11</i> or <i>htp-3</i> knocked down	133

Appendix Table 15: Primers 133

List of Figures

Figure 1: Major longevity pathways	17
Figure 2: <i>C. elegans</i> germline and meiotic progression.....	20
Figure 3: Overview of <i>C. elegans</i> meiosis.....	24
Figure 4: Representative lifespan of mutants of genes in different aspects of meiosis compared to WT	34
Figure 5: Lifespans of meiotic mutants and germline-specific RNAi knockdown of <i>htp-3</i>, <i>spo-11</i>, and <i>dsb-2</i>.	38
Figure 6: Impact of meiosis mutants in germlineless background.....	40
Figure 7: Healthspan of <i>dsb-2</i>, <i>spo-11</i>, and <i>htp-3</i> mutants	46
Figure 8: Protein homeostasis of <i>dsb-2</i>, <i>spo-11</i>, and <i>htp-3</i> mutants.....	52
Figure 9: Differentially expressed genes in meiosis mutants.	69
Figure 10: GO terms associated with differentially regulated genes in <i>dsb-2</i>, <i>htp-3</i> and <i>spo-11</i> mutants.....	71
Figure 11: Comparison of differentially-expressed genes in <i>spo-11</i> and <i>htp-3</i> mutants with aging studies.	74
Figure 12: Mechanisms of meiotic gene control of aging	91
Figure 13: Auxin exposure increases lifespan	101
Figure 14: Strains expressing TIR1 and degron tagged proteins extend lifespan	104

Preface

I would like to thank everyone who has made this possible. First, I would like to thank my advisor, Dr. Arjumand Ghazi, for her support and mentorship during my graduate training. Thank you for taking me on as a first year graduate student excited about reproductive biology and training me to become a scientist. Thank you to all of the past and present members of the Ghazi lab for providing a positive environment to do research. Thank you especially to Francis for all of his help and advice during graduate school.

Thank you to the wider research community at the University of Pittsburgh. To my committee for their advice and input throughout graduate school. I would especially like to thank Dr. Judith Yanowitz for her guidance during my graduate training. To the University of Pittsburgh worm community for their feedback on my research, advice on techniques, and shared reagents. Thank you to the Molecular Genetics and Developmental Biology graduate program for support during my training.

I would like to thank everyone who has supported me outside of the lab. I would like to thank Sarel and Josh for the many weekend hikes and conversations about graduate school and life. To my parents for instilling in me a love of learning and supporting me through years of school. Finally, I would like to thank Charlie for his unwavering support through the highs and lows of graduate school.

1.0 Introduction

With age, organisms accumulate damage and mechanisms have evolved to clear or repair damage. Over time, however, the repair mechanisms cannot compensate for the increased load of damage or the repair mechanisms themselves accumulate damage which eventually leads to dysfunction and results in aging. Additionally, aging is a risk factor for many diseases and life-threatening conditions including cancer, neurodegeneration, and cardiovascular disease (1). It is predicted that by 2030, older people are going to outnumber children, and by 2050, there will be more people over the age of 60 than adolescents and young adults (10-24) (2). With increased life expectancy, there will only be more people living with these age-related diseases. Research targeted towards understanding the mechanisms of aging in model organisms has demonstrated that delaying aging can often delay the onset of age-associated diseases. Therefore, it is of great importance and interest to public health to further understand the mechanisms and relationships that impact aging as a method to combat many of these diseases.

1.1 Classical theories of aging

One of the first theories of the cause of aging was developed with the assumption that like machines, organisms degrade with use and time and eventually stop working. This premise formed the basis of the “Wear and Tear Theory of Aging”, posited by evolutionary biologist, August Weismann, in 1882 (3). Over the next few decades, there were multiple theories that focused on

the specific cause of aging as different contributors to the accumulation of damage. In 1942, Johan Bjorksten presented the “Cross-Linking Theory” that suggested that with age, proteins become crosslinked, which leads to slower functioning and eventually death. (4). Harman proposed the “Free Radical Theory of Aging” that suggested that the harmful side effects of metabolic by-products, the free radicals, caused oxidative damage that led to aging (5). In 1972, Harman expanded this theory further, stating that mitochondria play a key role in both producing reactive oxygen species and serving as a target for the harmful effects of reactive oxygen. This led to the influential “Mitochondrial Free Radical Theory of Aging” (6).

In 1952, Peter Medawar developed the “Accumulated Mutation Theory”, which suggested that there may be evolutionary selection for self-maintenance that declines with age (3). There is greater selective pressure for mutations that are deleterious in younger organisms, considering that the mutations would decrease fitness. But as animals age and are no longer reproducing, there would be less selective pressure against these deleterious mutations. This would imply that harmful mutations are likely to accumulate freely in older organisms, which then cause aging. George Williams published a theory in 1957, which expanded upon Medawar’s idea that there was no selective pressure on genes that negatively impact an organism in old age (7). His “Antagonistic Pleiotrophy Theory” posited that there is selection for genes which benefit early life but impair late life. Together, these ‘classical’ theories substantiated the concept that there must be an evolutionary trade-off during an animal’s lifetime between reproducing and living.

1.1.1 The Disposable Soma Theory of Aging

In 1979, Thomas Kirkwood and Robin Holliday developed the “Disposable Soma Theory of Aging” which builds upon the “Antagonistic Pleiotrophy Theory” with an emphasis on the energy involved in either reproduction or maintaining an aging organism through repair (8). This theory stated that in order for an organism to survive, it must repair and maintain against many extrinsic forces that are detrimental to survival, including predation, lack of resources, and environmental stress, while still combatting intrinsic damage. But to be evolutionarily successful, an organism must survive until it is able to reproduce. It would not be beneficial for an organism to continue to put resources into repair and maintenance at the disadvantage of its progeny, specifically during the post-reproductive phase of an organism’s life (8). This theory accepts that accumulation of cellular and molecular damage results in aging. However, there are limited resources that can be allocated either to maintaining the organism and repairing the damage that accumulates or to reproduction. Therefore, there are mechanisms in place that control aging through the allocation of resources into either repair of the soma, or through investment into reproduction (8). This theory also highlights the dichotomy between germ line and soma: that the germ line is immortal and passed on in a pristine state to the future generations, while the soma is mortal and accumulates age-related damage. This theory was highly influential in shaping the dogma about an antagonistic relationship existing between reproductive fitness and longevity.

1.2 The relationship between reproduction and aging

The “Disposable Soma Theory of Aging” set up the seemingly simple, antagonistic relationship between fertility and longevity. Studies exploring this relationship have been conducted in laboratory animals, in nature and on human populations. The resulting evidence has provided support for the existence of trade-off. However, innumerable exceptions and contrary relationships have been observed that cannot be explained by simplistic trade-off between reproduction and aging. This relationship has been explored both as the impact of reproduction on aging and the opposite relationship of the impact of aging on reproduction. In the following sections, key studies in humans, mammals as well as model organisms are described to underscore the complexity of the reproduction-aging relationship.

1.2.1 Antagonistic and beneficial relationships between reproduction and longevity

The “Disposable Soma Theory of Aging” would suggest that organisms that reproduce have a shorter lifespan than their counterparts that do not have progeny. This hypothesis has been applied to different historical populations to better understand how reproduction, or the lack thereof, impacts aging. Kirkwood found that female longevity of a population of British Aristocrats was negatively correlated with the number of children a woman produced (9). However, this study has been criticized for its analytical methods (10). Later studies of other historical populations that try to answer the same question have resulted in mixed conclusions of no correlation, positive correlation or negative correlation between reproduction and longevity (10). Studies and reviews of historical populations from Gagnon et al., and Hurt et al., have found no association between

lifespan and number of children (11, 12). Many of these studies have focused on the trade-off of reproduction and longevity in women, but the “Disposable Soma Theory of Aging” has also been applied to men. Another group identified that in a population of Korean eunuchs, which was composed of a group of castrated men, the sterile men were found to have lived 14.4-19.1 years longer than non-castrated men of similar socio-economic status (13). Therefore, the analysis of historical populations resulted in differing opinions about reproduction’s effect on longevity.

In addition to these analyses of historical data, modern populations have also been analyzed, including a study of women in England, Wales, and Austria that found having no children was in fact correlated with higher mortality (14). A study of women from England and Wales during the 20th century found that mortality and number of children resulted in a “U” shaped curve, in which women who have no children or more than five children had the highest rates of mortality (15). This study suggests that the physical strain of bearing more than five children may have a negative effect on mortality (15). However, it is worth noting that just comparing number of children to longevity does not always give a conclusive answer to the trade-off between reproduction and longevity. There are other factors, such as the cost of breastfeeding, raising the child, socioeconomic factors, and resources, that make much of this data difficult to interpret for a causative effect (16).

The “Disposable Soma Theory of Aging” has been applied outside of human populations as well. Analysis of 30 species of mammals and birds in captivity determined that there was no relationship between number of offspring and longevity (17). Another study of 20 datasets of terrestrial vertebrates found that those with earlier age-at-first-procreation had faster senescence rates (18). These studies illustrate the complex, context-dependent links between reproduction and aging, but lack the causative evidence to suggest that there is a trade-off of resources.

1.2.2 Impact of the timing of reproduction on aging

The relationship between reproduction and longevity has also been studied in the context of the timing of reproduction. The “Disposable Soma Theory of Aging” would suggest that an organism has either a long lifespan or a successful reproductive span (8). Many of the previous studies measured reproductive success by the number of progeny or the absence of progeny. Reproductive success can also be considered through the length of time of successful reproduction. Many studies in human populations have shown that early reproduction is detrimental to longevity, and that women who were able to bear children later in life had the highest post-reproductive survival (14, 15, 19-25). However, while there seems to be a benefit towards delayed reproduction in terms of mortality, there is still risk of pregnancy that is higher in very young or older mothers, including hypertension, preeclampsia, gestational diabetes, preterm birth, and post-partum hemorrhage (20). Also, while some studies find that mortality risk is decreased with delayed age-at-first births, other studies find an increase in breast cancer risk that accompanies an increase in age-at-first birth (20). Similar to the controversy surrounding the previously mentioned conclusions about a trade-off between number of children and longevity, re-analysis of historical datasets has found no impact of age at first or last reproduction on longevity (26). Studies in model systems also present conflicting results on the relationship between lifespan and timing of reproduction. This question has been asked experimentally in the fruitfly, *Drosophila melanogaster*, in which selection for animals with longer reproductive spans resulted in isolation of strains with longer lifespan (27). Experiments that manipulated the timing of reproduction of the nematode *Caenorhabditis elegans*, through the use of sperm to mate with genetic females, found that early reproduction does not impact reproductive aging (28).

More recently, menopause has been utilized as an indicator for mortality risk as early menopause in women has been found to be associated with increased mortality risk in later life (29-33). Similarly, premature ovarian insufficiency has been linked to increased risk of cardiovascular disease and increased mortality rate (34). Early age at natural menopause has also been found to be associated with increased marks of epigenetic aging (35). Overall, evidence from these diverse areas of investigation have made clear that reproductive health and germline status impact somatic aging; however, it remains unclear as to what the extent is or through what mechanism(s). Many of these observations are correlative in nature and exemplify the difficulty in determining causality.

1.2.3 Impact of mating and pregnancy on aging

Some molecular hallmarks of aging can be observed in women during pregnancy or are prevalent in complications that arise due to pregnancy. Reactive oxygen species (ROS) can cause damage through creating DNA breaks, and this is combatted by antioxidant defense. With age, there can be a buildup of ROS. Similarly, the balance of ROS and antioxidants shifts during pregnancy and has been found to be associated with pre-eclampsia, hypertension and spontaneous abortion (36, 37). Inflammation also has a key role during aging, with immune activation beneficial at low levels, but chronic activation of the immune system, or ‘inflammaging’, causing cellular damage. Throughout pregnancy, there are major shifts to the immune profiles of women(38). Genetic and epigenetic observations have suggested that the number of pregnancies a women has correlates with a decrease in telomere length and an increase in markers of age-related DNA-methylation (39).

Benefits and harmful side effects of mating have been also observed in both mammalian systems and invertebrate model organisms. Male mice release a pheromone that accelerates female puberty and can also increase body mass and stress responses (40, 41). Mating is detrimental to female *D. melanogaster* due to transfer of proteins in the male seminal fluid that shorten female longevity (42). In *C. elegans*, mating causes female shrinkage and a decrease in lifespan, in addition to onset of aging features, including slowed movement, increase in paralysis, and a decline in tissue structure (43, 44). It was recently discovered that young *C. elegans* are protected from the harmful effects by self-sperm and this protective mechanism functions in other *Caenorhabditis* species as well (45). In worms, the harmful side effects of mating were found to originate from both the seminal fluid from the males as well as the pheromones released by the males (43, 44). The small compound nacq #1, which is produced by males, impacts the lifespan of hermaphrodites (46). However, aside from the evolutionary benefit of reproducing, there is also evidence to suggest that mating can be beneficial in some organisms. For example, arthropod males transfer edible gifts that increase the fitness of their mate, while female butterflies also gain nutrients through mating (47, 48). Reproduction is also positively correlated with longevity in ant queens, African mole rats, and some bird species (49-51)

1.2.4 Effects of aging on fertility: reproductive aging across species

The impact that increasing maternal age has on female fertility has been well documented. Decline of female reproductive fitness is one of the first indicators of aging. Reproductive aging in females begins many years before the end of life and over a decade before menopause, marked by oocyte depletion (52). Data from historical studies and *in vitro* fertilization demonstrate the

sharp decline of fertility with age as well as an increase in aneuploidy and miscarriage (53). Research in humans and mammalian model organisms suggest that one of the primary causes of reproductive senescence is the gradual depletion of the oocyte pool that females are born with, in addition to the decline in oocyte quality with age (53). During development, germ cells go through a series of mitotic divisions and arrest in prophase (54). Only one oocyte per cycle will enter the first stage of meiosis, and if fertilized, will complete the second stage of meiosis (54). This long process and state of arrested division have been thought to contribute to the increased opportunity for damage and dysfunction with age (54).

Humans and *C. elegans* both display reproductive declines as early signs of aging before the end of life. Also, both organisms arrest oocytes at meiotic prophase 1 (55). In *C. elegans* reproduction begins to decline by Day 5 of adulthood, while the animal survives for another 10-15 days. And while the number of progeny declines rapidly around this time, there are not many other markers of aging in the soma of the animal at this time. The reduction in progeny number is also accompanied by an increase in embryonic lethality and the laying of unhatched oocytes (56). Morphologically, young oocytes are large and closely packed together in the germ line, whereas, oocytes in older worms appear smaller, and showing more cavities between oocytes (57). Older oocytes are also more prone to stressors as tested in the laboratory such as bleaching (57).

While the exact cause of reproductive aging is still being investigated, oocyte quality is one of the main contributing factors to reproductive decline in both worms and humans (55). Similar to humans, *C. elegans* exhibit increased chromosomal abnormalities with age (55, 58). Another possible mechanism of reproductive aging is through DNA damage caused by impaired DNA damage repair mechanisms, reviewed in (58). Chromosomal nondisjunction is also increased with maternal age in multiple organisms, including humans, *Drosophila*, and *C. elegans*, reviewed

in (58). Specifically, this may be due to the loss of cohesion, which holds sister chromatids together during meiosis, or through dysfunction of the spindle assembly checkpoint, which ensures proper chromosomal segregation during meiosis, reviewed in (58). Proteostasis, the mechanism through which cells ensure proteins are properly folded and that damaged proteins are disposed of, also contributes to reproductive aging. In *C. elegans*, there is an increase in protein aggregation in maturing oocytes (59). Accordingly, the transcriptional changes observed in older oocytes include a decline in pathways related to oocyte maintenance and function, such as chromosome segregation, cell cycle, DNA damage response, and proteolytic pathways. Indeed, the human homologs of many of these genes undergo aging-associated transcriptional changes in human oocytes (55).

Genetic mutations that result in extended reproductive span have provided fundamental insights into the genetic pathways regulating reproductive aging in *C. elegans*. Pathways that sense nutrient availability, growth and development are potential candidates for impacting reproductive aging. It was determined that mutations in the insulin/IGF-1 signaling pathway which results in extended lifespan also result in extended reproductive span (28). Another longevity pathway, through dietary restriction, has also been shown to extend reproductive longevity (28). The influence of these two pathways on reproduction indicates that environmental stressors and nutrient status influence reproductive longevity in addition to somatic aging. And while these reproductive aging pathways were first shown in *C. elegans*, there have also been studies to suggest that these pathways shape reproductive aging in other organisms including as flies and mice, reviewed in (60). The transforming growth factor β (TGF- β) pathway, which in *C. elegans* includes two branches, the dauer and the Sma/Mab pathway, has also been studied as a regulator of reproductive aging (61). Interestingly, mutations in *sma-2*, of the TGF- β branch, increase

reproductive span without impacting the longevity of the animal, acting through an independent pathway outside of the known longevity pathways (62). More recently it was determined that TGF- β functions in the hypodermis to regulate aging of the germ line, with the *C. elegans* cAMP response binding element (CREB) functioning downstream and regulating a Hedgehog signaling factor, WRT-10 in the hypodermis (63, 64). Although *daf-2* mutants with reduced insulin signaling and *sma-2* mutants with reduced TGF- β Sma/Mab signaling have reduced progeny production, it is not reduced oocyte usage that underlies the extended reproductive span (62). Instead, *daf-2* and *sma-2* mutants produce successfully fertilized embryos later in life, whereas, older wild type animals lay unfertilized oocytes suggesting that oocyte quality is maintained with age (62). In fact, these two mutants also have a decrease in the number of chromosomal errors observed in older oocytes of wild type animals (62). The rates of DNA damage-induced apoptosis are maintained in *daf-2* and *sma-2* mutants compared to the decline observed in aging wild type animals (62). However, *sma-2* mutants produce fewer progeny in the first days of reproduction and along with *daf-2* mutants have smaller brood sizes (62, 65). Therefore, in both of these pathways in *C. elegans*, reproductive span can be uncoupled from lifespan, demonstrating the complexity of this relationship. *C. elegans* signaling pathways that regulate reproductive aging have been implicated in mammalian reproductive aging as well (55). Genes found to be upregulated in TGF- β Sma-Mab mutants with extended reproductive spans, show overlap with genes that have been found to decline in older mouse and human oocytes (55).

1.3 Using *C. elegans* as a model to study aging and reproduction

C. elegans was established as a model organism by Sydney Brenner in 1963 and has since proven to be a useful platform to investigate innumerable biological processes. It offers numerous advantages as a model system including ease of growth and maintenance. They are very small at only 1mm in length and grow on an agar plate with *Escherichia coli* as a food source and can survive for months without food in the dauer state (66). They develop quickly from eggs to adults in about three days. Each hermaphrodite produces about 300 progeny that are genetically identical to the parent. It serves as a powerful genetic tool and was the first metazoan to have its genome sequenced. It was determined that 83% of the worm proteome also had human homologs (67). They are also transparent, allowing for the use of genetic tools with fluorescent tags to study live animals. In addition, RNAi libraries generated by two labs cover 94% of the genome, and more recently, CRISPR has been adapted extensively for use in *C. elegans* (68-70).

1.3.1 Using *C. elegans* as a model system to study aging

In addition to the general benefits of *C. elegans* as a model system, worms offer particular advantages for studying aging. Their lifespan is only 2-3 weeks, which allows for researchers to quickly determine impacts on aging due to a specific genetic mutation, drug intervention, or environmental condition. Their small size and easy maintenance allow for large screens to identify conditions that extend or shorten lifespan. In addition to a short length of life, *C. elegans* demonstrate age-related decline that can be easily quantified in the lab, and some of these characteristics of aging have similarities to those in humans (71). Many of the physiological or

behavioral changes that decline with age can be easily measured in the lab to further understand the impact of aging from a mutation or intervention, as later discussed in Section 1.3.3 (71).

Anatomical changes associated with age can be easily visualized in *C. elegans* due to their transparent body. The cells of young adults have clear boundaries; with age, this definition is diminished and it becomes more difficult to identify nuclei with the appearance of necrotic cavities (72). While neurons appear to maintain their structural integrity well into old age, a decline in synaptic integrity that correlates with a functional decline in the neurons occurs in a measurable manner (73). The pharynx also degrades with age with the number of myofibrils and pharyngeal muscles declining with age (73). Considering that *C. elegans* in the laboratory consume *E. coli*, this accumulates in both the pharynx and intestine with age (73). The body wall muscles decline in structure and function with fewer myosin thick filaments and bent or broken thick filaments increase with age (74). The *C. elegans* reproductive system also shows signs of aging as described above in the section 1.2.4 .

At the cellular level, there are age-related changes in the nucleus and mitochondria. With age, there is a decline in the integrity of the nuclei, as well as a decline in the number and size of the intestinal nuclei (73). The nuclei in the muscle develop dark patches, and the nucleoli size increases with age. Also, the nuclear lamina becomes irregular (73).

There is a change in mitochondrial integrity too with age. The mitochondria in muscle cells becomes enlarged due to fusion, and there is an increase in fragmented mitochondria with age (73). At the molecular level, there is an increase in the level of reactive oxygen species, carbonylated proteins, and DNA damage (73). There is also the accumulation of fluorescent compounds mostly in the intestine of the animal, including lipofuscin that is oxidized, crosslinked macromolecules, and advanced glycosylation end products (75). The well-documented changes with age in *C.*

elegans have allowed researchers to discover mechanisms and genetic pathways that contribute to the length of life, as well as the different physiological and molecular changes associated with age.

1.3.2 Longevity pathways discovered and studied in *C. elegans*

Historically, aging was considered a ‘non-regulated’ random process that was a result of use over time (76). However, the discovery of single gene mutations that doubled worm lifespan were instrumental in establishing that aging is regulated through genetic pathways. In 1977, Klass determined that *C. elegans* could be used for aging studies and observed that altering the temperature or the food intake changes the lifespan. Klass conducted a genetic screen for mutants with altered lifespan and identified mutants with extended lifespan (77). It was later established that these mutants all mapped to the *age-1* gene (78). The *age-1* gene encodes for the catalytic subunit of PI 3-kinase, which functions in insulin/IGF-1 signaling (IIS) (79). These exciting discoveries determined that a single mutation has the potential to alter lifespan, paving the way for further researchers to identify other genetic determinants of lifespan.

One of the first interventions found to impact lifespan was dietary restriction, which has been shown in many species to both extend lifespan and delay the onset of disease, including cancer and neurodegeneration (80). It was later demonstrated that dietary restriction functions to increase longevity through other well studied pathways including the IIS, target of rapamycin (TOR) signaling, AMP kinase, and sirtuins (76). In *C. elegans*, *eat-2* mutants have been used as the genetic model to study dietary restriction. These mutants consume less food and display a 30% increase in lifespan (81). Research using the *eat-2* mutant has revealed the importance of autophagy and inhibition of mTOR for lifespan extension through dietary restriction (76).

As previously mentioned with the discovery of lifespan extension through the *age-1* mutation, IIS has been found to increase lifespan in *C. elegans*. Another mutation in this pathway, *daf-2*, an IGF-1/insulin receptor, has also been shown to double lifespan in *C. elegans* (82). This pathway converges on the activity of transcription factors especially the FOXO-family transcription factor, DAF-16, as well as other conserved transcription regulators such as heat shock factor, HSF-1, and the Nrf-like xenobiotic response factor, SKN-1 (76). These transcription factors regulate downstream genes to promote longevity (76). These pro-longevity genes include stress response, antimicrobial peptides, chaperones and lipases (76). Furthermore, this pathway does not seem to be specific to *C. elegans*, as inhibiting insulin/IGF-1 signaling in *Drosophila* extends lifespan (76). Mutations in the FOXO3A, the human homolog of DAF-16, as well as the human IGF-1 receptor and other components of the IIS pathway, have been linked to extraordinary longevity in centenarians (76).

Other pathways involved in nutrient sensing have been identified as important regulators of longevity. The TOR pathway, a nutrient sensor, also has a role in longevity in *C. elegans*. In the presence of abundant resources, the TOR kinase stimulates growth and blocks salvage pathways, while TOR inhibition causes a shift towards tissue maintenance (76). Inhibition of TOR extends the lifespan of *C. elegans* through a pathway that is distinct from the IIS/IGF-1 pathway (76). Specifically, the transcription factor PHA-4 is required by which autophagy is stimulated and inactivation of S6 kinase downregulates translation (83). AMP Kinase (AMPK) is another nutrient sensor and its overexpression in *C. elegans* increases lifespan (84). Interestingly, treatment with Metformin, which increases AMPK activity, promotes healthy aging and increases lifespan in mice (85). In *C. elegans*, overexpression of *aak-2*, which encodes one of the AMPK paralogs, extends lifespan and activates DAF-16 (84). There is also a timing component involved in the various

nutrient sensors' impacts on longevity. When calories are restricted in middle aged *C. elegans*, AMPK is required for lifespan extension, but AMPK is not required for caloric restriction for the entirety of the animals lifespan (76). Sirtuins, NAD⁺ dependent protein deacetylases, also have a role in regulating lifespan. In *C. elegans*, overexpression of the sirtuin gene, *sir-2.1*, extends lifespan through DAF-16 (86). This same pathway has been found to be extend lifespan in yeast and flies (76). Lastly, *C. elegans* studies provided initial evidence that signals from the reproductive system can impact longevity beyond the simplistic trade-off assumption as detailed in section 1.3.5 below. These pathways are summarized in Figure 1.

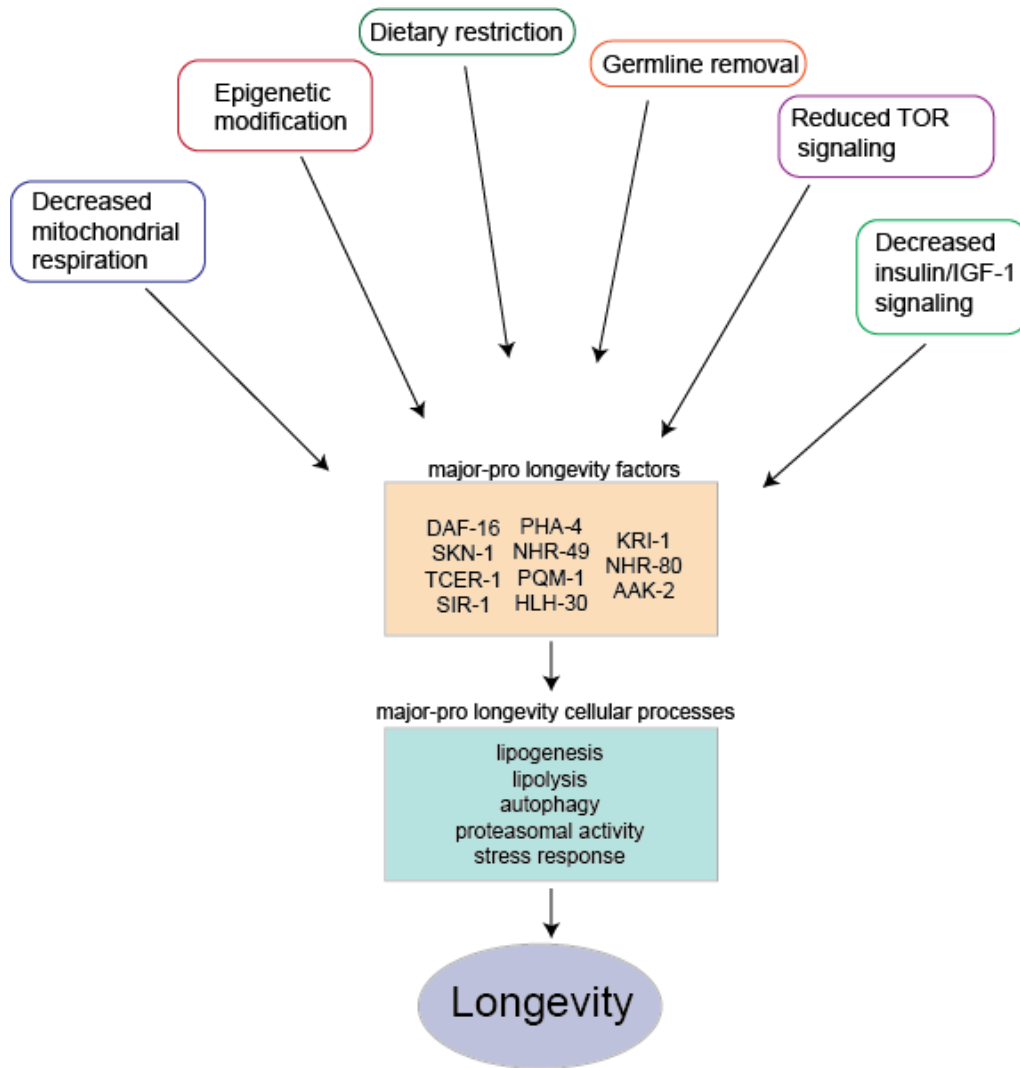


Figure 1: Major longevity pathways

Examples of major longevity pathways with a focus on pathways discovered or studied in *C. elegans*. Key transcription factors and key downstream cellular processes are also listed

1.3.3 Investigating healthspan using *C. elegans*

Initially, the length of life was the only determinant for identifying regulators of aging. This was especially the case for large screens, where lifespan was an easy and quantitatively precise readout. However, lifespan can be modulated while other aspects of aging remain constant

or vice versa. Therefore, in addition to quantifying lifespan, it is important to study healthspan, which encompasses many of the above-mentioned qualities of aging. Many assays have been developed to measure these age-related traits, especially in *C. elegans* (71). With age, there is a decline in muscle function that can be identified through locomotion. This healthspan assay can be measured by quantifying the number of body bends, or thrashes, in liquid (71). Another healthspan assay measures muscle function through locomotion by instead measuring movement on a solid agar plate through speed (71). Muscle function can be measured in other parts of the animal, for example, through pharyngeal pumping, which the animal uses to grind and eat *E. coli* which can be quantified by counting the number of pharyngeal pumps over time (71). The molecular changes that occur in *C. elegans* with age can also be utilized as measurements of healthspan. This includes the accumulation of lipofuscin, which can be visualized with fluorescence microscopy (71). The response to stress also declines with age and this can be measured by exposing animals to various stressors at different ages (87). Of the abiotic stressors, animals can be exposed to low or high temperatures, oxidative stress, and xenobiotic compounds. There are also biotic stress assays, including exposure to pathogenic bacteria such as *Pseudomonas aeruginosa* and *Staphylococcus aureus*. Pathogenic stress response can be measured by replacing the animals normal *E. coli* food with a pathogenic bacteria and determining the survival rate, similar to lifespan (71).

Many mutations that extend the lifespan of *C. elegans* also delay the age-related decline of characteristics associated with aging. Animals with a mutation in *daf-2* showed similar signs of tissue aging; however, this timeline was delayed compared to wild type (72). Knockdown of heat shock factor, *hsf-1*, shortened the lifespan of animals, but also accelerated aging based on qualitative measurements of tissue aging (72). These studies have contributed to our understanding

of aging as not simply an animal that dies faster due to sickness, but due to acceleration of tissue-specific aging mechanisms. Another study asked if healthspan and lifespan are correlated by measuring both aspects in a group of long-lived and short-lived mutants (88). It was determined that body movement and pharyngeal pumping were positively correlated with lifespan; however, reproductive span was not correlated with lifespan, body movement, or pumping (89). Another study examined healthspan in long-lived strains – *clk-2*, *daf-2*, *ife-2*, *eat-2*, which are known long-lived strains with mutations in genes with roles in mitochondrial signaling, IIS, protein translation and dietary restriction (90). This study tested resistance against stressors (heat and oxidative), distance moved on solid media, thrashing in liquid, pharyngeal pumping, and autofluorescence, and concluded that the rate of decline was similar in all long-lived mutants and wild-type animals (90). Another study examined the relationship between short-lived mutants and healthspan parameters and found that short-lived mutants included *daf-16*, *mev-1*, *hsf-1*, and *sir-1*, which have roles in the IIS pathway, mitochondria, heat shock response, and metabolic homeostasis, have reduced locomotion but not reduced resistance to heat stress (91). Other mutants affect healthspan but not lifespan. Two mutations *hpa-1* and *hpa-2*, were found to act through the EGF pathway to increase healthspan (swimming, lipofuscin accumulation, decreased advanced glycation end-product accumulation) with only a small increase in median and mean lifespan (92). Interestingly, there are other examples of transcription factors that are necessary for longevity but suppress aspects of healthspan, such as stress resistance, as exemplified later in the supplemental chapter of this thesis (93). Evidence from many of these studies emphasizes both the importance of measuring both lifespan and healthspan, since these are not interchangeable and also that doing so provides a better understanding of the impact a mutation or intervention has on an organism.

1.3.4 Using *C. elegans* to study reproduction

In addition to studying aging, *C. elegans* has also been an incredibly useful system to study germ line development and reproductive biology. The *C. elegans* reproductive system consists of two arms, with the somatic distal tip cell at the end of the arms, where signals from LIN-12/Notch pathway regulate germ cell proliferation (94). After proliferation, the germ cells begin meiosis in the transition zone (Figure 2). Multiple fundamental discoveries on germ-cell proliferation and differentiation, oogenesis, and spermatogenesis have been made through worm studies. One of these areas is the process of meiosis which is also a major focus of the work in this thesis and hence is detailed below.

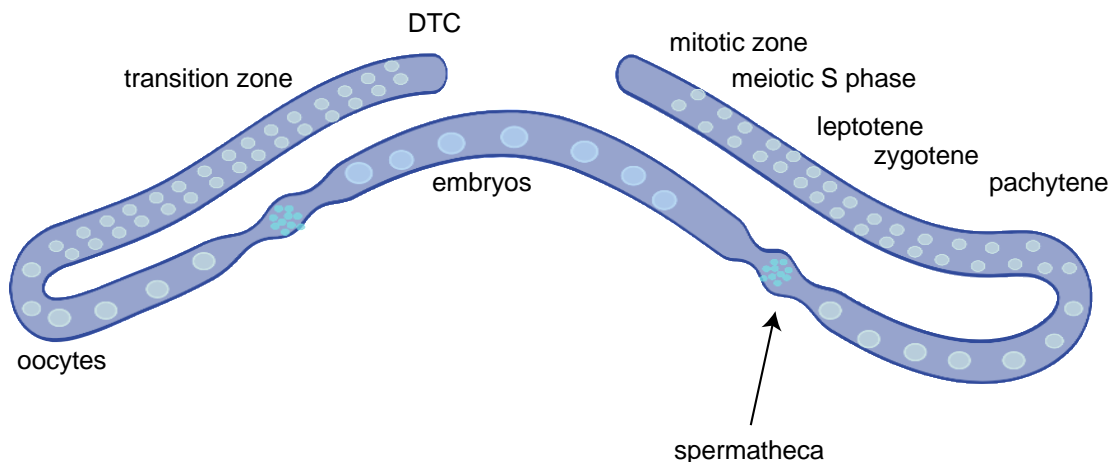


Figure 2: *C. elegans* germline and meiotic progression

The *C. elegans* germ line is composed of two gonad arms. Meiosis progresses in a spatiotemporal manner. Oocytes are then fertilized from sperm stored in the spermatheca. Created using BioRender.com

Meiosis in *C. elegans*: Meiosis is required for the generation of haploid gametes, sperm or eggs, which contain one copy of each chromosome. In worms, the stages of meiosis I are spaced spatio-temporally along the gonad arms (Fig 2) (94). To finish with four haploid gametes, DNA replication is followed by two rounds of division, meiosis I and meiosis II, where first homologous chromosomes segregate, then sister chromatids separate respectively. During replication, sister chromatid cohesion is established to hold together sister chromatids. Meiotic-specific cohesion proteins REC-8, COH-3, and COH-4 are important for holding together sister chromatids during the first meiotic division, which occurs during anaphase I (95). These proteins are also important for assembly of the synaptonemal complex (SC) assembly, the protein structure which forms between homologous chromosomes (95). The second meiotic division is similar to mitosis, with sister chromosomes separating but results haploid gametes. During the first meiotic division, homologous chromosomes must pair, synapse, and then exchange genetic material during crossover recombination (Fig 3). Meiotic prophase consists of leptotene, zygotene, pachytene, diplotene and diakinesis. During leptotene and zygotene, homologous chromosomes must first find and pair with each other. To enable this process, chromosome ends become tethered to the nuclear envelope, which is facilitated by pairing centers (PCs) (96). Each PC is bound by one of the four C2H2 zinc finger proteins, HIM-8, ZIM-1, ZIM-2 or ZIM-3, which are required for proper chromosome pairing and synapsis (96). The PC nucleoprotein complex acts as a recruitment site for polo kinase, PLK-2 (and PLK-1) (97). PLK-2 then triggers the structural reorganization of the nuclear envelope, including inner and outer nuclear envelope proteins, SUN-1 and ZYG-12, which aggregate to where PCs localize on the nuclear envelope (98, 99). SUN-1 and ZYG-12 form a SUN/KASH protein complex that connects the chromosomes to the cytoskeleton (98, 100). The formation of SUN-1/ZYG-12 aggregates and connections to the PCs are essential for pairing and

SC assembly (100). The SC begins to form during zygotene, with four *C. elegans* HORMA-domain proteins HIM-3, HTP-1, HTP-2, and HTP-3, making up the axial element of the SC (101). The central structure of the SC consists of SYP-1, SYP-2, SYP-3, SYP-4, SYP-5 and SYP-6 (102-106).

One requirement for proper chromosome segregation in meiosis is recombination, which structurally helps to hold homologous chromosomes together. Meiotic recombination is initiated by the formation of double-strand breaks by the conserved topoisomerase-like enzyme SPO-11 (107). Other proteins functioning to promote break formation include HIM-17, DSB-1, DSB-2, XND-1, MRE-11 and HIM-5 (108-112). SPO-11 is covalently bound to the DNA, which has to be removed by an endonuclease and then the DNA strand is resected to generate 3' single strand DNA tails. These processes are carried out by a complex of proteins including MRE-11 (or EXO-1, if MRE-11 is absent), RAD-50, NBS-1 along with COM-1 (113). COM-1 and NBS-1 also promote crossover formation via homologous recombination (HR) by inhibiting repair via non-homologous end joining (NHEJ) (114). The ssDNA gets coated with RAD-51, which then promotes homology search and strand invasion of the homologous chromosome. The coated filaments invade the homologous chromosome at the same DNA sequence, resulting in a D loop and then extension occurs (113, 115). The nucleation of the RAD-51 filament and stabilization requires BRC-2 (116). RAD-54 promotes strand invasion of the homologous DNA, along with HELQ-1 and RFS-1 (117, 118). After strand exchange, the DSB can either be repaired as a crossover (CO) or noncrossover (NCO). Meiosis specific proteins MSH-4 and MSH-5, as well as COSA-1 and ZHP-3, are important for CO designation (104, 119, 120). The COs are resolved through the actions of resolvases, which include SLX-4, and complexes XPF-1/HIM-6 and SLX-1/ MUS-81 (121). Alternatively, repair via NCO requires RTEL-1 and the DSBs are repaired via synthesis dependent

strand annealing (122). The SMC-5/6 complex and BRC-1 function during repair via inter-homolog NCO or inter-sister repair (123).

The formation of chiasmata, or physical linkages that results from CO events, connects homologous chromosomes. (124). In diplotene, the synaptonemal complex disassembles and in diakinesis chromosomes are condensed (125). The homologous chromosomes are then oriented so that during anaphase of meiosis 1, homologous chromosomes segregate away from one another (125). During meiosis II, the sister chromatids segregate to opposite poles, resulting in haploid gametes (126). Oocytes are arrested during meiotic prophase I, and sperm trigger oocyte meiotic maturation and the onset of the cell divisions just described (94). Once meiotic maturation is complete, the oocyte is ovulated through the spermatheca, where the sperm are stored, and into the uterus where fertilization and the cell divisions are completed. The fertilized embryo can then be laid (94).

C. elegans have proven to be an excellent model for studying reproduction due to their transparent nature and spatiotemporal layout for meiosis. Also, because males arise during events of chromosomal nondisjunction, it is relatively easy to track meiotic errors or mutations that result in an excess of males (127). *C. elegans* hermaphrodites have two copies of the X chromosomes, while males have only one copy of the X chromosome, therefore mistakes during meiosis are easily quantified through increase in male production. From a normal wild-type hermaphrodite mother, males are produced only at a frequency of about 0.2% (127). Therefore, in addition to studying aging, *C. elegans* have proven to be a useful model for studying questions related to meiosis and reproductions, and the mechanisms and pathways that shape these processes.

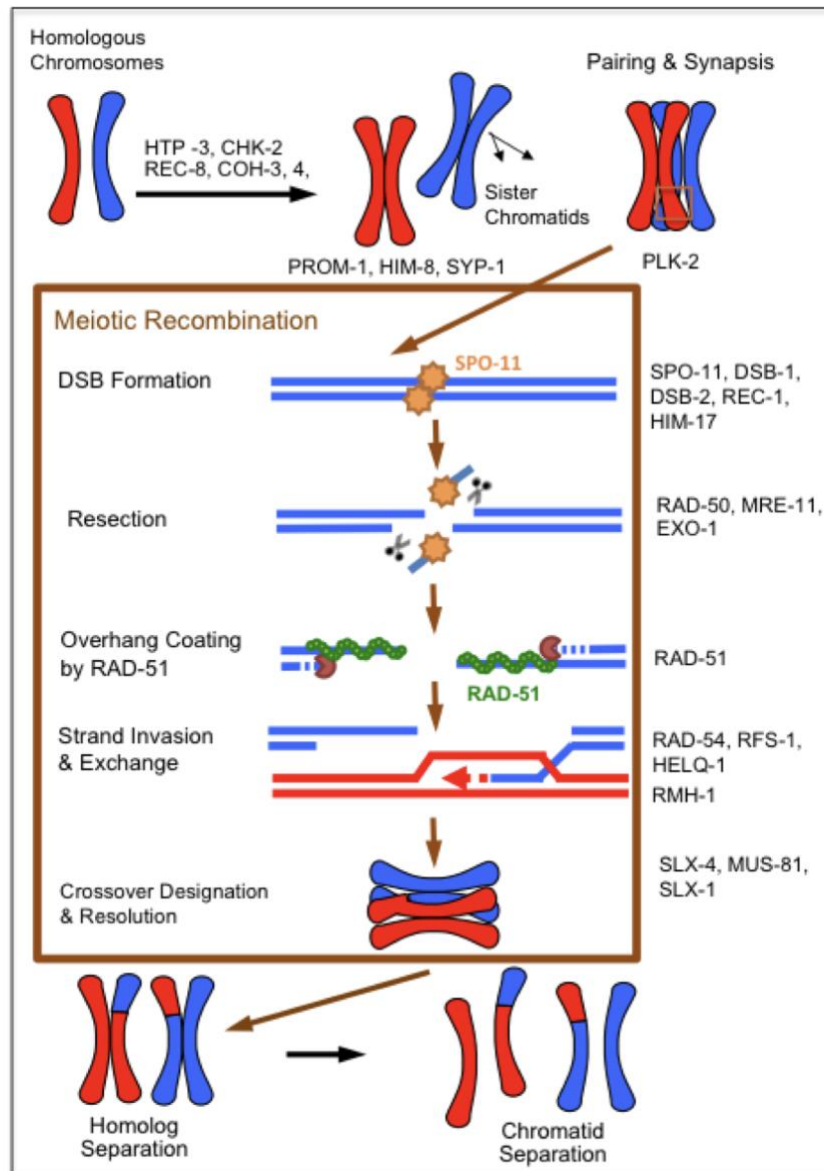


Figure 3: Overview of *C. elegans* meiosis

Chromosomes replicate, then homologous chromosomes pair and synapse. During meiotic recombination a double-strand break is formed which can be repaired via crossover or noncrossover. After homolog separation, this results in four haploid gametes. Some of the major proteins studied in this thesis are listed next to the step of meiosis.

Thanks to Dr. Judith Yanowitz for generation of this figure

1.3.5 Germline signals impact aging

As mentioned previously, one of the major regulators of lifespan discovered in *C. elegans* is the proliferation of germline stem cells. It was discovered that the lifespan of *C. elegans* is significantly increased, up to 60%, when the germline stem cells are ablated (128). Similarly in *Drosophila*, germ line ablation also increases lifespan (129). On the face of it, these observations would seem to reinforce the “Disposable Soma Theory of Aging”. However, further research has suggested a more nuanced relationship. For instance, removal of the entire gonad, not just the germline stem cells, does not result in extended longevity (128, 130). Other mutations that result in sterility of *C. elegans* do not always extend lifespan (130). Instead, it has been determined that the proliferating germline stem cells (GSCs) regulate lifespan, through signaling pathways that are tissue- and stage-specific in *C. elegans* (130).

The signaling network responsible for longevity upon *C. elegans* GSC ablation involves a network of transcriptional changes that occur in the soma following GSC removal. One of those is through intestinal nuclear relocation of DAF-16, the worm homolog of FOXO3A, which also has a role in IIS longevity (128). Although there is some overlap in the transcription factors necessary for IIS longevity and germline signaling of longevity, the two longevity paradigms are additive in terms of lifespan extension (131). One of the specific factors needed for longevity via GSC-loss is *kri-1*, encoding an Ankyrin-repeat containing protein, which stimulates the nuclear localization of DAF-16 (132). This gene was found to be necessary for lifespan extension only in the background of a *glp-1* mutant, while lifespan is not impacted in wild type animals or *daf-2* mutants (132). Considering that DAF-16 accumulates in the nucleus in the intestine, but the signal originates in the germ line, the signal should be communicated from the germ line to the intestine.

Researchers found that *kri-1* expression in the intestine and the pharynx rescued the lifespan extension of a *glp-1;kri-1* mutant (132). Another factor that is specific to the longevity of *glp-1* mutants is the transcription elongation and splicing factor, TCER-1 (133). Studying TCER-1 has revealed that germline stem cell removal increases the expression of *tcer-1* which promotes the expression of a set of DAF-16 target genes that are important for longevity (133).

Reproductive control of aging involves hormone and steroid signaling. This includes, DAF-12, a nuclear hormone receptor, which is required for germline ablation to extend lifespan (128). DAF-12 induces DAF-16 nuclear localization and upregulates downstream pro-longevity targets (128, 132, 134). In a wild type animal, DAF-12 is involved in reproductive development in *C. elegans* and responds to the binding of the ligand, dafachronic acids (DA) (134). Other components of this pathway that are also important for *glp-1* longevity, including DAF-9 and DAF-36, are required for DAF-12 ligand biosynthesis (134, 135). Research has found that DAF-12 must be bound to DA and be transcriptionally active for longevity, but supplementation with DA restores the longevity in animals with mutations in either *daf-9* or *daf-12* (135). Interestingly, DAF-12 seems to have roles other than merely the nuclear localization of DAF-16, potentially through its own targets independent of DAF-16 activity (132). This was found through an experiment using constitutively nuclear localized DAF-16, in which *daf-9* and *kri-1* are not necessary for lifespan extension, but *daf-12* is still required (132). DAF-12 has also been shown to stimulate microRNAs, including *mir-84* and *mir-241*, and function in the longevity pathway through DAF-16 (136). Another microRNA, *mir-71*, has also been shown to have a role in germline longevity, independent of DAF-12 activation. It was determined that *mir-71* deletion results in reduced DAF-16 nuclear localization (137).

In addition to the requirement of the above-mentioned transcription factors, researchers have identified the cellular processes that change upon GSC-removal. Some of these cellular processes include lipid metabolism, stress resistance, autophagy, and proteasomal degradation, many of which are hallmarks of aging (138). When considering the re-allocation of resources from reproduction that are shifted towards longevity, it was discovered that both the processes of fat production and degradation increase in germlineless mutants (139). Another nuclear hormone receptor, NHR-80 was also found to be necessary, specifically for the longevity of GSC-less animals, by promotion of fatty acid desaturation (140). Nuclear hormone receptor, NHR-49 is also essential and specific for the GSC-less longevity pathways (141). In germlineless animals, *nhr-49* is upregulated by both TCER-1 and DAF-16, and has a role in the of metabolic changes of germlineless animals that help facilitate extended lifespan (141). Another cellular process, autophagy, has also been shown to be upregulated upon GSC-removal, through the transcription factor PHA-4 (142). Autophagy is a process that degrades damages organelles or proteins in the cytoplasm of the cell. This process has been shown to have an important role in many longevity paradigms in *C. elegans*, including through reduced insulin signaling, dietary restriction, and reduced mitochondrial respiration (143). HLH-30 also has a role in autophagy during GSC-less longevity; however, it is required for many longevity pathways, not only in the context of GSC-loss (144). Additionally, it was determined that MML-1 and MXL-2 promote the nuclear localization of HLH-30 and are needed for GSC-less longevity (145).

glp-1 animals also exhibit increased stress resistance and multiple factors involved in stress response pathways have been identified as important for germline pathway of longevity (138). SKN-1 which regulates stress response pathways in many different longevity paradigms, promotes longevity in GSC-less mutants as well. (146). Heat shock factor, *hsf-1*, which is involved stress

response, was also found to be required for lifespan extension of a GSC-less animal (147). The proteasome, which in normal animals decreases in function with age, is also more active in a *glp-1* mutant (148). The proteasome includes the ubiquitin proteasome system, which functions to correctly fold proteins as well as degrading misfolded or aggregating proteins. In addition to an increased ability to combat proteotoxic stress, *glp-1* animals have demonstrated an upregulation of other stress responses such as pathogen stress, heat stress, and oxidative stress (138). Research into the transcriptional and cellular changes, which occur upon germline stem cell removal and contribute to longevity, indicate that there is not a simple trade-off between reproduction and longevity. Rather, there are widespread changes in many different cellular processes that culminate in increased lifespan.

1.3.6 Molecular mechanisms linking somatic health and reproductive aging

Nine cellular and molecular hallmarks of aging that contribute to the decline of an organism have been identified across species. These hallmarks were selected for their prevalence in mammalian aging and for their simple quantification in organisms such as *C. elegans* (149). The hallmarks are genomic instability, telomere attrition, epigenetic alterations, loss of proteostasis, deregulated nutrient sensing, mitochondrial dysfunction, cellular senescence, stem cell exhaustion, and altered intercellular communication (149). One of these hallmarks, the decline of protein homeostasis, is particularly interesting due to its connection with the germ line. Aging and age-related diseases, especially neurodegenerative diseases, are linked to the loss of protein homeostasis with age.

Studies in *C. elegans* demonstrate that proteostasis decline in germ cells begins during the onset of reproduction (150). Additionally, mutations that arrest germline stem cell proliferation (*glp-1*) also delay proteostasis decline (150). Protein homeostasis includes the maintenance of proper protein folding and degradation of misfolded proteins. The proteasome consists of the ubiquitin proteasome system and autophagy. While somatic proteostasis declines with age, cells such as embryonic stem cells and germline stem cells must maintain increased proteasomal activity in order to pass on high quality genetic information (151). Interestingly, while the *glp-1* animals are sterile, there is a shift to increased proteasomal activity in the soma (148). To maintain an immortal germ line in *C. elegans*, the oxidized proteins in the germline cells that accumulate are removed during oocyte maturation (152). It was also discovered that in *C. elegans*, there is a lysosomal switch that is stimulated by sperm to clear protein damage (153). A more recent study expanded this pathway to include the endoplasmic reticulum and also links genes involved in germline protein aggregation clearance with somatic protein homeostasis (154).

In conclusion *C. elegans* have proven to be an excellent model system in which to study both reproduction and aging. Research in this system has contributed towards the understanding of the genetics of aging, as well as different aspects of reproduction, including meiosis and reproductive aging. However, there remain many unknowns in these fields, and a core question lingers about the causative role of the germline health status on somatic aging. Studies in the *glp-1* animal, where the germline stem cells are not proliferating, have enhanced our knowledge of how germline status controls aging. However, the results of these studies are complicated by the reliance upon animals without a germ line. Therefore, to understand the causative role between germline integrity and somatic aging, another approach must be utilized. This thesis provides an alternative approach by examining the role that mutations in meiosis have on somatic aging.

2.0 Meiotic dysfunction shortens lifespan and diminishes healthspan

2.1 Introduction

The global aging population is growing rapidly with older people estimated to outnumber children by 2050 (10-24) (2). Considering that with increased age there is a dramatic increase in susceptibility to many diseases including cardiovascular disease, neurodegenerative disease, osteoporosis and cancer, it is of public health interest to understand the pathways and factors that influence aging (155). One of the most influential evolutionary theories of aging, The “Disposable Soma Theory of Aging”, suggested that aging is a consequence of animals investing their cellular resources towards maintaining their germ line to be passed to the next generation in a pristine state, and diverting them away from maintenance of the mortal somatic tissues (9). This implies an energy trade-off --and hence an antagonistic relationship-- between reproduction and longevity. There has been evidence in nature, laboratory models and human studies (discussed in detail in chapter 1) that both support and contradict this antagonistic relationship. For example in worms, flies and other species, mating shortens lifespan of the mother and increases immune-susceptibility (43, 44). Indeed, pregnancy was considered to be an extended state of generalized immunosuppression until recently, reviewed in (38). While it is now evident that immune alterations during pregnancy are complex and nuanced, it remains true that pregnant women exhibit increased susceptibility to, and severity during, many infections (38). But there is also evidence to suggest that mating and reproduction are beneficial for health and longevity across species. For example, in some species of insects, males transfer nuptial gift to females and in

eusocial animals such as ants, bees and African mole rats, increased procreation is associated with greater longevity (48-51). Transplantation of ovaries from younger mice into older mice has been shown to extend the lifespan and induce a cardio-protective advantage of older mice (156). The application of the “Disposable Soma Theory of Aging” to historical human records of births and deaths has led to conflicting results, in which reproduction has no impact on longevity and reproduction and number of progeny having a negative effect on aging (9, 10). Further, studies in females have found a link between the age at natural menopause and biomarkers of aging, as measured through epigenetic marks of DNA methylation (35). However, there is widespread evidence to suggest that the relationship between reproduction and aging is not based on a simple trade-off of resources, and that germline health and integrity are intimately connected with overall organismal health and aging. However, investigating this association and examining the cause-and-effect relationship is severely challenging in humans and mammalian systems.

To circumvent the limitations inherent in mammalian systems, we used *C. elegans* to investigate the relationship between germline integrity and organismal aging. To this end, we focused on the process of meiosis to tease apart the cause-and-effect relationship. Meiosis is a germline-restricted process that occurs in almost all multicellular organisms and leads to the production of haploid gametes. It is driven by a cascade of genes broadly conserved across species. In *C. elegans*, as in other organism, meiosis begins with the pairing and synapsis of homologous chromosomes (*htp-3*, *rec-8*, *coh-3,4*, *chk-2*, *him-8* and *zim* genes, *syp* genes, *prom-1*) (Fig 3). This is followed by a double-strand break during meiotic recombination (*spo-11*, *dsb-2*, *dsb-1*, *him-17*, *rec-1*, *dsb-3.xnd-1*, *mre-11*, *rad-50*) that is then resected (*exo-1*, *mre-11/rad-50/nbs-1* complex). Subsequently, the single-strand DNA end is coated by RAD-51 and repaired by crossover or non-crossover pathways that occur by strand invasion, strand exchange (*rad-54*, *rfs-1*, *helq-1*, *rmh-1*),

and distinct processing of NCO and CO intermediates. The crossovers are designated (*msh-4*, *msh-5*, *zhp-3*, *cosa-1*) and resolved (*xpf-1*, *him-6*, *slx-1*, *mus-81*, *slx-4*) (126). Some of these genes (*rad-51*, *rec-8*, *mre-11*, *rad-50*, *rad-54*) are also have roles in DNA damage repair in somatic cells (157). A recent genome wide association study (GWAS) that aimed to identify genetic determinants of age at natural menopause (ANM) found that many DNA damage response genes were associated with age at natural menopause, including various genes that function in meiosis (158). In mammals, it is difficult to tease apart the roles of many of these genes in their DNA damage repair in the soma and their role in meiosis in the germ line. However, in *C. elegans* all adult somatic cells are post-mitotic, allowing us to specifically examine the roles of such genes specifically in meiosis in the germ line.

We assessed the rate of aging of mutants of genes involved in different steps of meiosis utilizing three methods. First, we measured how long the mutants lived compared to wild type to understand if the meiotic mutations impact lifespan. Second, we were interested in determining if, in addition to the length of life, these mutations impacted other features of aging i.e. healthspan. *C. elegans* have conserved longevity pathways shared with humans, and there are also characteristics of aging which resemble mammalian aging (71, 76) as summarized in Chapter 1.3. We utilized a combination of these assays to measure healthspan to get a clearer picture for how these mutations impact aging beyond the length of life. Third, we wanted to examine molecular mechanisms through which meiotic dysfunction could impact aging of the soma. One of the potential mechanisms that we explored is protein homeostasis, one of the earliest age-related deficits in *C. elegans* (159). The results of our lifespan analyses, the impact of meiotic mutations on somatic healthspan and protein homeostasis are described below.

2.2 Results

2.2.1 Mutations in all aspects of meiosis impact lifespan

To address a potential causative role of the status of the germ line on organismal aging, we asked how mutations in genes involved in meiosis impact lifespan. We tested the lifespan of 38 strains that had at least one mutation in a gene involved in meiosis. These genes were selected for their variety of roles in meiosis, so we could unravel the impact of specific meiotic steps on lifespan. We found initially that 31 of these strains exhibited a shortened lifespan at least once (Appendix Table 1). Of the 31 strains, we selected for retesting 25 strains that exhibited the greatest impacts on lifespan and that affected genes that operate during different steps of meiosis. Of these, 13 showed reduced lifespan in at least two trials (Fig 4, Appendix Table 1). Interestingly, we found that genes associated with a reduced lifespan were not specific to a defined step of meiosis, but rather had diverse roles in meiosis, for example, double-strand break formation (*dsb-2*, *spo-11*), synaptonemal complex formation (*htp-3*) and meiotic DNA damage repair and crossover formation (*slx-1*, *rad-51*).

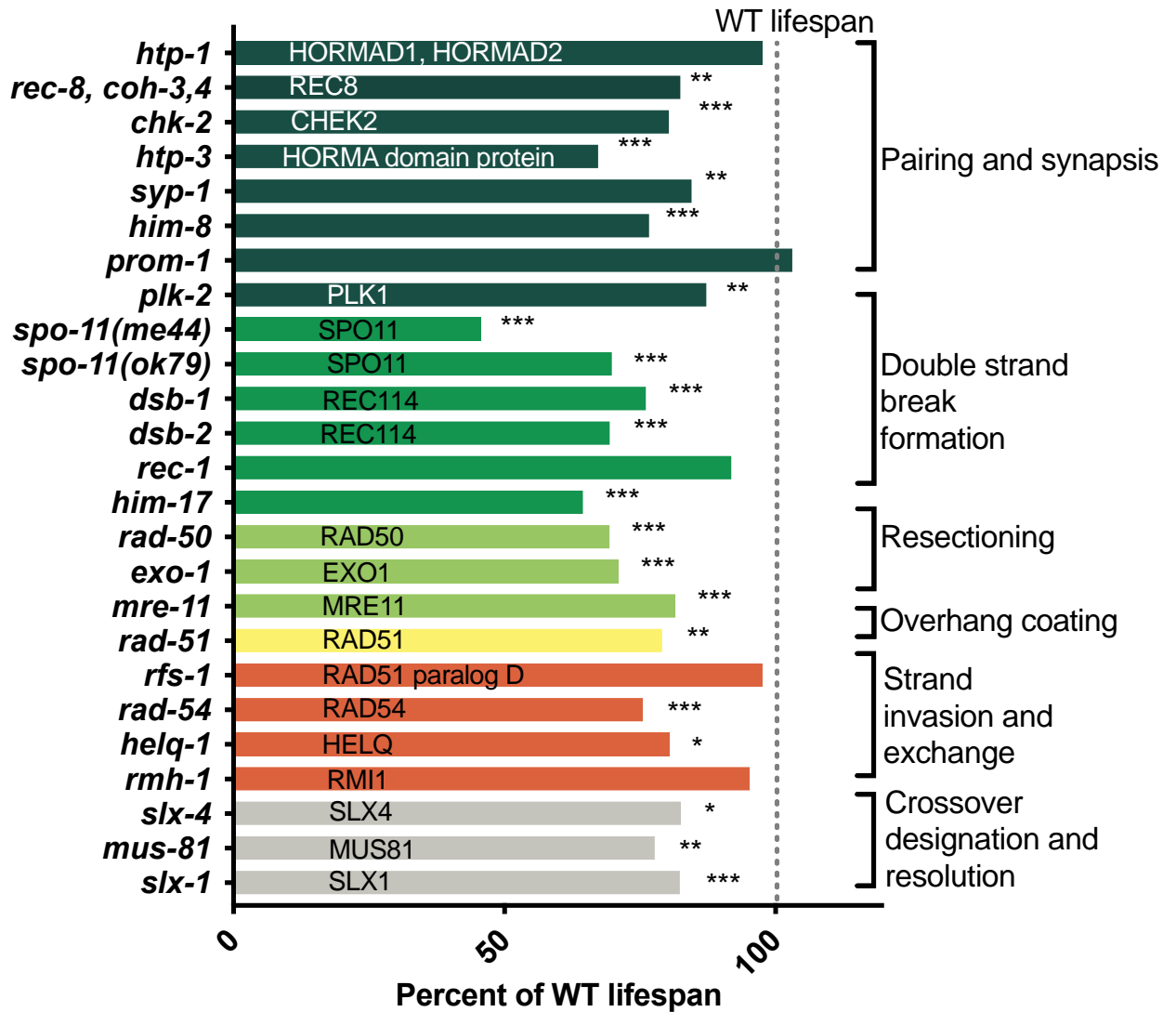


Figure 4: Representative lifespan of mutants of genes in different aspects of meiosis compared to WT

lifespan. Human homolog is indicated on each bar and the step of meiosis is grouped by color and indicated on the

right side * p <0.05, **p <0.001, ***p <0.0001

Table 1: Apoptosis, DNA breaks, and fertility phenotype of meiotic mutants with shortened lifespan

Gene/ mutation	Human ortholog	Avg. percent change in lifespan	DNA breaks (RAD-51 foci)	Germ cell apoptosis	fertility (% viable progeny)	Percentage of males
<i>chk-2(gk212)</i>	CHEK2	-19.68		WT levels (160)		
<i>htp-3(y428)</i>	HORMA domain protein	-32.70			88% and 39% survive to adulthood (161)	
<i>him-8(me4)</i>		-23.32	similar to WT but delayed repair (162)		96% (162)	39.70% (162)
<i>spo-11(me44)</i>	SPO11	-54.50	no breaks (163)		2.5% (109)	37% (109)
<i>spo-11(ok79)</i>	SPO11	-30.19	no breaks (163)	WT levels(164)	0.50% (107)	
<i>dsb-1(we11)</i>	REC114	-23.92	no breaks (109)		3.20% (109)	38% (109)
<i>dsb-2(me96)</i>	REC114	-30.61	decreased (110)		39% (110)	12% (110)
<i>him-17(e2707)</i>		-35.53	WT levels but delayed repair (108)		63% (108)	33% (108)
<i>rad-50(ok197)</i>	RAD50	-30.66	reduced (163)	increased (163)	1.2% (163)	19% (163)
<i>exo-1(tm1842)</i>	EXO1	-28.85	WT levels (113)		99.10% (165)	0.10% (165)
<i>mre-11(iow1)</i>	MRE11	-18.48	reduced (113)	increased (113)	0.2%(113)	
<i>rad-51(lg8701)</i>	RAD51	-20.93		increased (166)	0% (166)	
<i>slx-1(tm2644)</i>	SLX1	-17.63	WT levels but persist longer (167)	Increased (167)	92.70% (167)	0.40% (167)

Per the “Disposable Soma Theory of Aging” that postulates a trade-off of resources between somatic maintenance and reproductive fitness, mutations that cause a decrease in fertility would be predicted to result in an increase in lifespan. Indeed, sterile mutants have been shown to exhibit enhanced longevity in worms and flies (128, 168). We reviewed results from previously published papers describing the fertility defects in meiosis mutants. We found the mutations in our short-lived strains had a variety of fertility defects ranging from ones with less than 3% fertility

(*spo-11(ok79)*, *spo-11(me44)*, *rad-51*, *rad-50*, *mre-11*) to ones which produced >80% viable progeny (*slx-1*, *him-8*, *exo-1*) (162, 165, 167). Given previous observations that sterility and fertility loss are often associated with increased longevity, it was noteworthy that 9/13 mutants had >80% fertility loss but still exhibited significant lifespan reduction (Table 1). Defects in the DNA damage repair pathways, as well as excessive DNA breaks, have been reported to have an impact on aging (169). Of the 13 genes that reduced lifespan, 9 of the genes encode proteins that have no known roles in homologous recombination-mediated DNA repair. While many of the genes encode proteins that do not have a direct role in DNA repair, some of the mutations in these genes had reduced or very few breaks as indicated by RAD-51 foci (*dsb-2*, *dsb-1*, *rad-50*, *mre-11*, *spo-11*) (Table 1) (109, 110, 113, 163). Mutations in meiosis also can result in changes to the level of germ cell apoptosis including increased apoptosis in *rad-50*, *mre-11*, *rad-51*, and *slx-1* mutants with other mutants maintaining wild-type levels of apoptosis such as *chk-2* and *spo-11(ok79)* (Table 1) (113, 160, 163, 164, 166, 167). Thus, mutations in genes functioning at different steps of meiosis shortened lifespan significantly independent of their impacts on DNA repair, germline apoptosis or fertility.

To further understand how meiotic mutations impact reproduction, we selected three genes to further investigate. These genes included *spo-11* and *dsb-2*, which encodes proteins involved in the formation of the double-strand break during meiotic recombination, and *htp-3*, encodes a component of the synaptonemal complex (125). We selected these genes because of their specific role in meiosis, predicted germline-restricted expression, and the consistent reduction of lifespan that we observed in their mutants. We found that mutations in *spo-11(me44)* reduced mean lifespan from 26-54% (Fig 5A), *htp-3* mutants reduced mean lifespan from 17% - 33% (Fig 5B), and *dsb-2* mutants reduced mean lifespan from 6% to 31% (Fig 5C).

2.2.2 Germline-specific inactivation of meiotic genes shortens lifespan

Many, but not all meiotic genes, including *spo-11*, *dsb-2* and *htp-3*, are germline-restricted in expression. To test if their lifespan impacts were due to germline function, and to determine their sites of action, we asked if germline-specific RNAi inactivation of these genes shortened lifespan of worms. We used a recently developed transgenic strain in which mutant strain of *rde-1* (which encodes an Argonaute protein, a key component of the RNAi machinery pathway and essential for response to feeding RNAi) expresses the RDE-1 protein solely in the germ line (driven by the germline-specific promoter, *sun-1*). This strain has been used widely for germline-specific RNAi knockdown of genes (170-172). We found that if we initiated RNAi inactivation from early larval stages and maintained it throughout the entirety of the animal's lifespan, there was a reduction of mean lifespan by 12%-17% when *htp-3* was knocked down, 19-20% when *spo-11* was knocked down, and 19% when *dsb-2* was knocked down (Fig 5D, Appendix Table 2). *C. elegans* produce sperm during larval stage 3 (L3), then switch to producing oocytes in early adulthood and continue to do so throughout the rest of the reproductive span (126). To obtain a temporal perspective on the meiotic genes function, we inactivated *dsb-2*, *htp-3* and *spo-11*, only in adulthood by initiating RNAi in larval stage 4 (L4) poised on the cusp of adulthood. We found that 'adult-only' RNAi of any of the three genes had no impact on lifespan (Fig 5E). These results demonstrated that knockdown of *dsb-2*, *htp-3*, or *spo-11* in the germ line is sufficient to decrease lifespan, but the timing of the knockdown is important.

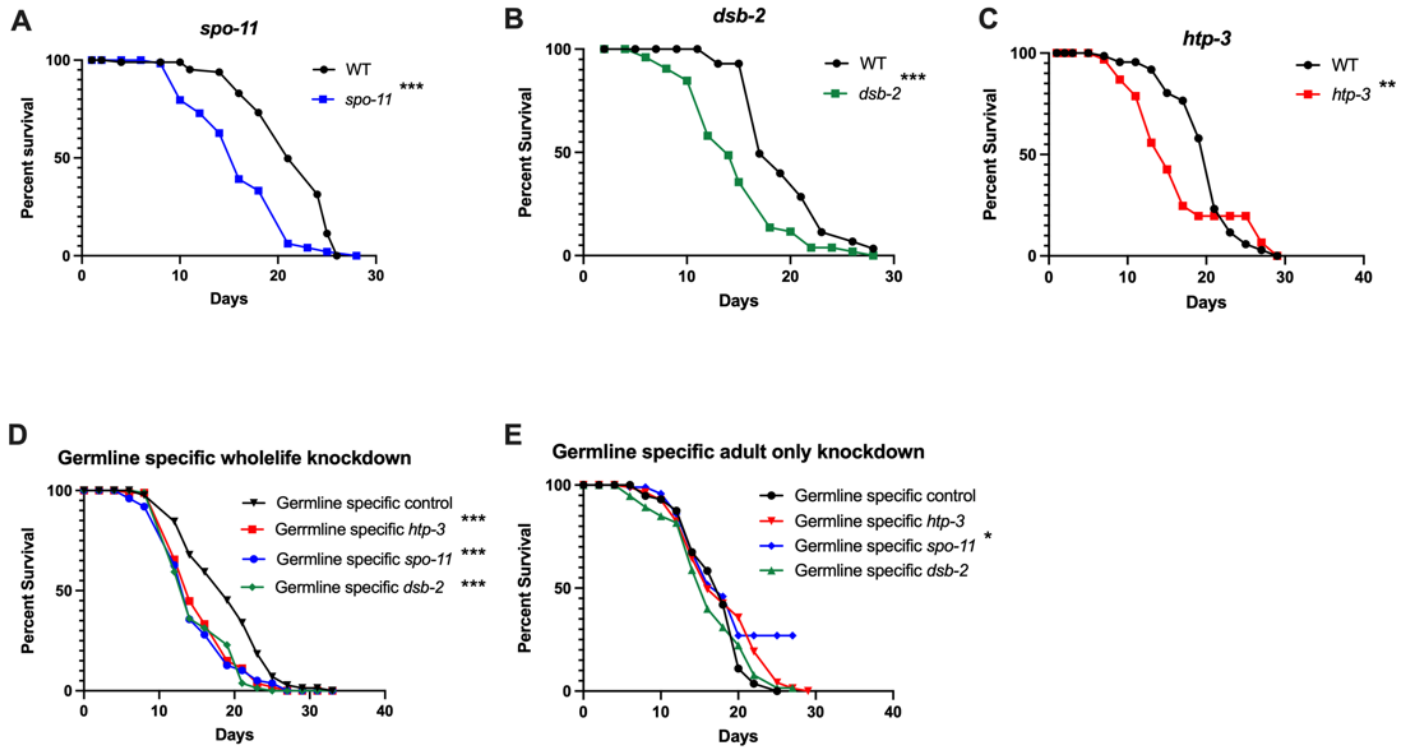


Figure 5: Lifespans of meiotic mutants and germline-specific RNAi knockdown of *htp-3*, *spo-11*, and *dsb-2*.

(A) N2 (m = 19.49 ± 0.62) n = 43/100, *spo-11(ok79)* n = 53/80 (m = 16.33 ± 0.62) P vs. N2 0.0008. (B) N2 (m = 19.55 ± 0.53) n = 49/72, *dsb-2* n = 62/78 (m = 14.84 ± 0.58) P vs. N2 <0.001 (C) N2 (m = 19.8 ± 0.58) n = 45/100, *htp-3* n = 52/80 (m = 16.42 ± 0.81) P vs N2 = 0.0014. (D) *sun-1p::rde-1* on L4440 control RNAi (m = $18.94 \pm .8$) n = 75/90, *sun-1p::rde-1* on *htp-3* RNAi (m = $15.77 \pm .45$) n = 82/90 P vs *sun-1p::rde-1* on L4440 <0.0001, *sun-1p::rde-1* on *spo-11* RNAi (m = $15.04 \pm .48$) n = 89/107 P vs *sun-1p::rde-1* on L4440 <0.0001, *sun-1p::rde-1* on *dsb-2* RNAi (m = $15.36 \pm .42$) n = 86/107 P vs *sun-1p::rde-1* on L4440 <0.0001. (E) *sun-1p::rde-1* on L4440 control RNAi (m = 17.19 ± 0.53) n = 55/62, *sun-1p::rde-1* on *htp-3* RNAi (m = $17.94 \pm .61$) n = 74/106 P vs *sun-1p::rde-1* on L4440 0.0732, *sun-1p::rde-1* on *spo-11* RNAi (m = $17.43 \pm .41$) n = 66/107 P vs *sun-1p::rde-1* on L4440 0.0485, *sun-1p::rde-1* on *dsb-2* RNAi (m = $16.29 \pm .52$) n = 88/97 P vs *sun-1p::rde-1* on L4440 = 0.8605. Survival data analyzed using Kaplan Meier curve shown as mean lifespan (m) \pm standard error of the mean n = observed/total * p

<0.05, **p <0.001, ***p <0.0001

We further tested the germline-specific role by introducing the three meiotic mutations (independently) into temperature-sensitive mutants of the gene *glp-1*. It has been previously reported that the removal of germline-stem cells (GSC) increases the lifespan of *C. elegans* by about 60%, and this has been replicated genetically through a mutation in *glp-1*, which encodes the receptor for a germline proliferation signal (128, 130) These temperature-sensitive mutants have a defect in germline cell proliferation when shifted from the normal laboratory conditions of 20 °C to 25 °C. The loss of GSCs extends lifespan through a network of transcriptional changes and upregulation of pro-longevity genes (138). We hypothesized that if the meiotic mutations functioned in the germ line to impact lifespan, then in the germline-less *glp-1* mutant background, there would not be a reduction in lifespan. We found that the *glp-1;dsb-2* double mutant showed no significant difference in lifespan from the *glp-1* single mutant, as expected based on our hypothesis (Fig 6A, Appendix Table 4). The *htp-3;glp-1* mutant showed a partial shortening of lifespan compared to *glp-1* (Fig 6E, Appendix Table 4). Surprisingly, the *spo-11* mutation in the *glp-1* background produced a significant decrease in lifespan (Fig 6B, Appendix Table 4). A similar result was observed with two alleles of *spo-11*, *ok79* and *me44*. Since *glp-1* mutants have an extended lifespan compared to wild type, the interpretation of this result would be complicated due to the lifespan extending signals generated through *glp-1* mutation. To obviate this, we used another germline-less mutant, carrying the *glp-4(bn2)*, temperature sensitive mutation that prevents germline development, but does not have an extended lifespan in the wild-type background (173). Again we found that the *spo-11;glp-4* double mutants had a similar decrease in lifespan to the *spo-11* single mutant. (Fig 6D, Appendix Table 4).

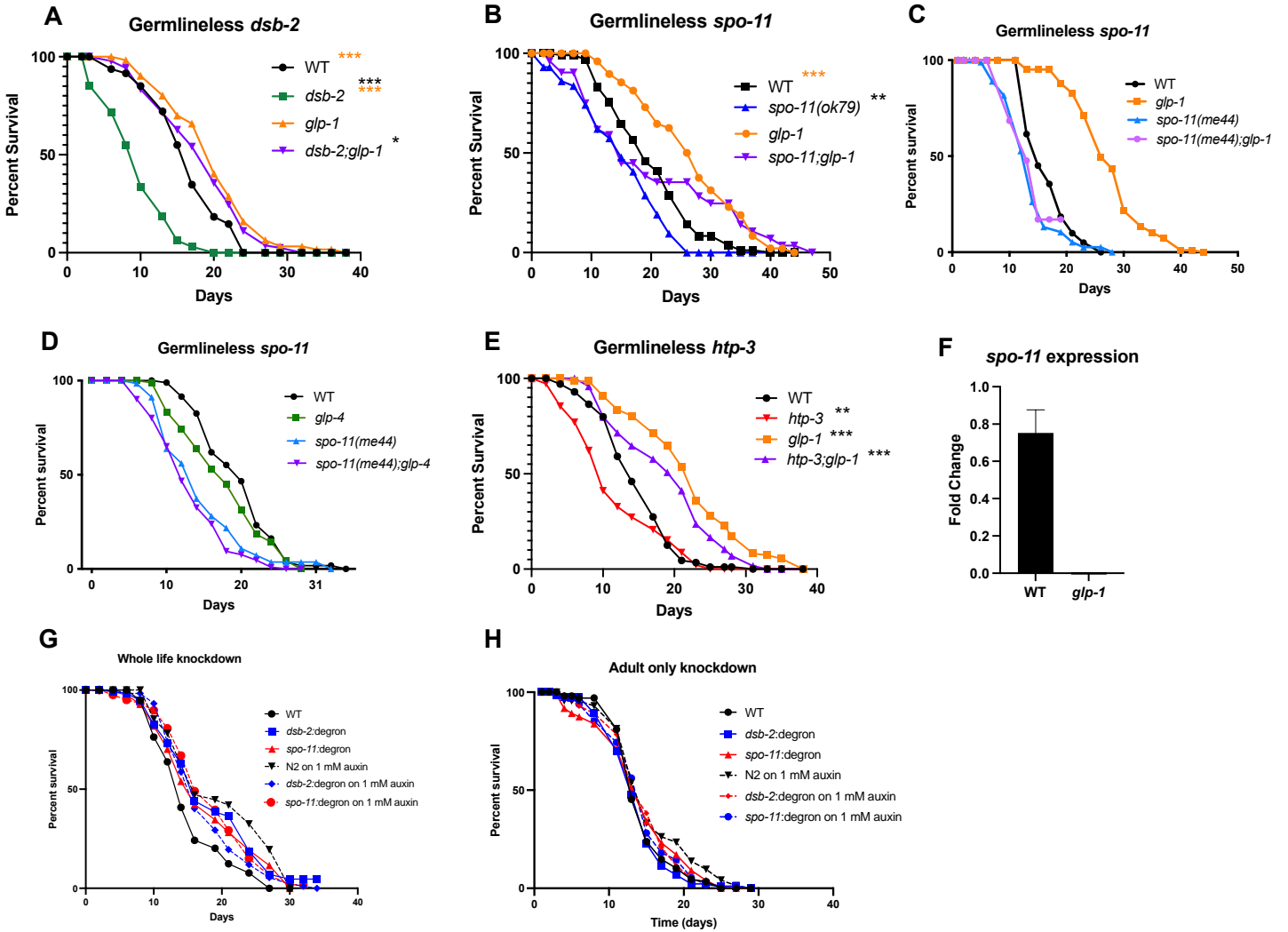


Figure 6: Impact of meiosis mutants in germlineless background.

(A) WT ($m=16.5 \pm 0.51$) $n = 71/113$ P vs *glp-1* <0.0001, *dsb-2* $n = 35/41$ ($m= 9.69 \pm .71$) P vs N2 <0.0001, P vs *glp-1* <0.0001, *glp-1* $n = 94/118$ ($m= 19.87 \pm .61$) P vs N2 <0.0001, *dsb-2;glp-1* $n = 82/95$ ($m= 18.33 \pm .67$) P vs N2 <0.0167, P vs *glp-1* 0.1325. (B) WT ($m=19.92 \pm 0.76$) $n = 87/111$ P vs *glp-1* <0.0001, *spo-11(ok79)* $n = 42/43$ ($m= 15.07 \pm .1.08$) P vs N2 0.0005, P vs *glp-1* <0.0001, *glp-1* $n = 48/49$ ($m= 26.53 \pm .1.25$) P vs N2 <0.0001, *spo-11(ok79);glp-1* $n = 36/52$ ($m= 20.22 \pm .1.99$) P vs N2 0.4799, P vs *glp-1* 0.0989. (C) WT ($m=16.56 \pm 0.56$) $n = 78/113$ P vs *glp-1* <0.0001, *spo-11(me44)* $n = 47/62$ ($m= 13.04 \pm .0.5$) P vs N2 <0.0001, P vs *glp-1* <0.0001, *glp-1* $n = 39/40$ ($m= 20.93 \pm 1.03$) P vs N2 <0.0001, *spo-11(me44);glp-1* $n = 38/61$ ($m= 11.05 \pm 0.64$) P vs N2 <0.0001, P vs *glp-1* <0.0001. (D) WT ($m=19.93 \pm 0.65$) $n = 60/122$ P vs *glp-4* <0.0625, *spo-11(me44)* $n = 57/70$ ($m= 14.66 \pm 0.78$) P vs N2 <0.0001, P vs *glp-4* <0.0013, *glp-4* $n = 75/124$ ($m= 17.92 \pm 0.66$) P vs N2 <0.0625, *spo-*

11(me44);glp-4 n = 118/125 (m= 13.27 ± 0.45) P vs N2 <0.0001, P vs *glp-4* <0.0001. (E): WT (m=14.71 ± 0.52) n = 91/102, *htp-3* n = 98/110 (m= 11.67 ± 0.61) P vs N2 <0.0001, *glp-1* n = 117/137 (m= 22.13 ± 0.68) P vs N2 <0.0001, *htp-3;glp-1* n = 116/121 (m= 19.03 ± 0.64) P vs N2 <0.0001, P vs *htp-3* <0.0001. (F): expression of *spo-11* in N2 animals and *glp-1* animals, statistical significances were calculated using a one-tailed t test, combined 3 biological replicates. (G): Whole life exposure: WT (m=15.25 ± 0.58) n = 75/123 P vs auxin <0.0001, *dsb-2:degron* n = 90/125 (m= 18.17 ± 0.68) P vs N2 on EtOH = 0.0015, P vs auxin = 0.2373, *spo-11:degron* n = 77/124 (m= 17.65 ± 0.76) P vs N2 = 0.0188, P vs auxin = 0.7307, WT on 1 mM auxin (m=19.64 ± 0.81) n = 69/120 P vs WT on EtOH <0.0001, *dsb-2:degron* on 1 mM auxin n = 93/129 (m= 17.42 ± 0.6) P vs N2 on EtOH = 0.0182, *spo-11:degron* on 1mM auxin n = 106/122 (m= 18.25 ± 0.61) P vs N2 = 0.0006. (H): Adult-only exposure WT (m=14.47 ± 0.39) n = 91/104 P vs auxin = 0.0503, *dsb-2:degron* n = 95/118 (m= 13.86 ± 0.4) P vs N2 on EtOH = 0.4258, P vs auxin = 0.1161, *spo-11:degron* n = 104/124 (m= 14.25 ± 0.52) P vs N2 = 0.5875, P vs auxin = 0.8986, WT on 1 mM auxin (m=15.55 ± 0.6) n = 75/92 P vs WT on EtOH = 0.0503, *dsb-2:degron* on 1 mM auxin n = 97/155 (m= 14.64 ± 0.45) P vs N2 on EtOH = 0.4259 *spo-11:degron* on 1mM auxin n = 112/141 (m= 14.36 ± 0.43) P vs N2 = 0.6288 Survival data analyzed using Kaplan Meier curve shown as mean lifespan (m) ± standard error of the mean n=observed/total * p <0.05, **p <0.001, ***p <0.0001

To address the discrepancy between the results of the germline-specific RNAi knockdown and the germline-less mutants, we sought another strategy to eliminate SPO-11 or DSB-2 protein specifically in the germ line using the Auxin-Inducible Degron (AID) system. Two strains had been previously developed that consisted of degron-tagged SPO-11 or DSB-2, which resulted in SPO-11 or DSB-2 proteins degrading specifically in the germ line and only in the presence of auxin (174). This tool would allow us to ask if loss of either of these two proteins specifically in the germ line impacted the lifespan of the animal. We found that degrading these proteins in the germ line, using two different concentrations of auxin (1mM or 4mM), either for the entire life of the animal or beginning during adulthood (L4 stage), does not impact lifespan of the animal (Fig

6 G,H, Appendix Table 3). However, these observations were also confounded by our discovery that both auxin exposure and the expression of the AID construct impacted lifespan (discussed in Chapter 5). Taken together, these experiments suggest that germline-specific whole life inactivation of meiotic genes is sufficient to shorten lifespan, but in some cases such as *spo-11* there may be somatic functions as well.

2.2.3 Mutations in meiosis impact healthspan

While conducting the lifespan experiments, we noticed that the meiosis mutants appeared older than the wild type animals of the same age. Considering that mutations in *dsb-2*, *htp-3*, and *spo-11* decrease lifespan, we were also interested in determining if these mutations also showed signs of accelerated aging i.e., diminished healthspan. It has been well documented that *C. elegans* show age-related decline in many different physiological, cellular, and molecular parameters as detailed in Chapter 1.3 (75). Multiple assays that measure aspects of age-related deterioration in anatomic, physiological and molecular aspects have been developed by our lab and others that together help assess the rate of aging of the animal (71). We assessed the meiotic mutants using these parameters. First, we tested if there were changes to the tissue integrity with age. The transparent nature of *C. elegans* allows for visualization of specific tissues that change with age (72). As the animals get older, the clearly defined nuclear boundaries in certain tissues, such as muscle cells, are less defined and necrotic cavities appear (72). The pharynx of the animals also shows clear degradation with age, with the older animals showing signs of degraded tissue and bacteria packing in the pharynx (72). We imaged middle-aged (Day 5) animals and found that the appearance of the *spo-11* mutants, compared to wild type animals of the same age, appeared to

show a marked decline in tissue integrity (Fig 7A, B). We quantified this by taking images of three different ages throughout the lifespan (Day 1, 5, and 10) of wild type animals and *spo-11* mutants and asked researchers who work with *C. elegans* across the University of Pittsburgh to blindly score the animals on a scale of 1-3, with 1 being the healthiest and 3 being the unhealthiest, with example images of each score provided for training purposes. The images were blinded for both genotype and age of the animal. The results from these examinations resulted in *spo-11* mutants on Day 5 and Day 10 of adulthood consistently receiving a score of 3 at a significantly higher rate than age-matched wild-type animals (Fig 7C). Interestingly, *dsb-2* and *htp-3* mutants appeared indistinguishable from their wild-type counterparts at all ages.

Another hallmark of aging in *C. elegans* is loss of mobility (175). Loss of mobility, as a measure of healthspan, can be quantified in *C. elegans* through a variety of different assays (71). Here we used thrashing rate, which we measured by counting the number of body bends each animal made while swimming in liquid during a set amount of time (see methods). Wild-type animals exhibit a well-documented, steady decline in thrashing rate between young (Day 2), middle (Day 5) and old (Day 7 or later) ages (Fig 7D-F, Appendix Table 5.). We found that animals with a mutation in *spo-11* exhibited an accelerated decline in their thrashing rate between Day 5 and Day 7 of adulthood (Fig 7D, Appendix Table 5). *htp-3* mutant animal demonstrated an accelerated decline in thrashing rate later in life, between Day 7 to 9 of adulthood (Fig 7E, Appendix Table 5). However, *dsb-2* mutants showed a similar decline in thrashing rate from Day 2 to Day 9 of adulthood as the wild-type animals (Fig 7F, Appendix Table 5). Thrashing was initially measured starting at Day 2 of adulthood, but to rule out that the mutations caused developmental defects that impaired movement, we also quantified thrashing rate in L4 larvae. We found that only *dsb-2* mutants had a reduced thrashing rate during this developmental stage, while

spo-11 and *htp-3* mutants had a similar thrashing rate as wild type. Interestingly, the *dsb-2* mutant animal was the only animal that we examined in which thrashing rate did not demonstrate an accelerated decline with age (Fig 7O).

C. elegans process their food, the normal lab diet of *E. Coli*, through grinding of their pharyngeal muscle, which is a neuromuscular organ whose rhythmic ‘pumping’ contractions break down bacterial cells (75). Wild-type pumping rates peak at Day 2 of adulthood and then decline throughout the rest of an animal’s lifespan (75). We found that *htp-3* mutant animals had an accelerated decline in pumping rate compared to wild-type, specifically between Day 5 and Day 7 of adulthood (Fig 7H, Appendix Table 6). Animals with a mutation in *spo-11* or *dsb-2* showed a similar rate of decline in pumping as wild type (Fig 7G, I, Appendix Table 6).

The fourth healthspan feature that we measured was neuronal function, as assessed by chemotaxis and short-term memory. Remarkably, the nervous system remains structurally intact during aging, but associative learning and long-term associative memory decline with age (176). Using an established associative learning assay, we trained the animals to associate the scent of butanone with food and then 30 minutes later, quantified the number of animals on an nematode growth media (NGM) plate that moved towards a drop of butanone versus a drop of the control (ethanol) (176). We measured this neurological function on Days 1 and 5 of adulthood. We found that *dsb-2* mutants demonstrated an accelerated decline in neurological function with age, while *htp-3* and *spo-11* mutants had no change compared to wild type (Fig 7J-L, Appendix Table 7).

As in many species, the ability of *C. elegans* to combat stress declines with age (71). One source of stress that can be easily quantified in the lab is exposure to pathogenic bacteria. The decline in resistance against pathogen attack, immunosenescence, is well documented in worms (177). This was the fifth healthspan feature that we measured, by exposing the animals to the

opportunistic pathogen *Pseudomonas aeruginosa* strain PA14 (PA14). *C. elegans* are typically grown on plates that are seeded with *E. coli* as food, but to measure pathogen stress resistance, worms grown on normal *E. coli* lawn during development can be transferred to plates seeded with the pathogenic PA14 strain and survival measured over time. We found that upon exposure to PA14, *dsb-2* mutant animals had a shorter survival time compared to wild-type animals (Fig 7M, Appendix Table 8). Thus, at least one meiotic mutant exhibited immune-susceptibility.

Lastly, we asked if in addition to premature signs of anatomical and physiological decline, the meiotic mutants also showed early induction of molecular markers of aging. Many previous studies have identified genes that undergo age-related gene expression changes in *C. elegans* (178-180). The expression of one such gene, *ins-7*, was upregulated earlier in *dsb-2* mutants compared to wild type and the other mutant animals (Fig 7N). Overall, these experiments demonstrated that, in addition to reducing lifespan, mutations in *dsb-2*, *spo-11* and *htp-3* also caused accelerated decline in healthspan features. Interestingly each mutant demonstrated a decline in at least one healthspan feature, however, there was not a single healthspan feature that we measured for which all of the mutants demonstrated an accelerated decline. These experiments led us to conclude that disrupted meiosis not only shortened lifespan, but also impaired healthspan.

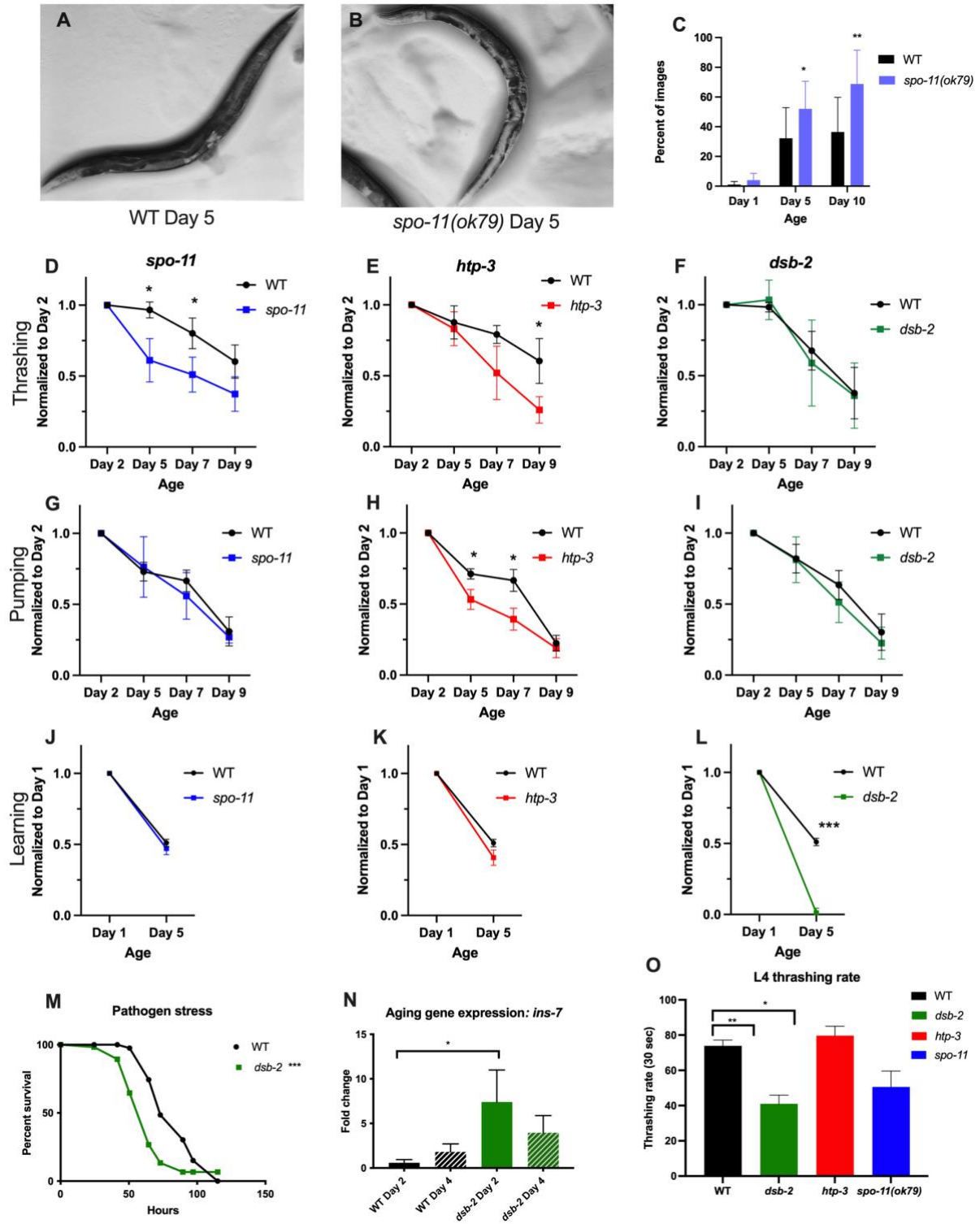


Figure 7: Healthspan of *dsb-2*, *spo-11*, and *htp-3* mutants

Image of wild type (A) or *spo-11(ok79)* (B) Day 5 adult. (C) Average percent of images, given the unhealthiest looking score. Statistical significance was calculated using a one-tailed t test, averaging data from 10 different people scoring images Fig D-E: Thrashing compared between wild type (WT, black) and *spo-11(ok79)* (blue) (D), *htp-3* (red) (E), and *dsb-2* (green) (F). Data shown are combined from 3 (or 4 for *dsb-2*) independent biological replicates with 20 animals tested per strain, per replicate. Values for each biological replicate are normalized to the thrashing rate for Day 2 of each strain. Statistical significance was calculated using an unpaired two-tailed t test (G-I): Pumping compared between wild type (WT, black) and *spo-11(ok79)* (blue) (G), *htp-3* (red) (H), and *dsb-2* (green) (I). Data shown are combined from 3 independent biological replicates with 20 animals tested per strain, per replicate. Values for each biological replicate are normalized to the pumping rate for Day 2 of each strain Statistical significance was calculated using an unpaired two-tailed t test (J-L): Learning compared between wild type (WT, black) and *spo-11(ok79)* (blue), (J), *htp-3* (red) (K), or *dsb-2* (green) (L). Data shown are combined from 3 independent biological replicates with 20 animals tested per strain, per replicate. More details for how learning index was calculated are in the methods section. Values for each biological replicate are normalized to the learning index for Day 2 of each strain Statistical significance was calculated using an unpaired two-tailed t test. (M) Pathogen exposure to *P. aeruginosa* (PA14) WT (m=83.49 ± 2.26) n = 57/87 *dsb-2* n = 42/58 (m= 63.95 ± 2.06) P vs N2 <0.0001. survival data analyzed using Kaplan–Meier test, shown as mean lifespan in hours (m) ± standard error of the mean (SEM). ‘n’ refers to number of animals analyzed/total number in experiment (see Methods for details) (N) expression of *ins-7* in N2 animals and *dsb-2* animals, statistical significances were calculated using a one-tailed t test, combined 3 biological replicates (O) Thrashing rate of L4 animals of N2(WT), *dsb-2*, *htp-3*, and *spo-11* strains, with data shown combined for 3 biological replicates. Statistical significance was calculated using one tailed t test Asterisks indicate statistical significance <0.05 (*), <0.001 (**), <0.0001 (***)

2.2.4 Mutations in meiosis impact protein homeostasis

Loss of protein homeostasis is one of the hallmarks of aging across species and is linked with age-related and neurodegenerative diseases, including Alzheimer’s disease and Parkinson’s disease (149). Protein homeostasis is imperative for maintaining protein quality control in a cell

through proper protein folding and clearance of misfolded proteins. These processes require chaperone-mediated protein folding, the autophagy-lysosomal system, and the ubiquitin-proteasome system (181). Aging-associated proteostatic collapse can cause the accumulation of protein aggregates, some of which have toxic properties and contribute to disease (181). Research using *C. elegans* has contributed towards our understanding of the functional importance of components of protein homeostasis in aging. Multiple models for measuring protein homeostasis decline in aging and neurodegenerative diseases, have been developed for use in *C. elegans*. For example, strains expressing the A β peptide and polyglutamine stretches have been used extensively to study the biology of Alzheimer's Disease and Huntington's Disease respectively (181). These models were developed to answer specific questions about these diseases, but they can be used more generally to understand protein homeostasis. In fact, studies in *C. elegans* have led to the discovery that animals that overexpress specific chaperones live longer, and that interventions in *C. elegans* that activate autophagy can also extend lifespan (182, 183). In addition to the role of protein homeostasis as one of the hallmarks of aging, there have also been studies that identified a link between reproduction and the timing of reproduction with protein homeostasis. This includes the finding that the loss of protein homeostasis is one of the first markers of aging, and interestingly, occurs as soon as the animals begin reproducing (159). There is also evidence to suggest that the germ line is involved in controlling somatic protein homeostasis, including evidence to suggest germline protein homeostasis impacts protein homeostasis in various somatic tissues (150, 154).

We asked if, in addition to the lifespan and healthspan declines, protein homeostasis was also diminished in meiotic mutants, which would point then towards a potential underlying mechanism. We used the aforementioned models and additional assays of protein accumulation to

determine if the trajectory of protein-homeostasis decline was altered in *dsb-2*, *htp-3* or *spo-11* mutants. The first model that we used was a previously developed strain that expresses the RNA binding protein, PAB-1, tagged to the fluorescent reporter, tagRFP (184). This protein tends to aggregate with age and the level of aggregation in the worm pharynx was found to be correlated with longevity and overall fitness (184). In order to understand if aggregation was altered in meiosis mutants, we categorized each animal as having low, medium, or high aggregation, as described in the original publication (184). These categories correspond to either less than 10 aggregates in the posterior pharyngeal bulb (low), more than 10 aggregates in the posterior bulb (medium), or more than 10 aggregates in the anterior bulb (high). As reported in the original publication, we also saw that wild-type animals had an increase in the number of animals with medium or high aggregation from Day 5 to Day 8 from about 5%-50% of animals to about 65%-85% of animals (Fig 8A-C, Appendix Table 9). In addition to these three previously published categories, we observed a fourth category in older animals: “diffuse” florescence where the aggregates lost discrete boundaries. Few animals belonging to this category were observed in wild type and rarely before Day 8. *dsb-2* mutants had a similar increase in worms with medium, high, or diffuse aggregation (Fig 8D-F, Appendix Table 9). The *spo-11* mutants had about 95% of animals with medium, high, or diffuse aggregation on Day 5, and in 2 of 3 trials, 100% of animals had medium, high, or diffuse aggregation on Day 8 (Fig 8G-I, Appendix Table 9). Surprisingly, 80%-100% of the *spo-11* mutants showed diffuse aggregation on Days 8 and Day 10 of adulthood, whereas only about 2% of wild-type animals did. *htp-3* mutant animals across three trials had an increase in the number of animals with medium, high, or diffuse aggregation from Day 5 to Day 8 from about 25%-60% to 60% - 80% (Fig 8J-L, Appendix Table 9). In *htp-3* mutants, 40-75% of animals displayed diffuse aggregation on day 12. The reasons underlying the production of the

'diffuse' aggregates remains unclear, however in *spo-11* and *htp-3* mutants, diffuse fluorescence manifests earlier and at higher rates. These data suggest that in at least two of the three meiotic mutants, age-related protein aggregation occurred prematurely and at high levels.

We also examined protein aggregation using a *C. elegans* strain expressing 35 Glutamine repeats (CAG repeats, or polyQ aggregation). PolyQ expansions have been identified as having a role in cellular toxicity during Huntington's disease, and researchers have expressed these repeats in model organisms, such as *C. elegans* to study further (185). It has been determined through genetic studies and studies in model organisms that 35-40 repeats causes proteotoxic stress (185). Previous research has identified that animals with 40 repeats (Q40) quickly develop aggregates within 1-2 days, Q29 animals show aggregates after a week, while animals with Q33 or Q35 develop aggregates in about 4-5 days (185). We asked if there was a change in the development of these polyQ aggregates in the meiosis mutants. The Q35 animals have Q35 tagged to YFP, under the promoter *unc-54*, which allows for expression in the muscle. With age, these proteins aggregate and can be visualized in the muscle of the animals. We found that there was no difference in the number or rate of aggregation formation in wild type and in *spo-11* mutants (Fig 8 M,N). We did not test the accumulation of polyQ 35 aggregates in the other meiosis mutants, *dsb-2* or *htp-3*.

Another method that we used to test the efficiency of the protein folding environment was a mutant with a known protein destabilizing mutation. *unc-52* encodes the worm homolog of mammalian Perlecan protein that is critical for myofilament function. A temperature sensitive mutation in *unc-52* results in age-dependent paralysis (159). We asked how knockdown of *dsb-2*, *htp-3*, or *spo-11* impacted the misfolding of UNC-52 as measured by the paralysis of the animal. We kept the animals at 15 °C and then shifted the animals to the 20 °C and checked for paralysis

every 4-12 hours. We found that animals with *dsb-2* or *spo-11* knocked down showed an early increase in the number of paralyzed animals, with about 80% of animals paralyzed after 2 days of adulthood (Fig 8O, Appendix Table 10).

Lastly, we also assessed protein homeostasis by measuring the expression levels of three heat shock proteins. Previously, the expression of genes encoding several chaperones/heat-shock proteins have been reported to increase with age in *C. elegans* (186). *hsp-16.2* encodes a heat shock protein predicted to enable unfolded protein binding activity when part of the heat-shock response (HSR) is upregulated. We asked if the meiotic mutants showed this upregulation prematurely compared to wild-type animals of a similar age. Using quantitative PCR (qPCR), we compared the *hsp-16.2* mRNA levels of Day 1 adults from three meiotic mutants with age-matched wild-type controls. We found that in Day 1 *htp-3* and *spo-11* mutants, there was an increase in *hsp-16.2* expression of 8- and 19-fold, respectively, compared to wild type (Fig 8P). We measured the expression of two other heat shock proteins *hsp-6*, which functions in the mitochondrial unfolded protein response (UPR_{mt}), and *hsp-4*, which regulates the endoplasmic reticulum unfolded protein response (UPR_{er}). *hsp-6* had 1.5- and 1.2 fold elevated expression in *spo-11* and *htp-3* mutants, respectively, compared to wild type (Fig 8Q). No differences were observed in *hsp-4* mRNA levels between the strains (Fig 8R). Overall, these experiments provided significant evidence that protein homeostasis was disrupted in the meiotic mutants and at an earlier age than wild type.

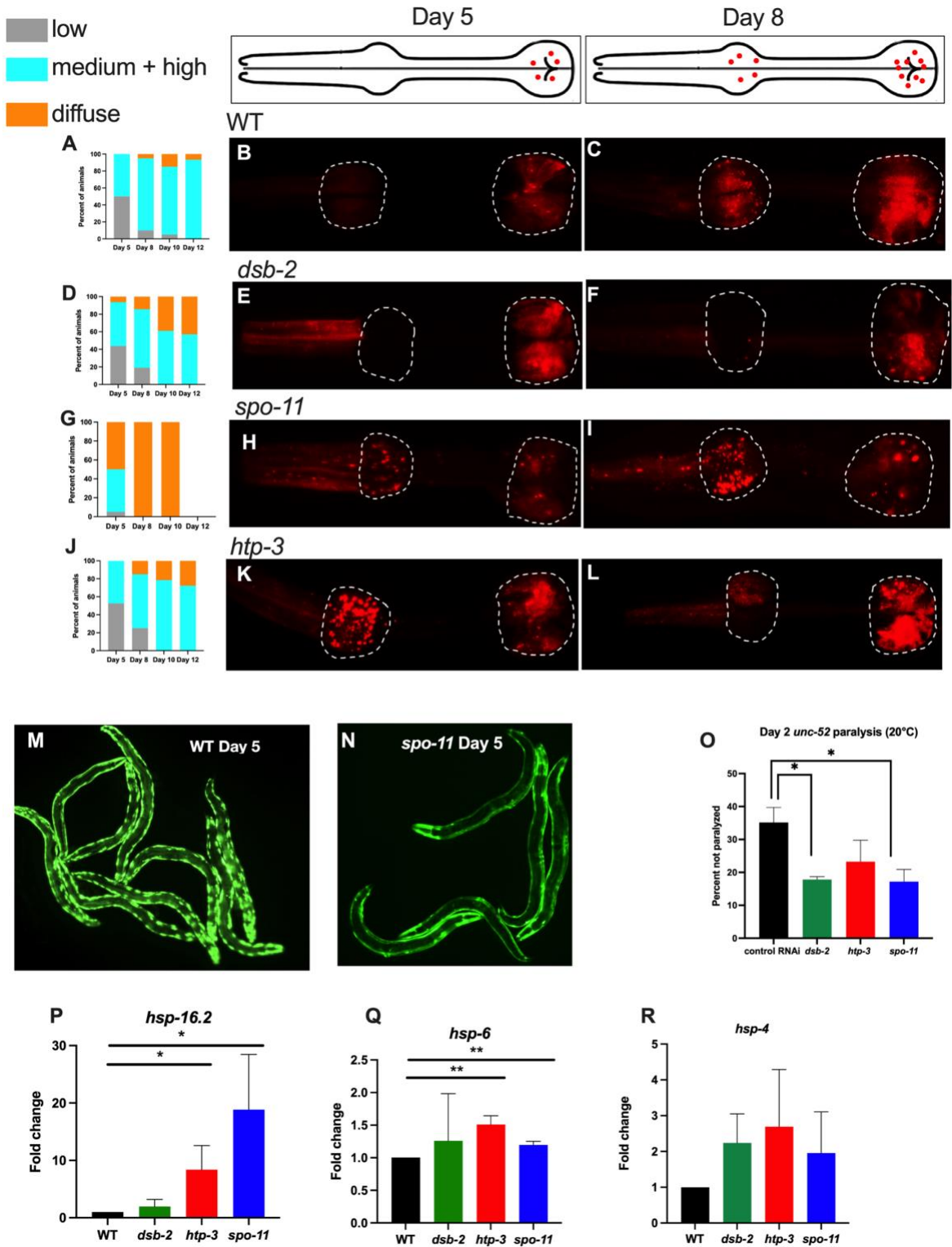


Figure 8: Protein homeostasis of *dsb-2*, *spo-11*, and *htp-3* mutants.

(A-L) Quantification of percent of animals in each category of aggregation levels with age. Low aggregation (grey) <10 aggregates in posterior pharyngeal bulb. Medium + high aggregation (blue) includes animals with >10 aggregates in posterior pharyngeal bulb or high >10 aggregates in anterior bulb. Diffuse aggregation (orange) animals with aggregates without clear boundaries. Data shown in one representative trial with 20 animals per strain per timepoint, other trials shown in supplemental table. Cartoon representation of aggregate levels in anterior and posterior pharyngeal bulbs in Day 5 and Day 8 animals. Representative images of Day 5 WT (B), *dsb-2* (E), *spo-11* (H), *htp-3* (K) animals in tagRFP::*pab-1* strain background. Representative images of Day 8 WT (C), *dsb-2* (F), *spo-11* (I), *htp-3* (L) animals in tagRFP::*pab-1* strain background. (M, N) Images of Day 5 WT animals or *spo-11* mutants in the background of *unc-54p::Q35::YFP* animals. (O) Percent of animals paralyzed after exposure to increased temperature of 20 °C for two days with control RNAi strain (L4440, black), *dsb-2*, (green), *htp-3* (red), or *spo-11* (blue) *knocked down*. Details about experiment are in the methods section. Data is combined from 2 biological replicates with 82-99 animals observed per strain per biological replicate. Statistical significance was calculated using one-tailed t test. (P-R): mRNA expression levels of *hsp-16.2* (P), *hsp-6* (Q), and *hsp-4* (R) in WT (black) *dsb-2* (green), *htp-3*(red), and *spo-11* (blue) mutants, statistical significances were calculated using a one-tailed t test, combined 3 biological replicates.

2.3 Discussion

Correlative evidence suggests a relationship between reproduction and aging; however, it is difficult to study the causative role of germline status on organismal aging. Here we used the model organism, *C. elegans*, and the germline-restricted process of meiosis to ask how mutations in meiosis impact aging. We found that overall, many mutations in meiosis reduce lifespan and specifically, mutations in *dsb-2*, *htp-3* and *spo-11* reduce healthspan in addition to lifespan. We also found that knockdown in the germ line of *dsb-2*, *htp-3*, or *spo-11* is sufficient to reduce lifespan. In addition to the many healthspan parameters we measured, such as tissue integrity,

muscle function, mobility, stress resistance, and gene expression changes, we also found that there was an early decline in protein homeostasis as measured by various models.

2.3.1 Mutations in meiosis impact lifespan

While genes involved in meiosis have been extensively studied to understand reproduction and their roles in meiosis, very few studies have examined how these mutations impact aging. However, genes involved in other aspects of the germ line, such as *glp-1*, have been extensively studied in terms of how germline stem cell arrest impacts somatic health (130). In addition to *C. elegans*, there is also evidence in flies that blocked oogenesis extends longevity (168). In humans and rodents, castration increases lifespan (13, 187), but there are also mutations in *C. elegans* that result in sterility which do not increase lifespan (130). Based on previous research, we found that while the majority of meiotic mutants impacting lifespan had a decrease in fertility, some mutants had very little impact on fertility (*exo-1*, *him-8*, *slx-1*) (162, 165, 167). According to the “Disposable Soma Theory of Aging”, animals that do not invest resources into reproduction invest energy and resources into somatic maintenance. Therefore, it is surprising that these mutants, which have reduced fertility and, in some cases, have below 5% viable progeny (*spo-11(me44)*, *spo-11(ok79)*, *dsb-1*, *rad-50*, *mre-11*, *rad-51*), reduced, instead of extended, lifespan (107, 109, 113, 163, 166)

Another process that has previously been found to impact aging and health is DNA break repair. Other studies have identified that mutations in DNA damage repair genes, including *brc-1* and *xpf-1*, which are involved in various DNA damage repair pathways such as homologous recombination, interstrand crosslink repair, and nucleotide excision repair, impair stress resistance

and reduce lifespans (169). Additionally, *exo-3*, an AP endonuclease, shortens lifespan and functions in the gonad as well as the soma (188). However, another study found that DNA damage in germ cells actually increases stress resistance in the soma (189). Previous research has identified that some mutants that we examined had altered numbers and persistence of DNA double-strand breaks, as measured by RAD-51 (*him-17*, *slx-1*, *exo-1*, *him-8*), while some mutants had either no breaks or reduced breaks (*htp-3*, *dsb-2*, *dsb-1*, *spo-11*, *rad-50*, *mre-11*) (108-110, 113, 162, 163, 167). Prior evidence suggested that apoptosis plays a role in oocyte quality; however, blocking apoptosis does not impact lifespan (56, 72). Mutants that reduced lifespan in this study had variable impacts on levels of apoptosis. Some mutants exhibited WT levels or decreased levels of apoptosis (*chk-2*, *spo-11*) and some mutants displayed increased levels of apoptosis (*mre-11*, *rad-50*, *rad-51*, *slx-1*) (113, 160, 163, 164, 166, 167). Interestingly, while the majority of the mutants that we tested impacted lifespan, there were some genes for which mutations had no impact on lifespan (*htp-1*, *rfs-1*, *rec-1*, *helq-1*, *rad-54*, *sws-1*, *rmh-1*) or had increased lifespan (*plk-2*). This could be due to redundancy in function in meiosis. We also did not test every gene that functions in meiosis. Instead, we focused on examining mutations in genes that are specific to meiosis or have predicted mostly germline expression, while also testing genes from a variety of different molecular processes in meiosis.

2.3.2 Knockdown of *dsb-2*, *htp-3* and *spo-11* in the germ line for the entirety of the animal's life decreases lifespan

We utilized three different methods to understand if meiotic genes in the germ line impact lifespan. Utilizing germline restricted RNAi, we found that knockdown of *dsb-2*, *htp-3*, and *spo-*

11 reduced lifespan. However, we found that lifespan was only reduced when the animals were exposed to the RNAi over the entire duration of the animal's life. When we asked if knocking down these genes during the young adult (L4) stage impacts lifespan, we did not find a lifespan change. This indicates that the stage for which the function of these genes is important for aging and might begin earlier than the start of reproduction. *C. elegans* first produce sperm and then switch to oogenesis in the L4 stage. Future studies could determine if the meiotic genes are impacting either oogenesis or spermatogenesis by also studying the impact of meiotic mutations in males or animals that only produce oocytes due to a genetic mutation.

We were surprised that a mutation in *htp-3* in the germline-less background had a small reduction in lifespan. We also found that *spo-11* mutants had a similar reduction in lifespan in the germline-less background as they do in wild type. We found this to also occur in the other germline-less background, *glp-4*, which has a normal lifespan. We used two different alleles of the *spo-11* mutation to rule out the possibility that this was a mutation specific result. Interestingly, we measured the expression level of *spo-11* in *glp-1* animals and found no gene expression in day 1 adults (Fig 7F). These results could indicate that the level of *spo-11* expression in *glp-1* animals is undetectable by qPCR or potentially that it is expressed before Day 1. This could be examined in the future by using another tool to quantify *spo-11* expression in germline-less animals such as smFISH or by conducting qPCR on L4 germline-less animals.

Utilizing the auxin inducible degradation system, we attempted to knockdown SPO-11 and DSB-2 in the germ line for either the entirety of the animal's lifespan, or just for adulthood. These results were confounded due to the impact of auxin and the AID strains on lifespan (discussed further in Chapter 5). Interestingly, we found that while knockdown of SPO-11 caused sterility, these effects were reversed later in the animal's reproductive span. This potentially could indicate

that the effects of auxin did not stretch beyond a few days. We addressed this by frequently transferring the animals to fresh plates containing auxin, and by increasing the concentration of auxin. However, this did not change the phenotype of return of fertility. This indicates that SPO-11 may not have been completely knocked down for the entirety of the animals' lifespan and that could explain why we did not see a change in lifespan.

2.3.3 Mutations in meiosis have variable impacts on healthspan and protein homeostasis

We found that there was not a single measure of healthspan for which all three meiosis mutants had a faster decline compared to wild type. Similarly, no single mutant we tested displayed healthspan deficits in all assays. This is similar to other short-lived and long-lived mutants, where some aspects of healthspan correlate with lifespan, while other measurements of healthspan do not (90, 91). Therefore, this seems to be a consistent feature of aging such that different characteristics or healthspan features decline at different rates. While we tested a variety of healthspan parameters, there are a number of aspects that we did not test such as gut autofluorescence, heat stress, oxidative stress and pathogen stress for *htp-3* and *spo-11*. Therefore, the possibility that all meiotic mutants share an impact on a healthspan measure cannot be overruled without further analyses.

2.3.4 Mutations in *dsb-2*, *htp-3*, and *spo-11* impact the status of protein homeostasis

We were interested in the mechanism through which mutations in meiosis impact aging and wanted to determine if any of the common hallmarks of aging were altered. Interestingly, the meiosis mutants, specifically *spo-11*, had variable impacts on the different models of protein

homeostasis we tested. We found that there was a premature decline in protein homeostasis using the PAB-1-aggregation model. Similarly, using the temperature sensitive *unc-52* protein-folding model, we observed protein homeostasis defects upon inactivation of *spo-11* and *dsb-2* mutant. However, there was no difference observed in the number of poly Q aggregates. The PAB-1::RFP protein homeostasis model is expressed in the pharynx of the animal. Both the PolyQ aggregation model is under the control of body wall muscle, *unc-54* promoter and *unc-52(ts)* is also expressed in the in the body wall muscle. Therefore, there may be differences in the tissue-specific impact of germline dysfunction on protein homeostasis in the soma. Additionally, protein homeostasis was slightly altered in *htp-3* mutants using the PAB-1 model and the *unc-52* model, whereas in *dsb-2* mutants, there was no significant change in the protein homeostasis models and the *dsb-2* mutants, other than the slight change to paralysis of the *unc-52(ts)* mutant. Therefore, even though lifespan and healthspan are altered in these mutant animals, there may be tissue specificity.

In conclusion, we found that while the “Disposable Soma Theory of Aging” predicts that meiotic mutations would increase lifespan, our data shows that this relationship is much more complex because we find mutations in meiosis that decrease lifespan. We found that three of these mutants, *dsb-2*, *htp-3*, and *spo-11*, have a decline in healthspan as well. Our data points to protein homeostasis as a potential mechanism through which disruption of meiosis impacts aging. In contrast to the predictions of the “Disposable Soma Theory of Aging”, animals which have mutations which alter reproduction to produce fewer progeny also have a shorter lifespan. In the future, it will be interesting to determine exactly how germline disruption is sensed by the animal to alter lifespan.

2.4 Methods

2.4.1 *C. elegans* strains and culture

Strains were maintained at 20 °C on nematode growth media (NGM) plates seeded with *E. coli* strain OP50. Strains were acquired from the CGC or shared by the Yanowitz lab. These strains include N2 (WT), DCL569 *mkcSi13* [*sun-1p::rde-1::sun-1* 3'UTR + *unc-119(+)*] II, CF1903 *glp-1(e2144)*, SS104 *glp-4(bn4)*, AGP285 *spo-11(ok79)/nT1;glp-1*, AGP310 *spo-11(me44);glp-4*, AGP304 *dsb-2(me96);glp-1*, AGP322 *htp-3;glp-1*, CA1421 *meIs8* [*pie-1p::GFP::cosa-1* + *unc-119(+)*] II. *ieSi38* [*sun-1p::TIR1::mRuby::sun-1* 3'UTR + *Cbr-unc-119(+)*] IV, CA1423 *meIs8* [*pie-1p::GFP::cosa-1* + *unc-119(+)*] II. *ieSi38* [*sun-1p::TIR1::mRuby::sun-1* 3'UTR + *Cbr-unc-119(+)*] IV, WS3455 *chk-2(gk212)*, QP1298 *rec-8/nT1;coh-3,4*, QP0455 *htp-1(gsk150)*, *htp-1(gk174);htp-2(tm2543)*, *htp-2(t2543)*, TY4986 *htp-3(y428)* *ccls4251* *l/hT2* [*bli-4(e937)* *let-?(q782)* *qIs48*] (I,III)., CA1230 *htp-3(tm3655)/hT2*, AV307 *syp-1(me17)/nT1g*, AC276 *syp-2(ok307)/nT1*, CV2 *syp-3(ok758)/hT2*, CA998 *ieDf2/mLs11*, CA151 *him-8(me4)*, RB1183 *prom-1(ok1140)*, RB1582 *plk-2(ok1936)*, AV157 *spo-11(me44)/nT1*, AV106, *spo-11(ok79)/nT1*, RB1562 *him-5(ok1896)*, CA1117 *dsb-1(we11)/nT1g*, QP938 *dsb-2(me96)*, KR5301 *rec-1(h2875)*, CB5423 *him-17(e2707)*, AV473 *rad-50(ok197)*, SSM72 *exo-1(tm1842)*, QP0900 *mre-11(iow)/nTg*, CA538 *rad-51(lg8701)/nTg*, *brc-1(tm1842)*, RB1279 *rfs-1(ok1372)*, VC531 *rad-54(ok615)*, TG1792 *helq-1(tm2134)*, QP1208 *sws-1(ea12)*, *rmh-1(ad92)*, *him-14(ok230)/mln1*, AV115 *msh-5(me23)/nTiU*, CV98 *him-18(tm2181)III/qCq* *dpy-19(e1259)glp-1(q339)nls189* III, TG1760 *mus-81(tm1937)*, TG1868 *slx-1(tm2644)*, VC193 *him-6(ok412)*, CB1487 *xpf-1(e1487)*. To generate double mutants we crossed genetic strains using standard genetic cross methods and

confirmed homozygous or heterozygous mutations using PCR or DNA sequencing. For strains which are balanced, animals were maintained as heterozygotes and homozygotes were picked for the experiment.

2.4.2 Lifespans

All lifespan experiments were conducted at 20 °C on *E. coli* OP50 plates, unless otherwise noted. Between 20 and 30 L4 hermaphrodites were transferred to 4-5 plates per strain. For experiments involving RNAi, NGM plates were supplemented with 1 mL 100 mg/mL Ampicillin and 1 mL 1 M IPTG (Isopropyl- β -D-1-thiogalactopyranoside) per liter of NGM. The plates were observed at 24–48 h intervals to record live, dead or censored (animals that were missing or bagged). For lifespan assays that included strains with the temperature sensitive *glp-1* or *glp-4* mutation, all eggs for that experiment were picked and transferred to 25 °C for 48 h. Then the animals were transferred to fresh plates for the lifespan and maintained at 20 °C. RNAi strains were acquired from Ahringer or Vidal Library (69, 70). The lifespan assays were analyzed using the program Online Application of Survival Analysis (OASIS 2) and Kaplan Meier survival curves to calculate P-values (190). GraphPad prism (version 9) was used to graph the results.

2.4.3 Thrashing assay

Thrashing assay was based on a previously optimized protocol (191). To measure thrashing rate with age, L4-stage larvae were picked and maintained at 20 °C. On day 2, adults were transferred to an unseeded NGM plate (to remove excess OP50 from the body of the animal), then

transferred one at a time into 1 ml of M9 media in an unseeded 3 cm plate. The animals were allowed to acclimate for 5 minutes in the liquid, then the number of body bends counted for a 30 second interval. A body bend constituted the movement of the head and/or tail beyond the midline of the body. Thrashing rate was measured similarly on animals aged to 5, 7, and 9 days of adulthood at 20 °C. Thrashing was quantified for 10-20 animals per timepoint per strain and repeated for a total of 3 biological replicates. Both strains were normalized to the average number of thrashes in 30 seconds for that biological replicate for Day 2. P values were calculated for each timepoint between the mutant strain and the wild-type strain using Student's t test.

2.4.4 Pumping assay

To measure pumping rate with age, L4-stage larvae were picked and maintained at 20 °C. On day 2, about 20 adults were transferred to a fresh NGM plate seeded with OP50. The animals were allowed to acclimate for about 2-5 minutes. The number of pumps in the terminal bulb was counted for 30 seconds using a counter for every 5 pumps. The count was repeated on the same worm 3 times. Pumping rate was measured similarly on animals aged 5, 7, and 9 days of adulthood at 20 °C. Pumping was quantified for 10-20 animals per timepoint per strain and then repeated for a total of 3 biological replicates. Both strains were normalized to the average number of pumps in 30 seconds, for that biological replicate for Day 2. P values were calculated for each timepoint between the mutant strain and the wild-type strain using Student's t test.

2.4.5 Learning

Chemotaxis response was measured from a sample size of 20-40 worms per trial and was repeated three times. Methods used for the study were adapted from similar past studies (Kauffman et al., 2010). L4's were picked and maintained at 20 °C until D1 of adulthood. The population was then split into 2 groups of trained with the chemotaxis response and untrained control group. To perform the chemotaxis assay, 20-40 worms were placed at the center of a 10 cm plate, and their migration towards butanone (1µL 1:10 butanone:ethanol) and ethanol control (1µL ethanol) at opposite ends of the plate (1 cm away from the edge) was recorded. For the pre-training group, this assay was done immediately, after washing the worms in M9 buffer. For the other group, training consists of a short starvation period, 1 hour in M9 buffer, and conditioning 50 min with food and butanone (1:10 butanone:ethanol) on inside of the plate lid. The worms were then washed and kept on plates with food and no butanone for 30 min. After this brief starvation period the chemotaxis assay was completed as defined above. The same protocol was then repeated with animals from day 5 of adulthood. After each chemotaxis assay was performed, the chemotaxis index (CI) is calculated for each group.

$$CI = \frac{(\# \text{ at Butanone} - \# \text{ at Control})}{(\text{Total } \# - \# \text{ at Origin})}$$

CI was then used to calculate the learning index a measure of short-term associative memory.

$$\text{Learning index} = \text{Post CI} - \text{Pre CI}$$

Learning index was then used to compare the short-term associative memory (STAM) of day 1 animals to day 5 animals. Both strains were normalized to the learning index for Day 1, for

that biological replicate. P values were calculated for each timepoint between the mutant strain and the wild-type strain using Student's t test.

2.4.6 Aggregation assay

Protocol based on method previously developed by Lechler et al., (184). Animals were picked at the L4 stage and maintained on OP50 NGM plates at 20 °C. On Day 2 of adulthood, animals were imaged using a Leica M250 FA stereoscope to count the number of aggregates per animal. The animals were quantified as have low (<10 aggregates), medium (>10 aggregates in posterior bulb), high (>10 aggregates in anterior bulb), or diffuse aggregation (aggregates not countable). About 20 animals per strain per timepoint were categorized with three biological replicates. For the representative images a Nikon A1r confocal microscope was used to take 0.2 µm Z -stacks.

2.4.7 Pathogen stress assays

Frozen stocks of *Pseudomonas aeruginosa* (PA14) were streaked out on an LB plate and incubated overnight at 37 °C. A single colony was inoculated in Kings Broth, which was incubated overnight in a 37°C shaker incubator. Then 25 uL of the culture was seeded on NGM plates, which were modified to have high peptone (0.35%). The plates were then incubated overnight at 37 °C and sat at room temperature for 24 hours before use. Between 20-30 L4 animals were added to each PA14 seeded plate at 25°C, and the animals were monitored for survival every 6-12 hours. The animals were marked as live, dead, or censored animals to account for the bagged, exploded

or missing animals. The animals were transferred to fresh plates every day of the experiment until they stopped laying eggs. The survival data was analyzed using the program Online Application of Survival Analysis (OASIS 2) and a Kaplan Meier survival curve was used to calculate P-values (190). GraphPad prism (version 9) was used to graph the results.

2.4.8 qPCR

RNA was isolated from three biological replicates of Day 1 adults. These animals were picked as L4's and maintained on OP50 *E. coli* plates at 20 °C until collected for RNA. On day 1 of adulthood, the animals were washed with M9 three times. Then TRIzol was added to the rinsed pellet and stored at -80 °C. The samples were then freeze thawed 6 times and the RNA was isolated using a standard phenol chloroform method with ethanol precipitation (192). The concentration was determined using a Nanodrop. RNA was treated with DNase 1 (Sigma Aldrich) and cDNA was made using the High Capacity RNA-to-cDNA kit (Applied Biosystems). qPCR reactions were made using PowerUP SYBR Green Master mix (Thermo Fisher), 0.25 M primers, and 10 ng cDNA and conducted using the CFX Connect Real-Time PCR detection system.

2.4.9 *unc-52* paralysis assay

Paralysis assay was adapted from the method as described in Ben-Zvi et al., (159) *unc-52(e669su250)* animals were maintained at 15 °C, then L4 animals were picked and moved to RNAi or OP50 control plates at 20 °C to monitor for paralysis. For each experiment, 50-110 animals were used per condition, and the experiment was blinded for the RNAi clone that was

seeded on each plate. Paralysis was monitored every 4 - 12 hours by prodding the animal with a pick. If the animal did not immediately respond and move across the plate, the animals was marked as paralyzed. GraphPad prism (version 9) was used to graph the results for the percent of animals that were paralyzed at a specific timepoint and student's t-test was used to calculate P-value.

2.4.10 Generation of *dsb-2* RNAi clone

To generate the RNAi clone to knockdown *dsb-2*, PCR was used to amplify the region of interest (Appendix Table 15). The PCR product was then run on a gel, the single band was excised from the gel and purified using QIAquick gel extraction kit (ID: 28704). The fragment was then ligated into the L4440-TA vector (provided by Mainpal Rana, Yanowitz lab) using the NEBNext Quick Ligase Reaction kit (cat # E6056S). After verifying the sequence, the plasmid was transformed into HT115.

3.0 Meiotic mutants exhibit prematurely-aging transcriptional profiles

3.1 Introduction

One of the classical theories of aging, the “Antagonistic Pleiotropy Theory”, posited that aging was a consequence of evolutionary positive selection for genes that are beneficial to younger reproducing organisms but become detrimental to older ones (7). This theory ascribes a significance to age-related gene regulation that has also been supported by subsequent discoveries on the genetic regulation of aging. Hence, there has been intense interest in documenting the transcriptional changes that are associated with age across species, including in worms and individual human tissues. Studies investigating age-related gene expression changes have indicated that up to 30% of the *C. elegans* transcriptome may in fact changes with age (193). While the global transcriptional changes are not completely understood, there are some functional categories of genes that are known to be dysregulated with age in *C. elegans*. These transcriptional changes include differential expression of actin related genes, stress response, lipid metabolism and genes associated with cell death (73, 193). In addition to studying transcriptional changes that occur during normal aging, there has also been extensive research on the gene expression changes associated with long-lived and short-lived *C. elegans* mutants. This includes a mutation in *glp-1*, which is essential for germline proliferation. *glp-1* mutants are sterile and have a 60% increase in lifespan, which is specific to loss of the proliferating germline stem cells (128, 130). These mutants have been extensively studied to understand the underlying transcriptional changes associated with longevity. The transcriptional changes associated with the *glp-1* mutation include a shift in lipid

metabolism, autophagy, stress resistance and proteasomal degradation (138). Therefore, previous research has demonstrated that germline mutations can have a broad impact on somatic gene expression, including determinants of longevity.

Following our discoveries, that mutations in many different steps of meiosis decrease lifespan and diminish healthspan features, we investigated the underlying mechanisms causing this accelerated aging. We continued to focus on *dsb-2*, *spo-11* and *htp-3*, the three genes whose detailed lifespan and healthspan phenotypes we had documented so far. As described below, we applied large scale RNA sequencing to map the transcriptomes of these meiotic mutants and found transcriptional changes that were significantly shared between them as well as unique to each. Strikingly, the transcriptional changes associated with these mutations resembled changes observed in both older *C. elegans* and in genes differentially expressed with age in humans. Finally, using previously published datasets, as well as the results from our RNA sequencing study, we identified 10 genes which are differentially expressed with age in wild-type animals, and in *spo-11* and *htp-3* mutants. These represent homologs of human genes which change in expression with age. Overall, this study adds to our evidence that mutations in meiosis affect the normal aging of *C. elegans*.

3.2 Results

3.2.1 The meiotic mutants share significant fractions of their transcriptomes

We utilized RNA sequencing (RNAseq) to map the transcriptomes of the three mutants: *spo-11*, *dsb-2*, and *htp-3*. We chose these mutant animals because of their distinct roles in meiosis, together with our observations of the impact on aging from these mutants. Day 1 adults of the three mutant animals and wild-type animals were collected in three independent biological replicates for RNA isolation, library preparation and sequencing (75 bp single end reads). The resulting raw sequencing data was analyzed using two independent pipelines that are regularly used in our lab, the Galaxy pipeline and the CLC Genomics Workbench (194). The final lists of differentially expressed genes (DEGs) were derived from the CLC analysis with a cut off 2 fold change and a p value of <0.05 (Supplemental Table S1-6). We found that *spo-11* mutants had the most differentially regulated genes, with 7,654 genes upregulated, referred to as SPO-11 UP and 3,584 genes downregulated, referred to as SPO-11 DOWN. *htp-3* mutants had the second most differentially expressed genes, with 4,730 genes upregulated (HTP-3 UP) and 1,666 genes downregulated (HTP-3 DOWN). And *dsb-2* mutants had the fewest differentially expressed genes, with 106 genes upregulated (DSB-2 UP) and 91 genes downregulated (DSB-2 DOWN). We found that *htp-3* mutants shared 86% of their transcriptomes with *spo-11* mutants (4069/4730 UP, 1430/1666 DOWN; $P < 0.0001$, $P < 0.0001$) (Fig. 9). Additionally, despite the small number of DEGs identified in *dsb-2* mutants, it was striking that 63 of 106 DSB2-UP genes were also upregulated in both *spo-11* and *htp-3* mutants (Fig. 9).

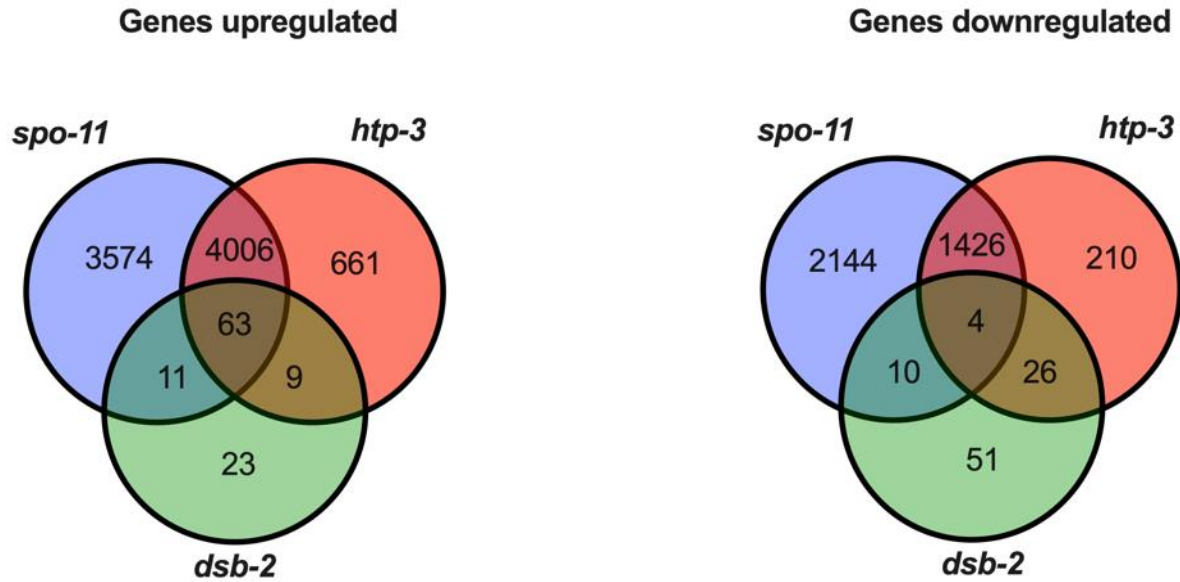


Figure 9: Differentially expressed genes in meiosis mutants.

(A) Number of genes upregulated in Day 1, *spo-11(me44)*, *htp-3*, and *dsb-2* mutant animals with overlapping number of genes shown between genotypes. (B) Number of genes downregulated in Day 1, *spo-11(me44)*, *htp-3*, and *dsb-2* mutant animals with overlapping number of genes shown between genotypes.

Using DAVID and WormBase Gene Expression Analysis to identify enriched functional categories, we found specific gene ontology (GO) terms that were differentially regulated in the three meiosis mutants (<https://wormbase.org/tools/enrichment/tea/tea.cgi>) (<https://david.ncifcrf.gov/>). In *dsb-2* mutants, the upregulated genes were enriched for GO terms associated with extracellular matrix, cell adhesion, and basement membrane organization, whereas, the downregulated gene list was enriched for the terms development and growth. The GO Terms associated with genes upregulated in *htp-3* mutants included immune response, biotic stimulus and response to other organisms and the downregulated terms include development and reproduction (Fig 10). GO terms associated with upregulated genes in *spo-11* mutants included immune response and transmembrane transport, whereas, the downregulated category was

enriched for development and reproduction functions (Table S1-6). We also examined the tissue-distribution of the DEGs identified using a previously described prediction pipeline and found them to be enriched for expression in the germ line and reproductive systems, expectedly, but also tissues such as the nervous system, intestine, hypodermis and muscle (Table S1-6) (195).

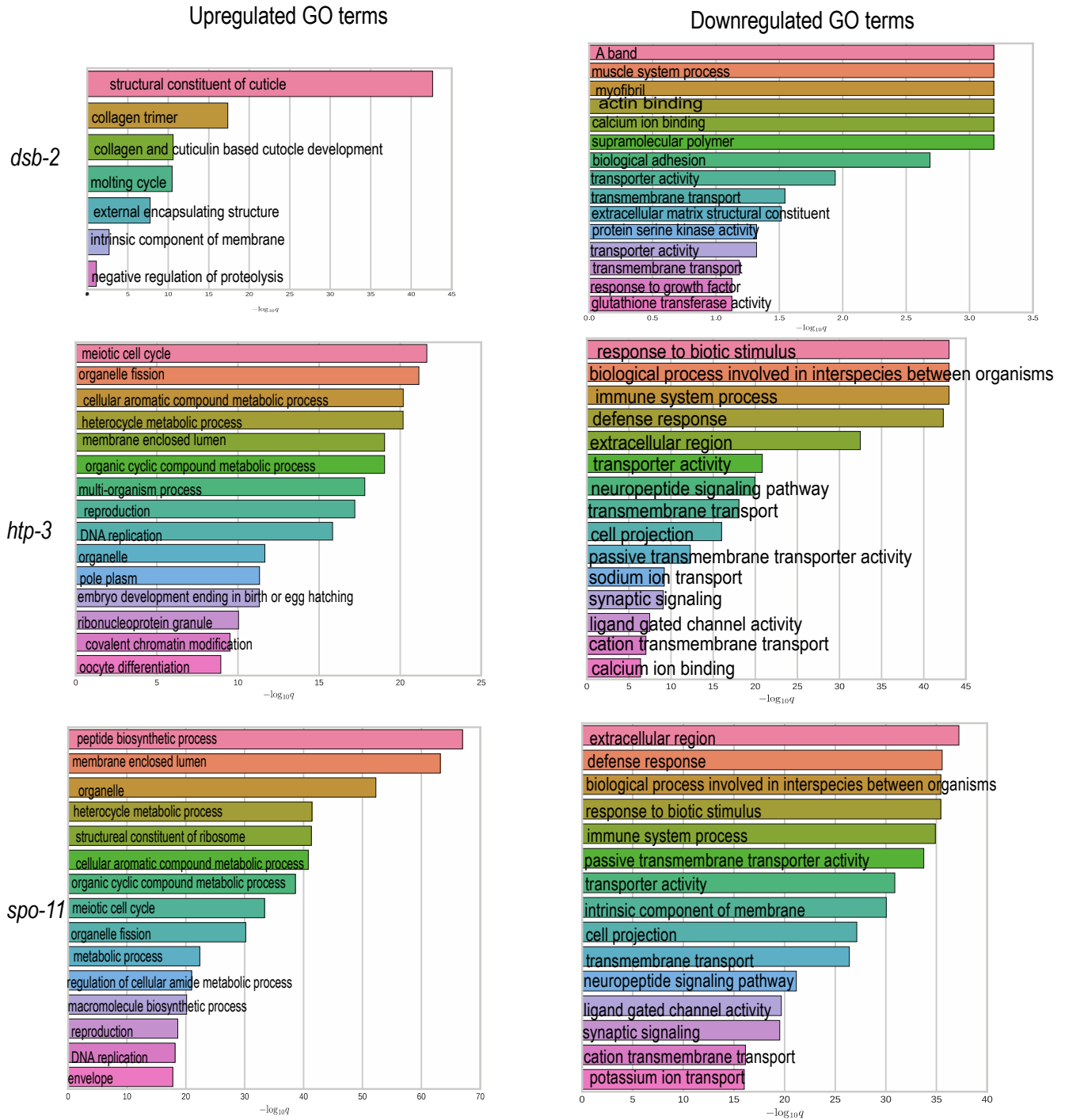


Figure 10: GO terms associated with differentially regulated genes in *dsb-2*, *htp-3* and *spo-11* mutants

WormBase Gene enrichment analysis was used to determine GO terms. The top significant terms are displayed

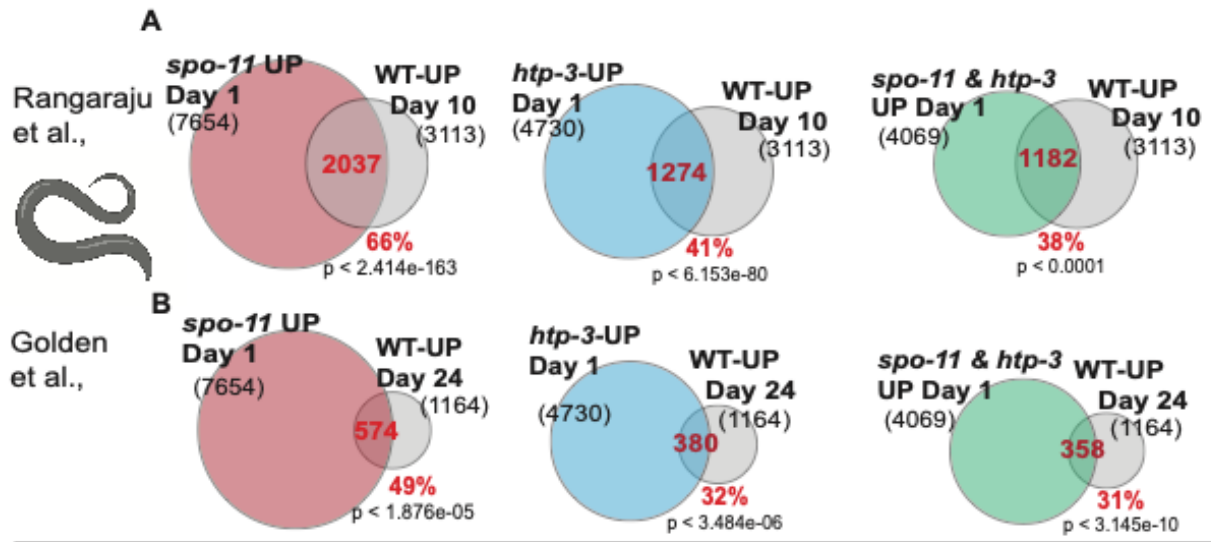
3.2.2 Genes differentially regulated in *htp-3* and *spo-11* mutants share similarities with *C. elegans* aging

We next asked if the gene-expression changes induced by meiotic dysfunction had any relevance to normal aging. We hypothesized that the mutants would exhibit a prematurely-aged transcriptional profile i.e., during young adulthood show high expression of genes normally upregulated in old WT animals. Due to the very small size of the *dsb-2* mutants' DEG list, we used the *spo-11* and *htp-3* mutants' DEGs for these analyses. We compared the transcriptomes of Day 1 *spo-11* and *htp-3* mutants with the datasets from Rangaraju et al., that comprises a comprehensive RNAseq map of the transcriptomic changes observed during middle age (Day 5) and aging (Day 10) in WT animals (196). We found significant overlap in SPO-11 UP with genes upregulated in Day 10 wild-type animals (66%, 2037/3113 genes, $p < 2.414e-163$) as well as SPO-11 DOWN and Day 10 wild-type downregulated genes (44% 1259/2834 genes, $p < 3.152e-182$) (Fig 11A, Table S10,11). We also found significant overlap when we compared the differentially expressed genes in the *htp-3* mutants, with 41% of the genes upregulated in Day 10 wild-type animals also upregulated in *htp-3* mutants (1274/3113 genes, $p < 6.15e-80$) and 26% (727/2834 genes, $p < 1.919e-177$) of the genes downregulated in Day 10 wild-type animals also downregulated in *htp-3* mutants (Fig 11A, Table S10,11) (196). The overlap with the middle-aged, Day 5 wild-type transcriptomes was also significant: 55% (1413/2548, R factor: 1.3, $P < 5.190e-40$) and 42% (1069/2548, R factor 1.6, $P < 3.40e-72$) for SPO11-UP and HTP3-UP gene lists, respectively (Table S9-12). Lastly, genes downregulated in Day 1 *spo-11* and *htp-3* mutants were also highly enriched for genes which were downregulated at Day 10 in wild-type animals with 40%

(1113/2834, R factor: 1.9, $P < 7.363e-145$) and 26% (727/2834, R factor: 2.7, $p < 1.919e-177$) overlap, respectively (Table S10,11).

We also compared our datasets to another *C. elegans* study in which Golden et al., conducted a microarray analysis on worms that were collected at 7 different times throughout the lifespan of the animal, from Day 4 to Day 24 (193). They identified sets of genes which increased for the entirety of the animals' lifespan as measured until Day 24. We found that of the 1164 genes upregulated with age in wild-type animals, 574 genes were also upregulated in *spo-11* mutants (49%, $p < 1.876e-05$) (Fig 11A). Similarly, we found that the *htp-3* mutants shared 380 genes that were also upregulated throughout the animal's lifespan (32% $p < 3.484e-06$) (Fig 11B). Between the genes upregulated in both *spo-11* and *htp-3* mutants, 358/1164 genes or 31% were also upregulated in the Golden et al., study of genes which increase throughout lifespan ($p < 3.145e-10$) (Fig 11B) (193). Through comparison with these two studies of the transcriptome of aging *C. elegans*, we identified that there are shared gene expression changes in *spo-11* and *htp-3* mutants that are associated with chronological as well as physiological age.

Overlap with Aging Worm Transcriptome



Overlap with Aging Human Transcriptomes

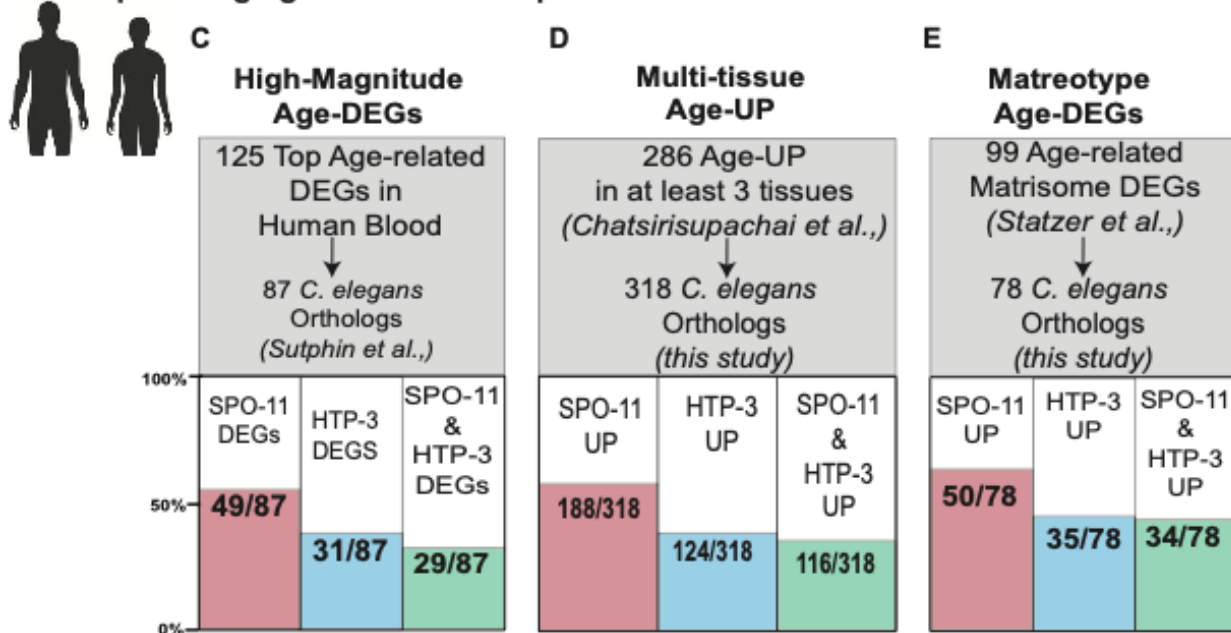


Figure 11: Comparison of differentially-expressed genes in *spo-11* and *htp-3* mutants with aging studies.

(A) Number of differentially regulated genes which are shared between this study of genes upregulated in Day 1 *spo-11* mutants, *htp-3* mutants, and genes shared between *spo-11* and *htp-3* mutants with genes upregulated in Rangaraju et al., study of genes upregulated in wild-type Day 10 animals. (B) Number of differentially regulated genes which are shared between this study of genes upregulated in Day 1 *spo-11* mutants, *htp-3* mutants, and genes

shared between *spo-11* and *htp-3* mutants with genes upregulated in Golden et al., study of genes upregulated with age up to Day 24 of adulthood. (C) Number of genes differentially regulated in our study of *spo-11*, *htp-3*, and *htp-3* and *spo-11* overlap, which overlap with the *C. elegans* orthologs of genes differentially regulated with age in human blood from Sutphin et al., study. (D) Number of genes upregulated in our study of SPO-11 UP, HTP-3 UP, and HTP-3 and SPO-11 UP overlap, which overlap with the *C. elegans* orthologs of genes upregulated with age in at least three tissues up regulated in human aging from Chatsirisupachai et al., study. (E) Number of genes upregulated in our study of SPO-11 UP, HTP-3 UP, and HTP-3 + SPO-11 UP overlap, which overlap with the *C. elegans* orthologs of matrisome genes upregulated with age in humans with age from Statzer et al., study.

3.2.3 Genes differentially regulated in *htp-3* and *spo-11* mutants share similarities with genes differentially regulated in human aging

We were also curious to determine if the gene expression changes we observed in the *htp-3* and *spo-11* mutants resembled the genes expression changes associated with human aging. Sutphin et al., analyzed gene expression changes using the Cohorts of Heart and Aging Research in Genomic Epidemiology (CHARGE) dataset of genes, which are differentially expressed with age in human peripheral blood (178). From that dataset, they wanted to determine if the *C. elegans* homologs of these genes had a functional impact on aging of the animal. First, they converted the top 125 genes that were differentially expressed with age to the predicted *C. elegans* ortholog using WORMHOLE and identified the corresponding 87 *C. elegans* orthologs (178). Of the 87 genes, we found 49 genes also in the *spo-11* mutant DEGs, 31/87 genes in the *htp-3* DEGs, and 29/87 genes differentially regulated in both *spo-11* and *htp-3* mutants (Fig 11C). Interestingly, Sutphin et al., identified five genes with the greatest impact on lifespan through RNAi knockdown, which included *kynu-1*, *iglr-1* (upregulated in *spo-11* and *htp-3*), *tsp-3* (upregulated in *spo-11* and *htp-3*),

rcan-1 (upregulated in *spo-11*), and *unc-36* (upregulated in *spo-11*) (178). Additionally, we were interested in the larger CHARGE dataset of 1,497 differentially expressed genes with age in human peripheral blood (197). We converted these human genes into *C. elegans* orthologs using OrthoList (<http://ortholist.shaye-lab.org/>) and found 1534 *C. elegans* genes corresponding to 891 of the 1497 human genes. The larger number of *C. elegans* genes may be due to gene duplication events in the *C. elegans* genome as well as the inclusion of orthologs with partial matches (198). Remarkably, 917 of the 1534 genes (60%, R factor 0.9 P < 3.458e-04) were included in the *spo-11* DEGs (Table S11,12), while 533 (35%, R factor 1.0 P < 0.094) were included in the *htp-3* DEGs (Table S9,10); 442 were shared between *spo-11* and *htp-3* DEGs (29%, R factor 0.9 p < 0.018) (Table S9-12). Therefore, in addition to sharing a similar transcriptome to differentially expressed genes in *C. elegans* with age, the *htp-3* and *spo-11* mutants also share a transcriptomic signature with the orthologs of genes associated with aging in human peripheral blood and some genes with functional significance to *C. elegans* lifespan.

While the CHARGE data set consists of the transcriptomic changes observed in human blood, we were also interested if there were other tissues that shared a transcriptomic signature with *htp-3* and *spo-11* mutants. In a previous study, Chatsirisupachai et al., analyzed gene-expression datasets from the Genotype-Tissue Expression (GTEx) project to identify age-related DEGs from 26 human tissues (199). We identified the top 10 tissues (adipose, adrenal, blood vessel, brain, colon, lung, muscle, ovary, prostate, and uterus) that had an extensive list of genes with an age-related increase in expression. The strongest overlaps were observed between genes SPO11-UP and HTP3-UP gene lists and those upregulated in muscle, ovary, prostate, adipose, uterus and the brain (21% to 32%) (Table S13). Interestingly, we found that there were very few genes that were common among the human homologs of the genes downregulated in *spo-11* or

htp-3 mutants and the genes downregulated in various human tissues with age (<10%) (Table S13). Since the number of upregulated genes varied between the top 10 tissues, we looked for genes that were commonly upregulated between the tissues. We found that 286 genes were upregulated between at least 3 of the 10 tissues (Table S13). *C. elegans* orthologs were identified for 135 of these 286 genes and resulted in 318 *C. elegans* orthologs (<http://ortholist.shaye-lab.org/>). Of those 318 *C. elegans* orthologs, 188 genes were upregulated in *spo-11* mutants (59%, R factor 1.4, $p < 1.086e-08$) and 124 genes upregulated in *htp-3* mutants (39%, R factor 1.5, $p < 1.348e-06$). We found that of the genes that were jointly upregulated between *spo-11* and *htp-3* mutants, 116 of the 318 genes were also upregulated in the different tissues (36%, R factor 1.6 $p < 4.021e-08$ (Fig 11D).

A recent study collected gene expression changes with age in humans and utilized multiple datasets with focus of identifying age-related changes in matrisome i.e., genes encoding extracellular matrix (ECM) components (200). 1027 protein encoding genes comprise the human matrisome (200). Many of these genes or functional categories associated with these genes are implicated in healthy aging. As such, this category of genes has been of interest to those studying aging. Statzer et al., identified 99 genes that encompass the human aging ‘matreotype,’ or matrisome genes that change with age (92 upregulated, 7 downregulated). Again, using OrthoList (<http://ortholist.shaye-lab.org/>), we identified, 78 *C. elegans* orthologs (corresponding to 59 of the 99 genes). Of these, 50 (64%, R factor 1.5, $P < 1.870e-04$), 35 (45%, R factor 1.7, $P < 4.598e-04$) and 34 (44%, R factor 1.9, $P < 4.854e-05$) were also upregulated in Day 1 *spo-11* mutants, *htp-3* mutants, and the common genes between both mutants, respectively (Fig 11E, S9-12). Overall, the transcriptional profiles of genes upregulated in *spo-11* and *htp-3* mutants showed similarities with three studies mapping age-related gene expression changes in a variety of human tissues. This

suggests that the prematurely-aging meiotic mutants may express a molecular signature shared with human aging.

In addition to determining if there was a broad transcriptional change, we also wanted to identify if there were specific genes that were upregulated in our dataset as well as the published datasets of genes upregulated with age in *C. elegans* and humans. We found that between the Rangaraju et al., Golden et al., and CHARGE dataset of genes, there are differentially expressed in *spo-11* and *htp-3* mutants, there is a common “aging signature.” This includes, 10 *C. elegans* genes encoding proteins involved in extracellular matrix and collagen binding (*spon-1* and *mua-3*), transport activity (*pgp-8*, *sulp-4*, *ncr-2*), a cytochrome P450 (*cyp43A*), ribosomal (*rpl-11.2*) and calpain genes (*clp-4*) and predicted transmembrane protein, (*tag-120*), and an annexin (*nex-2*).

3.3 Discussion

3.3.1 Differences between *spo-11*, *dsb-2*, and *htp-3* mutant transcriptomes

Overall, we found that *dsb-2*, *htp-3*, and *spo-11* mutations, which have predicted germline-restricted expression, impact the genes expressed in the entirety of the animal. Interestingly we found that there were few genes that were differentially expressed in *dsb-2* mutants, even though we found striking effects of the *dsb-2* mutation on both lifespan and healthspan. DSB-2 is involved in the double-strand break formation during meiotic recombination, as an accessory factor to SPO-11. However previous research has suggested that the *dsb-2* mutation has an age-related defect in meiosis (109). We sequenced the transcriptome of Day 1 animals, but in the future, it may be

interesting to sequence the transcriptome of older animals, considering the previous evidence from other reports that *dsb-2* mutants have more pronounced meiotic defects later in the reproductive ages.

While *spo-11* and *htp-3* shared DEGs, they also exhibited uniquely differential expressions that are likely due to their specific roles in meiosis. HTP-3 functions during the formation of the synaptonemal complex to pair and physically attach the homologous chromosomes together (125). SPO-11 functions to form the DNA double-strand break during meiotic recombination (107). There may be some compensatory mechanisms or other proteins involved in pairing and synapsis which prevents an even more widespread transcriptional change in *htp-3* mutants. There are four HORMA domain proteins in *C. elegans* that have overlapping function; however, HTP-3 has a specific role in sister chromatid cohesion and break formation (101). Interestingly, we found that in animals with a *spo-11* mutation, there was a drastic shift in the transcriptome. This could be because *spo-11* encodes an enzyme that is uniquely responsible for forming a double-strand break during meiosis. Considering that the break formation has a pivotal role during meiosis and thus reproduction, there may be a checkpoint or other signal triggered upon *spo-11* mutation.

3.3.2 Gene expression changes from meiosis mutations are widespread in different tissues

Our tissue-enrichment prediction analyses showed that the DEGs were expressed in the germ line as expected, but there was also enrichment in tissues such as the intestine, muscle and hypodermis. This is interesting because many of the regulators of *glp-1* longevity are required to be expressed in the intestine (134). In future studies, it will be interesting to conduct RNA Seq experiments on the soma and the germ line separately. It will also be interesting to determine if

there is a specific tissue that is responsible for signaling between the germ line and the soma to cause the aging defects we observed in the meiosis mutants. In the future, tissue specific rescue or knockdown experiments will be required to determine the somatic tissues that coordinate meiotic signals from the germ line to influence lifespan and healthspan.

3.3.3 Similarities between human aging transcriptomes and *spo-11* or *htp-3* mutant transcriptomes

While the length of life varies greatly between organisms, there are similarities between organisms in terms of the underlying mechanisms of aging. This includes the “hallmarks of aging” as well as some of the longevity pathways discovered in *C. elegans*, which have been found to be conserved in mice and humans (149, 201). Previous research has found similarities in the functions of the genes differentially regulated with age in multiple organisms (197, 202, 203). Therefore, it is not surprising to find an overlap between genes differentially regulated in *htp-3* and *spo-11* mutants and human homologs differentially regulated with age.

Finally, we identified 10 *C. elegans* genes that were commonly dysregulated with age in multiple published studies as well as in *spo-11* and *htp-3* mutants, including *pon-1*, *mua-3*, *pgp-8*, *sulp-4*, *ncr-2*, *cyp43A*, *rpl-11.2*, *clp-4*, *tag-120*, and *nex-2* (196, 197, 204). Some of these genes are related to pathways or functions known to impact longevity. For example, the extracellular matrix has been previously identified to have an important functional role in aging of multiple organisms (205). Additionally, *rpl-11.2* is required for upregulation of PHA-4 to respond to nucleolar stress, and *pha-4* has an important role in caloric restriction-induced longevity in *C. elegans* (206). This list of 10 genes also includes genes with known impacts on neurodegenerative

disorders including *clp-4*, which has been found to be upregulated in a transgenic *C. elegans* model used to study Alzheimer's Disease (207). Similarly, *ncr-2* encodes the *C. elegans* homolog of the human NPC1, which is implicated in a neurodegenerative disorder (208). One of the other genes identified, *pgp-8*, has been identified as having a role in endoplasmic reticulum stress resistance, which may contribute to the aging phenotype we observed (209). In the future, it would be interesting to determine if and how any of these genes have a functional impact on lifespan or healthspan of normal animals.

In conclusion we found that the genes differentially regulated in meiotic mutants share similarities with the genes differentially regulated in older *C. elegans* and the homologs of genes differentially regulated with age in humans. This supports our finding that meiotic mutations impact the length of the life and the physiological changes that occur during aging, as measured through healthspan. Thus, meiotic dysfunction not only shortens lifespan and diminishes healthspan, but also induces gene expression profiles highly similar to those of older animals.

3.4 Methods

3.4.1 *C. elegans* strains and culture

Strains were maintained at 20 °C on nematode growth media (NGM) plates seeded with *E. coli* strain OP50. Strains were acquired from the CGC or shared by the Yanowitz lab. These strains include N2 (WT), *TY4986 htp-3(y428) ccIs4251 I/hT2 [bli-4(e937) let-?(q782) qIs48] (I,III),*

AV157 *spo-11(me44)/nT1*, QP938 *dsb-2(me96)*. For strains which are balanced, animals were maintained as heterozygotes and homozygotes were picked for the experiment.

3.4.2 RNA Seq

RNA was isolated from Day 1 adults of 3 biological replicates of wild type, *dsb-2(me96)*, *htp-3(y428)*, and *spo-11(me44)* mutants, which were collected in Trizol (Invitrogen) and stored in the -80°C freezer until RNA was isolated. To isolate RNA, the animals were freeze thawed 6 times, and the RNA was harvested using the TRIzol method (192). RNA was checked for quality and concentration using the Agilent Tapestation and Qubit Fluorometry. The library was prepared using the NEBNext Poly(A) mRNA Magnetic Isolation module (E7490) and NEBNext Ultra II RNA Library Prep Kit for Illumina (E7775) with NEBNext Multiplex Oligos for Illumina. The DNA libraries were checked for quality and quantified using Tapestation D1000 and Qubit High Sensitivity. The sequencing was run on Illumina NextSeq 500 with 75 bp single end reads at the Health Sciences Sequencing Core at UPMC Children's Hospital of Pittsburgh. The sequencing data was then analyzed using CLC Genomics Workbench (version 21) using the RNA-Seq pipeline. Differentially regulated genes were filtered for significance using a fold change of greater than 2 and a p value <0.05.

3.4.3 Transcriptome analysis

Enrichment analysis was conducted for each gene group using Wormbase Gene Set Enrichment Analysis tool <https://wormbase.org/tools/enrichment/tea/tea.cgi>

<http://nemates.org/MA/progs/representation.stats.html> was utilized to determine if there was significant overlap between data sets of differently expressed genes. This program took into account the size of the gene lists for both sets, the size of the overlapping gene list and the size of the *C. elegans* genome. <http://ortholist.shaye-lab.org/> was used to convert the *C. elegans* genes lists into human homologs or the human genes into *C. elegans* homologs (210).

4.0 Molecular mechanisms underlying meiotic control of aging

4.1 Introduction

The studies described in this chapter address key mechanistic questions: What genes and molecules are involved in signaling meiotic dysfunction to the soma and subsequent lifespan reduction? Do the transcriptional changes associated with meiosis disruption have any functional relevance to organismal lifespan? *C. elegans* studies have not only been instrumental in identifying genetic pathways that modulate aging, they have also revealed fundamental knowledge about the cellular processes that these pathways act on to change the animal's lifespan. In mutants of *daf-2*, that encodes the worm insulin and IGF-1 receptor, extended lifespan is reliant upon the FOXO transcription factor, DAF-16, as well as other pro-longevity factors such as HSF-1, SKN-1 and others. Mapping the transcriptomes in *daf-2* mutants dictated by DAF-16 and other such factors led to the discovery of downstream targets that included stress response genes, antimicrobial peptides, protein homeostasis- and metabolic- factors (76). Functional studies with these downstream effectors helped establish that these pro-longevity factors acted by increasing stress resistance, immune-resistance, improving lipid homeostasis and proteostasis (76). Since then, studies in other model organisms and systems have consolidated evidence for these processes' roles in lifespan and health maintenance. This paradigm applies to dietary restriction (DR), i.e, increased longevity due to reduced caloric intake, a pro-longevity intervention found to be conserved across species (80). Notably, DR has been found to modulate these pathways to not only extend *C. elegans* lifespan, but also in *Drosophila*, mouse, and dog (76). Similarly, our laboratory,

and other studies, have used transcriptional profiling coupled to functional analysis of long-lived germline-less mutants to identify genes and processes that promote longevity upon GSC loss (139). While the studies described in the previous chapter demonstrated that one such process, protein homeostasis, is impaired in meiotic mutants, it remained unclear how this impairment is brought about and what the functional relevance of the transcriptional changes could be.

As described in the previous chapters, we identified that mutations in *C. elegans* meiosis impact aging. We focused on three genes, *spo-11* and *dsb-2*, which encode proteins that function during meiotic recombination to form double-strand breaks, and *htp-3*, which encodes a component of the synaptonemal complex. We identified that mutations in these three genes reduce lifespan and accelerate healthspan. We also found that *spo-11* and *htp-3* mutants share similarities to the gene expression profile of aging worms as well as the human homologs associated with human aging. But it remains mostly unknown through what mechanism or pathway mutations in *dsb-2*, *spo-11*, or *htp-3* were influencing somatic aging. Here, we explored the functional relevance of the DEGs identified through these mutants' RNAseq study. These studies also led us to explore the role of protein chaperones in this lifespan paradigm. We found that *rpn-6.1*, that encodes a subunit of the 19S proteasome, undergoes differential expression in meiotic mutants and its overexpression partially rescued the reduced lifespan of *spo-11* mutants (148). Additionally, we identified two genes, *irlid-53* and Y19D10A.5, as potential anti-longevity genes. These two genes were upregulated in short lived mutants, *dsb-2*, *htp-3*, and *spo-11*, and have predicted roles as transmembrane transporters. We found that inactivation of *irlid-53* and Y19D10A.5 extended the lifespan of wild-type animals underscoring their functional relevance to longevity.

4.2 Results

We wanted to understand how mutations in meiosis signal to the rest of the animal to impact somatic aging. To answer this question, we investigated the status of one common mechanism of aging, protein homeostasis (149). We utilized both the RNA sequencing data that we had previously collected as well as previous publications that studied pathways between the germ line and soma (211, 212).

4.2.1 Germline-to-soma signaling in meiotic mutants does not require coelomocyte endocytosis

While attempting to identify a potential mechanism responsible for signaling from the germ line to the soma, we asked if a physical link between the two tissues is necessary for the lifespan change. *C. elegans* have six coelomocytes that sit in the pseudocoelomic cavity and are physically connected to both the intestine and the germ line. They are phagocytic, taking up soluble macromolecules, and their function has been compared to the function of macrophages (213). CUP-4 is required for efficient endocytosis by *C. elegans* coelomocytes (214). A recent study from Lan et al., discovered that CUP-4 is required for germline to intestinal signaling to regulate UPRmt, AMPK, and lifespan (211). We hypothesized that if a similar endocytic pathway signaled meiotic dysfunction to the intestine, then preventing signal transmission by inactivating *cup-4* would rescue meiotic mutant's lifespan. However, we found that the *spo-11* mutants had the same shortened lifespan on control RNAi as on *cup-4* RNAi (Fig 12A, Appendix Table 11). This suggests that a physical connection between the germ line and soma may not be necessary for the

lifespan reduction in *spo-11* mutants, although this remains to be tested in the other mutants and by other means of coelomocyte elimination.

4.2.2 Wnt signaling does not impact the lifespan of *spo-11* or *htp-3* mutants

We next asked if longer range signaling molecules were responsible for the somatic aging in the meiosis mutants. A recent paper by Calculli et al., identified that a germline mutation impacted somatic protein aggregation and functioned through the Wnt ligand, *egl-20* (212). We hypothesized that since the meiotic mutations also impacted somatic protein homeostasis, the Wnt signaling pathway could be a potential mechanism for this role. *C. elegans* have five Wnt ligands that are encoded by *egl-20*, *lin-44*, *cwn-1*, *cwn-2*, and *mom-2* (215). Based on our RNA sequencing results, we found that *egl-20*, *lin-44*, and *cwn-2* were upregulated in *spo-11* and *htp-3* mutants, while *cwn-1* was upregulated in *spo-11* only. Expression of these genes remained the same in *dsb-2* mutants. Therefore, we asked if mutations in *spo-11* and *htp-3* functioned through a similar pathway to impact lifespan by knocking down these Wnt ligands in *spo-11* and *htp-3* mutants. We found that neither *cwn-1* nor *cwn-2* knockdown had an impact on lifespan in either the wild-type background or the *spo-11*, or *htp-3* mutants (Appendix Table 12). However, knockdown of *egl-20* increased the lifespan of wild-type animals in 2 of 3 trials and increased the lifespan of *spo-11* mutants in 1 of 3 trials; it had no impact on *htp-3* mutant lifespans (Fig 12B, Appendix Table 12). Thus, Wnt signaling did not appear to be a shared signaling pathway activated in all meiotic mutants, it may play a role in *spo-11* mutants.

4.2.3 Genes commonly upregulated in meiosis mutants impact lifespan

We also utilized the results from RNA sequencing to identify potential signals or pathways that have a functional impact on lifespan. First, we focused on the genes that were commonly upregulated in all three meiosis mutants and we identified 63 genes. This included genes with roles in cytoskeleton (*ttn-1*, *unc-54*, *che-3*, *myo-1*, *myo-2*, *epi-1*, *lam-2*, *ketn-1*), matrix/adherence (*him-4*, *dig-1*, *mua-3*), transmembrane transporters/signaling (*irl-53*, *irl-35*, Y19D10A.5, Y19D10A.4, F56A4.10, C01B4.8, C01B4.7, T26H5.9, *unc-2*, *nca-2*), and genes involved in known longevity pathways (*lrp-2*, *lrp-1*, *sma-1*), cytoskeleton (*ttn-1*, *unc-54*, *che-3*, *myo-1*, *myo-2*, *epi-1*, *lam-2*, *ketn-1*), matrix/adherence (*him-4*, *dig-1*, *mua-3*), transmembrane transporters/signaling (*irl-53*, *irl-35*, Y19D10A.5, Y19D10A.4, F56A4.10, C01B4.8, C01B4.7, T26H5.9, *unc-2*, *nca-2*), and genes previously identified for roles in known longevity pathways (*lrp-2*, *lrp-1*, *sma-1*). We hypothesized that if these genes were upregulated in short-lived mutants and performed anti-longevity functions, then inactivating them in wild-type animals could extend the lifespan of the latter. From the original list of 63 upregulated genes, we selected 12 based on previous roles in longevity pathways, predicted membrane and signaling functions and conservation with human proteins. Two genes encoding putative membrane proteins with insulin-receptor-like domains, *irl-35* and *irl-53*, were included in this group. Two of the four coding transcripts of *irl-53* share an identical sequence with the *irl-35* transcripts. We expected that the RNAi clone we created inactivated the expression of both genes simultaneously. Whole-life RNAi increased wild-type lifespan ~10-20% significantly and consistently (Table 2). Similarly, RNAi of Y19D10A.5, another putative membrane protein, also reliably increased by 10%-21% (Fig 12C, Appendix Table 13). Upon inactivation of C01B4.7, predicted to encode a transmembrane

transporter, lifespan was extended 11% but this was inconsistent across trials (Table 2) Knockdown of some genes tested did not impact lifespan (*mua-3*, *unc-2*, *F45D3.4*, and *lrp-2*), whereas, some shortened lifespan upon whole-life RNAi (*sma-1*, *ketrn-1*, *F39C12.1*, *him-4*, and *dig-1*) (Table 2). We wanted to distinguish if the gene knockdown was impacting aging or development by knocking down the genes beginning in adulthood, starting by L4. Similar to when we knocked down these genes during the entirety of the lifespan, we found that knockdown of the genes with predicted developmental roles, *sma-1*, *ketrn-1*, *dig-1*, and *him-4*, again reduced lifespan.

Table 2: Genes upregulated in *spo-11*, *dsb-2*, and *htp-3* mutants

Upregulated genes which were knocked down by RNAi are shown. The lifespan results for both knockdown during whole life or adult only are represented as a percent change in lifespan. Lifespans which were significantly different than wild type are highlighted based on if they increased lifespan (green) or decreased lifespan (red)

Genes upregulated by <i>dsb-2</i> , <i>htp-3</i> , <i>spo-11</i>	Impact on Lifespan (whole life)	Impact on lifespan (adult only)	Description
<i>irld-53</i>	9.97%, 21.2%	N.S.	Insulin/EGF Receptor L Domain protein; DD neuron-enriched putative insulin-binding protein
C01B4.7	10.61%, N.S.	N.S.	predicted to have transmembrane transporter activity, similar to human Anion/sugar transporter, solute carrier family 17
<i>ketrn-1</i>	-19.50%	-13.84%	enables actin filament binding activity
Y19D10A.5	9.46%, 20.4%, N.S.	N.S.	predicted to have transmembrane transporter activity - <i>daf-12</i> target
<i>him-4</i>	-80.72%	-21.93%	extracellular matrix structural constituent
<i>dig-1</i>	-15.71%	-7.80%	predicted to enable calcium ion binding activity
<i>sma-1</i>	-30.93%	-15.78%	Ortholog of human voltage-gated Ca ²⁺ channel, CACNA1A. Negative regulator of TGF β pathway
<i>unc-2</i>	N.S.	N.S.	predicted to have voltage-gated calcium channel activity, negative regulation of transforming growth factor beta receptor signaling
<i>mua-3</i>	N.S.	N.S.	Transmembrane protein linking epithelial cytoskeletal intermediate filaments in to cuticle
<i>lrp-2</i>	N.S.	N.S.	Ortholog of human LRP1 (Low Density Lipoprotein receptor related protein 1) implicated in Keratosis Pilaris Atrophicans & Alzheimer's Disease; Membrane-localized.
F39C12.1	-19.71%	N.S.	Ortholog of human GATOR complex protein MIOX involved in cellular response to amino acid starvation & positive regulation of TOR signaling
F45D3.4	N.S.	N.S.	Uncharacterized DAF-7 interactor; Impacts dauer development; HIF independent hypoxia-induced factor

4.2.4 Protein homeostasis genes are differentially regulated in *spo-11* and *htp-3* mutants and overexpression of *rpn-6.1* rescues *spo-11* mutant lifespan

Considering the earlier indication that somatic protein homeostasis was altered in *spo-11* and *htp-3* mutants, we identified several proteostasis genes that were downregulated in *spo-11* and *htp-3* mutants. We were particularly interested in *rpn-6.1*, encoding a subunit of the 19S proteasome, and chaperonin encoding genes, *cct-8* and *cct-2*, for their identified role in germline control of longevity (148, 154, 216). Overexpression of RPN-6.1 and CCT-2 extends lifespan at higher temperature (25 °C) and over expression of CCT-8 extends lifespan at normal temperature (20 °C) (148, 216). We found that while knockdown of *spo-11* in the control strain (*myo-3p::GFP*) decreased lifespan from 12% - 26.5 % consistent with our mutations studies, knockdown of *spo-11* in the RPN-6.1 overexpressing animals caused no lifespan shortening (Fig 12D, Appendix Table 14). Overexpression of neither CCT-2 nor CCT-8 did not provide similar protection against *spo-11*(RNAi)-induced lifespan shortening (Appendix Table 14).

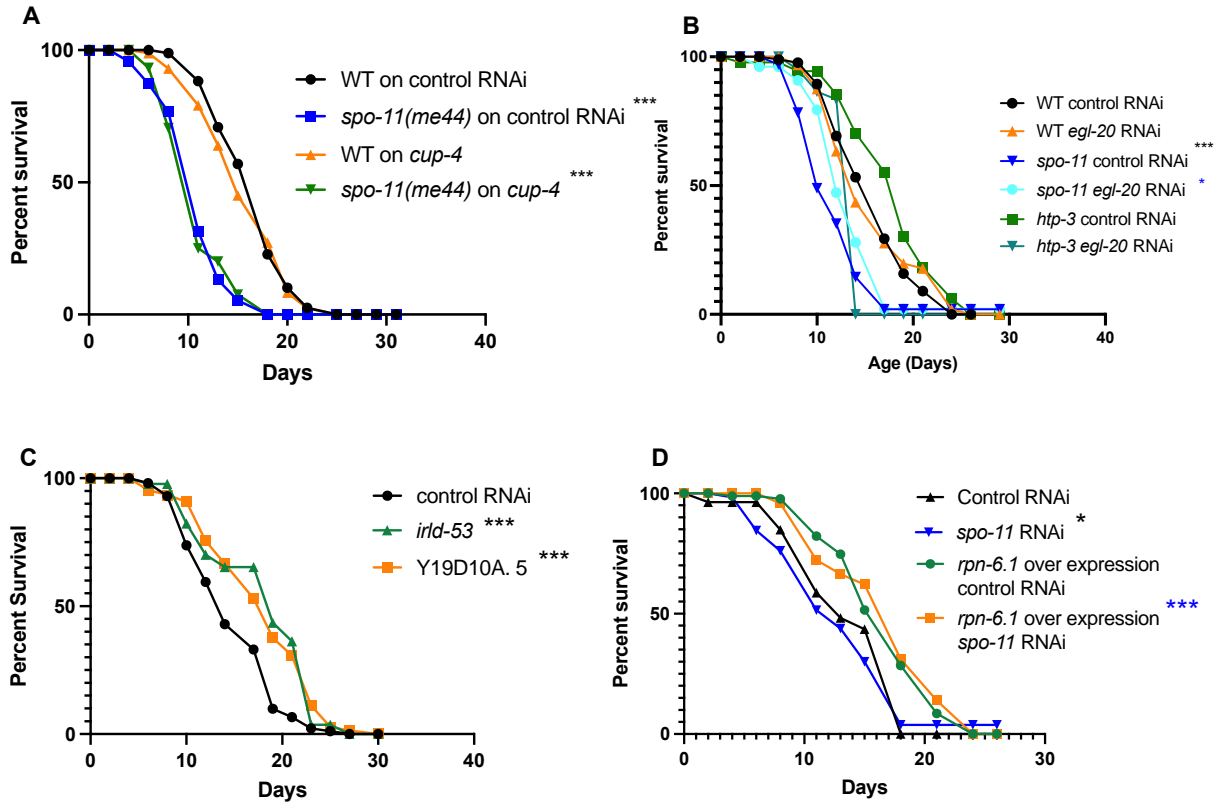


Figure 12: Mechanisms of meiotic gene control of aging

(A) Lifespan of *cup-4* RNAi knockdown WT on L4440 RNAi ($m=16.59 \pm 0.4$) $n = 80/98$ P vs *spo-11(me44)* <0.0001 , *spo-11(me44)* on L4440 $n = 43/47$ ($m= 11.01 \pm 0.46$) P vs N2 <0.0001 , WT *cup-4* RNAi $n = 85/91$ ($m= 15.76 \pm 0.45$) P vs N2 =0.439, *spo-11(me44) cup-4* RNAi $n = 43/45$ ($m= 11.11 \pm 0.47$) P vs N2 <0.0001 , P vs *spo-11(me44)* L4440 RNAi <0.0001 . (B) Lifespan of Wnt ligand knockdown WT on L4440 RNAi ($m=15.88 \pm 0.53$) $n = 55/93$, WT on *cwn-2* RNAi ($m=16.52 \pm 0.36$) $n = 84/113$, P vs N2 L4440 = 0.4299, WT on *egl-20* RNAi ($m=15.79 \pm 0.67$), $n= 52/111$ p vs N2 L4440 = 0.9184, *spo-11(me44)* on L4440 RNAi $n=51/78$ ($m=11.63 \pm 0.42$) p vs N2 L4440 < 0.0001 , *spo-11(me44)* on *cwn-2* RNAi $n=38/89$ ($m=12.04 \pm 0.35$) p vs N2 L4440 < 0.0001 , p vs *spo-11* on L4440 = 0.3516, *spo-11(me44)* on *egl-20* RNAi $n=50/78$ ($m=13.04 \pm 0.42$) p vs N2 L4440 < 0.0001 , p vs *spo-11* on L4440 = 0.035, *htp-3* on L4440 RNAi $n=20/46$ ($m=17.84 \pm 0.99$) p vs N2 L4440 =0.0658, *htp-3* on *cwn-2* RNAi $n=19/33$ ($m=19.51 \pm 0.74$) p vs N2 L4440 = 0.0007, p vs *htp-3* on L4440 = 0.2223, *htp-3* on *egl-20* RNAi $n=17/43$, ($m=14.79 \pm 0.45$) p vs N2 L4440 =0.1861, p vs *htp-3* on L4440 = 0.5898. (C) Lifespan of *irdl-53* and Y19D10A.5

knockdown. WT on L4440 RNAi ($m=14.83 \pm 0.47$) $n = 92/120$, WT on Y19D10A.5 RNAi ($m=17.85 \pm 0.6$) $n = 76/116$, P vs WT L4440 = 0.0001, WT on *irld-53* RNAi ($m=17.97 \pm 0.62$), $n= 59/95$ p vs N2 L4440 <0.0001 Other trials shown in supplemental data. (D) Lifespan of overexpression of *rpn-6.1 myo-3p::GFP* on L4440 RNAi ($m=14.49 \pm 0.6$) $n = 54/80$, *myo-3p::GFP* on *spo-11* RNAi ($m=12.75 \pm 0.64$) $n = 38/59$, P vs *myo-3p::GFP* L4440 = 0.0403, *sur-5p::rpn-6* on L4440 RNAi ($m=16.68 \pm 0.47$), $n= 73/89$ p vs *myo-3p::GFP* on L4440 = 0.2074, *sur-5p::rpn-6* on *spo-11* RNAi ($m=16.87 \pm 0.57$), $n= 67/78$ p vs *myo-3p::GFP* on *spo-11* RNAi <0.0001. Survival data analyzed using Kaplan Meier curve shown as mean lifespan (m) \pm standard error of the mean n =observed/total * p <0.05, **p <0.001, ***p <0.0001

4.3 Discussion

4.3.1 Wnt signaling does not affect lifespan in meiosis mutants

The Wnt signaling pathway has many important, conserved roles in development in regulating biological processes. Wnts are secreted lipid modified glycoproteins and trigger many functions during development such as cell fate, cell migration and polarity (217). We examined the role of Wnt signaling in meiotic mutants' longevity because Wnts were identified to be upregulated in two of our three meiotic mutants and because previous research has reported that knockdown of Wnt ligands has varying impacts on wild-type lifespan in worms. Lezzerini and Budovskaya found that *cwn-2* mutants have increased lifespan, and *egl-20* mutants and animals with *lin-44* knocked down both have decreased lifespan (218). Of the five Wnt ligands, *egl-20* has been found to be the only ligand that can function across long distances within the worm (219). *egl-20* has also found to be involved in signaling from the nervous system to other tissues to induce the mitochondrial unfolded protein response (220). However, our preliminary mechanistic studies

did not find a unifying role for Wnts in meiotic mutants' lifespan regulation. Considering that Calcutti et al., identified that the Wnt ligand *egl-20* was responsible for signaling from the germ line to impact somatic protein homeostasis, it would be interesting in future studies to determine if knockdown of *egl-20* altered the early decline in protein homeostasis that we observed in both *spo-11* and *htp-3* mutants (212).

4.3.2 *irld-53* and Y19D10A.5 knockdown increase lifespan

Interestingly some of the genes that were commonly upregulated in the *dsb-2*, *htp-3*, and *spo-11* mutants had known roles or encoded proteins in functional categories that have known roles in longevity. This includes genes involved in cytoskeletal integrity (*ttn-1*, *unc-54*, *che-3*, *myo-1*, *myo-2*, *epi-1*, *lam-2* and *ketn-1*). It has been previously demonstrated that genes involved in cytoskeletal integrity and integrin-signaling complexes, which have an important role in cytoskeletal organization and cell adhesion, also have roles in longevity and stress response (221, 222). The genes that we identified, which were upregulated in *spo-11*, *dsb-2*, and *htp-3* mutants, and whose knock down increased lifespan, were *irld-53*, *irld-35* and Y19D10A.5. These genes are predicted to encode transmembrane transporter proteins, which is interesting in terms of the functional role in signaling to impact lifespan. *irld-53* and *irld-35* encode an insulin/EGF-Receptor L domain protein; *irld-53* has been reported to be enriched in the neurons and intestine whereas *irld-35* expression domains remain unknown (223). Y19D10A.5 encodes a substrate transporter like protein and has been identified as a DAF-12 target (224). *daf-12* encodes a nuclear hormone receptor that modulates insulin-IGF-1 signaling as well as gonadal signals to regulate lifespan (128). A mutation in *daf-12(m20)* extends longevity of *daf-2* mutants (225). Considering that these

two genes were found to be upregulated in *dsb-2*, *htp-3*, and *spo-11* mutants, and have roles in both lifespan and insulin signaling, it would be interesting to further investigate the status of the insulin signaling pathways in the meiosis mutants. Pertinently, we found that the DAF-2 agonist, *ins-7*, was upregulated in *spo-11* and *htp-3* mutants. Previously it has been determined that reduction of *ins-7* extends *C. elegans* lifespan (226).

4.3.3 Overexpression of RPN-6.1 extends *spo-11* lifespan

One of the hallmarks of aging is decline in protein homeostasis (149). Therefore, it is not surprising that some of the genes that were differentially expressed in *dsb-2*, *htp-3*, and *spo-11* mutants included genes with roles in protein homeostasis. However, the identification of central chaperone-encoding genes with established pro-longevity functions, *rpn-6.1*, *cct-2* and *cct-8*, suggested a specific modulation of proteostasis in response to meiotic dysfunction. Indeed, we found that overexpression of *rpn-6.1* increased the lifespan in animals with *spo-11* knocked down. Previous research identified that overexpression of *rpn-6.1* increased proteasome activity in wild-type animals and increased the lifespan of wild-type animals at higher temperatures of 25°C, but not at 20°C (148). Vilchez et al., also identified that DAF-16 regulates *rpn-6.1* expression in germline-less animals to promote longevity (148). In the future, we could investigate the role of DAF-16 in response to meiotic mutations to determine if this transcription factor regulates the somatic aging program.

Overall, these studies suggest that the genes upregulated and downregulated upon meiosis impairment have functional roles in lifespan determination. Study of genes upregulated in *dsb-2*, *htp-3*, and *spo-11* identified anti-longevity candidates and a potential role for insulin signaling.

Study of genes downregulated in these mutants revealed the importance of a proteasomal subunit, RPN-6.1, in this process. The partial rescue of *spo-11* mutants' lifespan upon overexpression of the regulatory proteasomal subunit RPN-6.1, which has key roles in modulating somatic proteasome activity in the context of the long-lived germline-less *C. elegans* is pertinent. Further investigation into these known longevity pathways will reveal details of the mechanism through which meiotic mutations accelerate somatic aging.

4.4 Methods

4.4.1 *C. elegans* strains and culture

Strains were maintained at 20 °C on nematode growth media (NGM) plates seeded with *E. coli* strain OP50. Strains were acquired from the CGC and strains generously shared by the Vilchez lab. These strains include N2 (WT), AGD614 *uthEx633 [myo-3p::GFP]*, AGD598 *uthEx557 [sur-5p::rpn-6 + myo-3p::GFP]*, AGD597 *uthEx556 [sur-5p::rpn-6 + myo-3p::GFP]*, DVG9 *ocbEx9[myo3p::GFP]*, DVG47 *ocbEx47[psur5::cct-2, pmyo3::GFP]*, *ocbEx47[psur5::cct-2, pmyo3::GFP]*.

4.4.2 Lifespans

All lifespan experiments were conducted at 20 °C on NGM plates seeded with *E. coli* OP50 plates unless otherwise noted. Between 20 and 30 L4 hermaphrodites were transferred to 4-5 plates per strain. The plates were observed at 24–48 h intervals to record live, dead, or censored (animals

that were missing or bagged). For experiments involving RNAi, NGM plates were supplemented with 1 mL 100 mg/mL Ampicillin and 1 mL 1 M IPTG (Isopropyl- β -D-1-thiogalactopyranoside) per liter of NGM. RNAi strains were acquired from Ahringer or Vidal Libraries (69, 70). The lifespan assays were analyzed using the program Online Application of Survival Analysis (OASIS 2) and Kaplan Meier survival curves to calculate P-values (190). GraphPad prism (version 9) was used to graph the results.

4.4.3 Generation of *irld-53* RNAi clone

To generate the RNAi clone to knockdown *irld-53*, PCR was used to amplify the region of interest (Primers in Appendix Table 15). The PCR product was then run on a gel, the single band was excised from the gel and purified using QIAquick gel extraction kit (ID: 28704). The fragment was then ligated into the L4440-TA vector (provided by Mainpal Rana, Yanowitz lab) using the NEBNext Quick Ligase Reaction kit (cat # E6056S). After colony PCR and verified through sequencing, the plasmid was transformed into HT115.

5.0 Auxin treatment increases lifespan in *C. elegans*

This chapter is a modified version of Loose and Ghazi, 2021, Biology Open DOI: [10.1242/bio.058703](https://doi.org/10.1242/bio.058703). Licensed under a Creative Commons Attribution 4.0 International License.

5.1 Introduction

C. elegans has been a very useful model organism, in part because of the ease of gene knockdown or mutation. Gene knockdown through RNA interference (RNAi) was first discovered in *C. elegans*, and two libraries have been made that cover 94% of the genome (70, 227, 228). Recent advances have adapted CRISPR gene editing, condition gene depletion using FLP and CRE recombinases, the Q-system, and cGAL in *C. elegans* for conditional gene knockdown (68). These systems have their advantages to easily target knockdown of any gene, but disadvantages include off target effects. For example, the mutant *C. elegans* strain, *rrf-1*, which encodes a gene essential for amplification of the dsRNA signal in the soma, has been used to for restricting RNAi knockdown to only the germ line. But upon further investigation, researchers have found that there is also knockdown of the target genes in the soma (229). There have also been off-target cross reaction effects when the dsRNA shares sequence similarity with the target mRNA, which can occur if 25 nucleotides are shared between multiple genes (230, 231). While many of these systems target mRNA, there are instances where protein knockdown is the preferred tool. This includes

instances where the targeted gene is maternally deposited, or if there are temporal specific needs to observe rapid protein knockdown in, for example, an essential developmental gene (68)

Recently, Auxin inducible degradation (AID) has been developed by borrowing a system from plants that allows for a tissue specific, temporal specific, and reversible method for protein knockdown. The system was adopted from *Arabidopsis*, which uses the substrate recognition F-box protein TIR1, a component of an Skp1-Cullin-Fbox (SCF) E3 ubiquitin ligase complex. In the presence of auxin, TIR1 binds a short 44 amino acid degron sequence to target for protein degradation (Fig 13A). By tagging specific proteins with the degron sequence in tandem with expression of TIR1 driven by a tissue specific promoter, this results in tissue specific degradation that can be reverse upon removal of auxin (232). The AID system had previously been adapted for use in yeast and mammalian cell culture, but *C. elegans* were the first metazoan system where this method of protein degradation was successfully used (232).

The plant hormone indole-3-acetic acid, or auxin, functions in many developmental processes such as cell division, elongation and differentiation and was also identified as the stimulus that causes plants to move towards light (233). During the development of the AID system for use in *C. elegans*, researchers verified that both TIR1 expression as well as exposure to auxin do not impact normal development, fertility, or viability at normal 20 °C temperature and lower concentrations of auxin (1 mM) (232). Considering the benefits of using the AID system for understanding gene function in a temporal and spatially controlled manner, it would be useful in the context of aging. It has not been previously studied if and how auxin and expression of TIR1 impacts *C. elegans* over a longer period of time, during the aging process.

We were interested in understanding how germline integrity impacts somatic aging, and used previously developed AID *C. elegans* strains to target two germline-specific, meiosis

proteins, and a control strain with GFP tagged to the degron sequence (174, 232). We found that exposure to auxin for the entirety of the animal's lifespan increased the length of life, independent of beginning the auxin exposure at the egg stage or at the beginning of adulthood, L4. We also found that animals expressing TIR1 and the degron tagged proteins increased lifespan in two of the three strains. Therefore, it is important to exercise caution when using tools and interpreting data for studying effects on longevity.

5.2 Results

5.2.1 Auxin exposure beginning during development or beginning during adulthood extends lifespan

The AID system has been utilized in *C. elegans* for spatial and temporal specific protein knockdown. This system has been adapted in *C. elegans* by tagging the protein of interest with a degron tag in conjunction with TIR1 expression in the tissue of interest. Upon exposure of the animal to auxin, via supplementation of IAA to the NGM plates, the protein of interest is degraded. In order to determine if long-term exposure could be utilized for aging studies, we conducted experiments with control animals with different auxin concentrations to first determine the baseline impact on lifespan. We transferred the animals to fresh NGM plates containing either 1 mM or 4 mM auxin every 48 hours until the end of reproduction (Day 5). We found that exposing WT animals to either 1 mM auxin or 4 mM auxin for the entirety of the animals lifespan extended

lifespan during three of four trials, with two trials significantly extending lifespan (29% and 34%) (Fig 13B, C)

We wanted to understand if the increased longevity was due to developmental defects originating from auxin exposure. To test this, we kept the animals on normal NGM plates until the beginning of adulthood larval stage 4 (L4) and then transferred to plates containing auxin. We found that lifespan was significantly increased upon adult only exposure to 1 mM auxin by 37% and 7% (Fig 13D). Adult only exposure to 4 mM auxin extended lifespan by 12% but was not statistically significant (Fig 13E). Additionally, we found that transferring the animals to fresh NGM plates containing auxin more frequently (every 24 hours), did not further increase the lifespan in both the 1 mM or 4 mM auxin and exposure beginning as adult or eggs (Table 3).

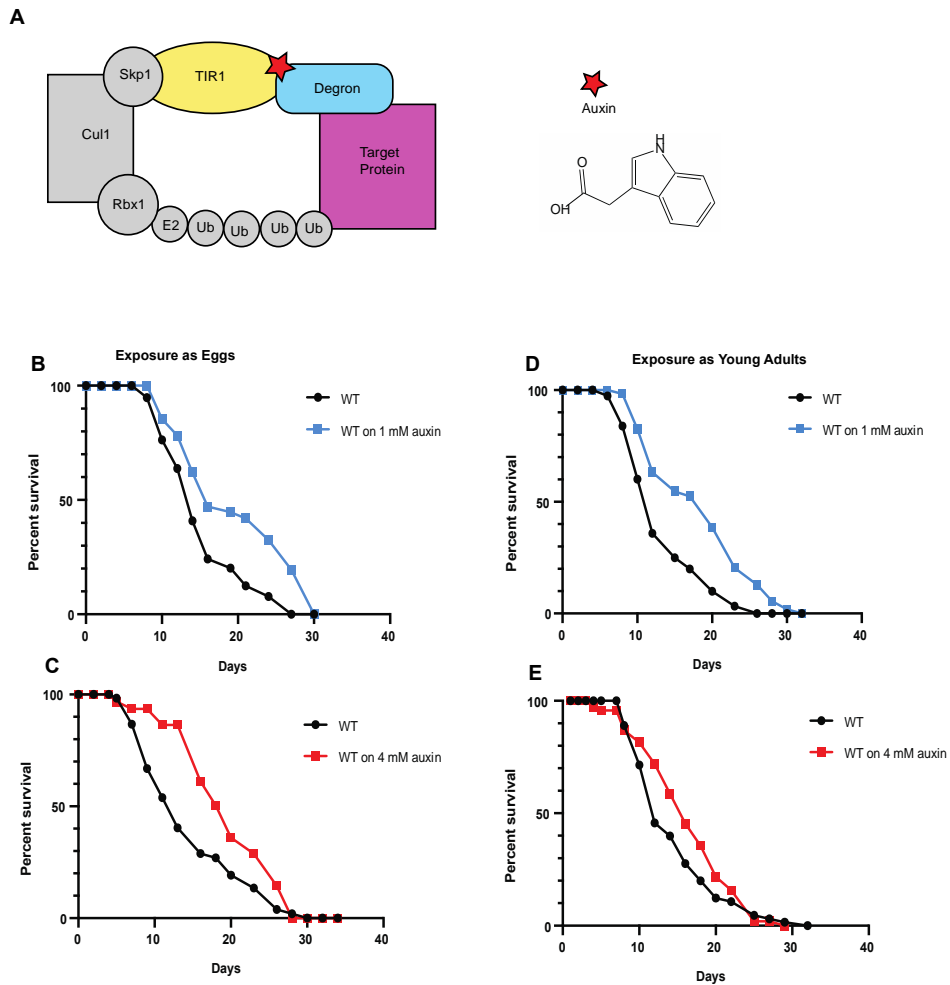


Figure 13: Auxin exposure increases lifespan

A. Schematic of auxin degradation system (B-E) Lifespans of N2 animals on either 2.5% ethanol control or 1mM or 4 mM auxin. (B) eggs placed on either auxin or EtOH plate. N2 on EtOH ($m= 15.25 \pm 0.58$, $n= 75/123$) N2 on 1 mM auxin ($m=19.64 \pm 0.81$, $n= 69/120$) (p vs N2 on EtOH > 0.0001) (C) eggs placed on either auxin or control plates. N2 on EtOH ($m= 14.54 \pm 0.89$, $n= 54/67$) N2 on 4 mM auxin ($m = 19.46 \pm 1.15$, $n= 28/45$) (p vs N2 on EtOH = 0.0083) (D) L4's placed on either auxin or control plates N on EtOH ($m= 13.4 \pm 0.49$, $n=104/118$) N2 on 1mM auxin ($m = 18.35 \pm 0.51$, $n= 91/125$) (p vs N2 on EtOH > 0.0001) (E) L4's placed on either auxin or control plates N2 on EtOH ($m= 14.64 \pm 0.66$, $n = 71/101$) N2 on 4 mM auxin ($m = 16.43 \pm 0.78$, $n = 53/90$) (p vs N2 on EtOH = 0.1343). The same controls for this experiment are also in Chapter 2, figure 5. Survival data analyzed using Kaplan Meier survival curve $m =$ mean lifespan \pm standard error, $n =$ animals observed/total animals.

Table 3: Lifespans of animals exposed to auxin

Lifespan of strains exposed to auxin (1 mM or 4 mM) during the entirety of lifespan or just adulthood. Results from this study were controls for auxin experiment in Chapter 2, figure 5 and Appendix Table 3

Lifespans of animals - exposure beginning during development				
Strain	Plate	Mean + S. E.	n = obs/tot	P vs N2 EtOH
N2	2.5% EtOH	15.25 + 0.58	75/123	
N2	auxin 1 mm	19.64 + 0.81	69/120	0.000017
CA1421	2.5% EtOH	18.17 + 0.68	90/125	0.0015
CA1423	2.5% EtOH	17.65 + 0.76	77/124	0.0188
N2	2.5% EtOH	14.87 + 0.5	93/119	
N2	auxin 1 mm	14.39 + 0.39	95/119	2.43E-01
CA1421	2.5% EtOH	14.54 + 0.39	104/127	0.3907
CA1423	2.5% EtOH	14.79 + 0.4	98/128	9.24E-01
N2	2.5% EtOH	14.5 + 0.67	74/93	
N2	auxin 4 mm	15.56 + 0.77	50/80	0.229
CA1202	2.5% EtOH	18.63 + 0.61	69/89	0.0002
CA1421	2.5% EtOH	16.71 + 0.76	62/92	0.0264
CA1423	2.5% EtOH	18.53 + 0.75	71/90	0.0004
N2	2.5% EtOH	14.54 + 0.89	54/67	
N2	auxin 4 mm	19.46 + 1.15	28/45	0.0083
CA1202	2.5% EtOH	16.23 + 1.15	42/80	0.159
CA1421	2.5% EtOH	17.81 + 0.82	61/99	0.0157
CA1423	2.5% EtOH	13.96 + 0.68	70/99	0.5062
Lifespans of animals - exposure beginning during adulthood				
Strain	Plate	Mean + S. E.	n = obs/tot	P vs N2 EtOH
N2	2.5% EtOH	13.4 + 0.49	104/118	
N2	auxin 1 mm	18.35 + 0.68	91/125	3.70E-09
CA1421	2.5% EtOH	16.49 + 0.63	88/115	0.0002
CA1423	2.5% EtOH	17.47 + 0.64	82/119	4.10E-07
N2	2.5% EtOH	14.47 + 0.39	91/104	
N2	auxin 1 mm	15.55 + 0.6	75/92	5.03E-02
CA1421	2.5% EtOH	13.86 + 0.4	95/118	0.4258
CA1423	2.5% EtOH	14.25 + 0.52	104/124	5.88E-01
N2	2.5% EtOH	14.64 + 0.66	71/101	
N2	auxin 4 mm	16.43 + 0.78	53/90	0.1343
CA1202	2.5% EtOH	15.59 + 0.66	83/125	0.3834
CA1421	2.5% EtOH	15.04 + 0.62	56/79	0.7827
CA1423	2.5% EtOH	15.71 + 0.71	82/100	0.3071

5.2.2 Strains facilitating AID-mediated germline depletion are long-lived

The *Arabidopsis* TIR1 protein was optimized for *C. elegans* expression to facilitate auxin dependent protein degradation by adding two codons and making two point mutations to increase auxin sensitivity and substrate affinity (232). Zhang et al., developed the system in *C. elegans*, and has created a variety of strains expressing TIR1 in different tissues, including the strains used in this study, which were initially used to investigate the roles of germline proteins in crossover during meiosis (174). Considering our interest in germline proteins involved in meiosis and how they impact aging, we were interested in determining how knockdown of these proteins specifically in the germ line impacts aging. We tested the lifespan of these strains, which have mRuby tagged TIR1 under the control of the promoter and 3'UTR of *sun-1* (*Psun-1::TIR1::mRuby*). The two strains in which we were interested also have the *spo-11* or *dsb-2* locus tagged with the degron sequence and a 3xFLAG epitope (Fig 14A). We used a third strain as a control for our experiments, which has the mRuby-tagged TIR1 and GFP tagged to a degron sequence under the control of the promoter of *eft-3*, which has universal somatic expression (174, 232). We found that two of the three strains were significantly longer lived than the wild-type animals under the control conditions, without exposure to auxin. We found that CA1421 (DSB-2::degron) exhibited a lifespan increase in five of seven trials with an extension of 3% to 23% (Fig 14B, Table 3). The CA1423 (SPO-11::degron) strain was long-lived in five of seven trials with an extension of 6% to 28% (Fig 14C, Table 3). The third strain CA1202, showed a 6% to 28% lifespan extension in all three trials with one trial significantly longer lived (Fig 14D, Table 3).

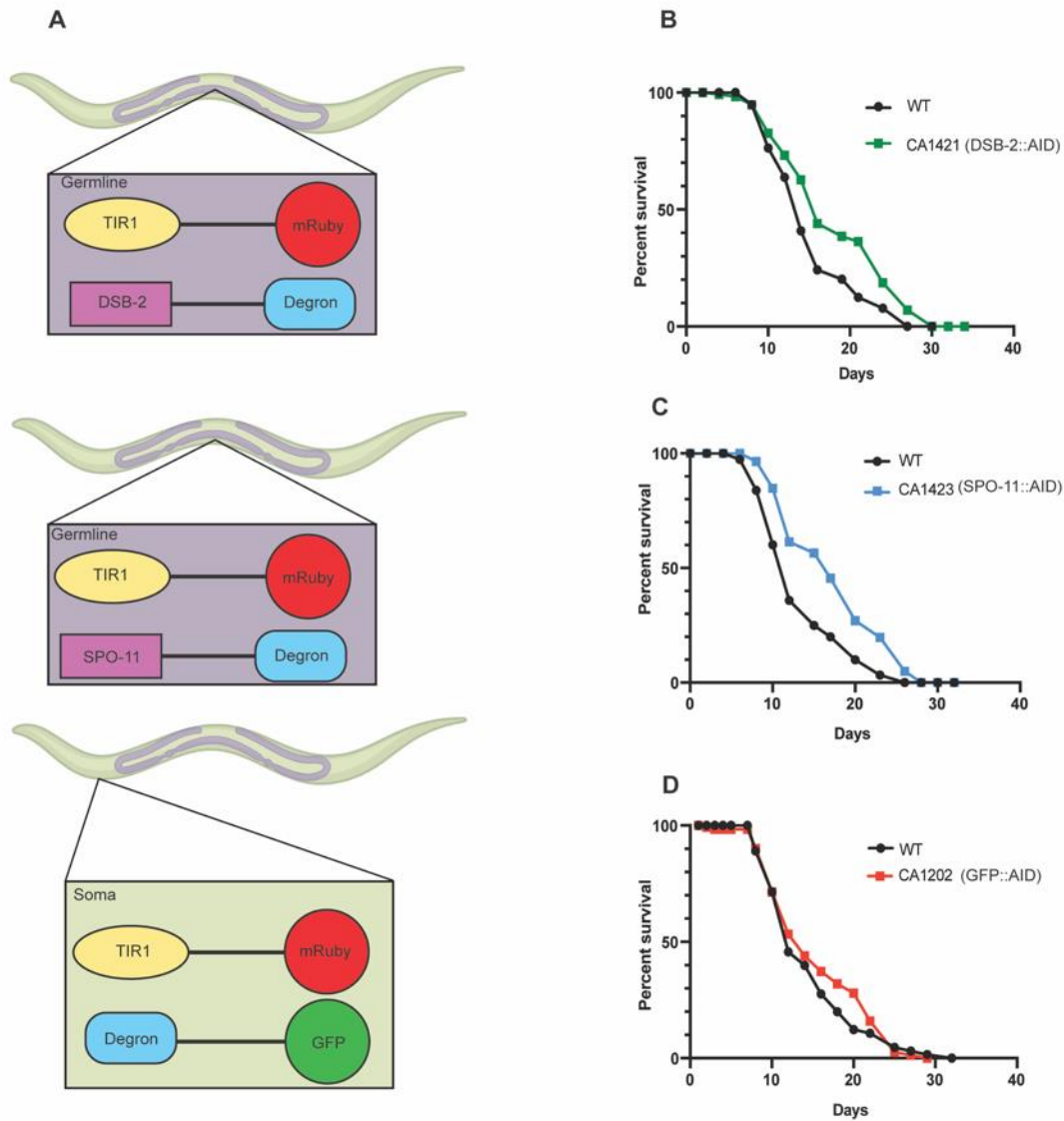


Figure 14: Strains expressing TIR1 and degron tagged proteins extend lifespan

(A) Schematics of transgenic animals expressing TIR1 in either the germ line (CA1421 and CA1423) or soma (CA1202) with degron tagged protein (B) Lifespan of N2 ($m = 15.25 \pm 0.58$, $n = 75/123$) CA1421 ($m = 18.17 \pm 0.68$, $n = 90/125$) (p vs N2 = 0.0015) (C) N2 on 2.5% EtOH ($m = 13.4 \pm 0.9$, $n = 104/118$) CA1423 ($m = 17.47 \pm 0.64$, $n = 88/115$) (p vs N2 > 0.0001) (D) N2 ($m = 14.5 \pm 0.67$, $n = 74/93$) CA1202 ($m = 18.63 \pm 0.61$, $n = 69/89$) (p vs N2 = 0.0002) All lifespans conducted on NGM plates containing 2.5% ethanol. The same controls for this experiment are also in Chapter 2, figure 5. Survival data analyzed using Kaplan Meier survival curve $m = \text{mean lifespan} \pm \text{standard error}$, $n = \text{animals observed/total animals}$. Created using BioRender.com

5.3 Discussion

In exploring the impact of meiotic genes on somatic longevity, we made the serendipitous discovery that two features of the auxin inducible degradation system increase lifespan. We found that exposing wild-type animals to two different concentrations of auxin during two different type periods increased lifespan. We also found that the expression of the TIR1 protein increased lifespan in these transgenic animals independent of exposure to auxin.

Other studies have found that altering the level of indoles, which are precursors to auxin, impact aging in *C. elegans*, *Drosophila*, and mice. Sonowal et al., found that exposure to *E. coli*-derived indoles extend lifespan and healthspan in *C. elegans*, including increased thrashing and pharyngeal pumping (234). Lee et al., discovered that exposure to indole deficient versus indole producing bacteria decreased survival of *C. elegans* in a dose dependent manner, with 0.5 mM indole reducing survival by 8 days and 1mM indole reducing lifespan by 12 days (235). Interestingly, *C. elegans* may have developed defense against higher levels of indoles. Its metabolite, 2-oxindole reduced survival, but N- β -D-glucopyranosyl-indole did not decrease survival (235). In addition to lifespan, it was determined that exposing animals to auxin functions through the XBP-1 branch of the Unfolded Protein Response (UPR) to promote resistance to endoplasmic reticulum stress, which could have an indirect role in regulating aging (236, 237). Also, it is noteworthy that our experiments were conducted using live *E. coli*. It is possible that there was impact on *E. coli* from the auxin treatment that indirectly effected longevity in the *C. elegans* feeding off of the *E. coli*. Additionally, the auxin we used in these experiments, IAA, was not water soluble, so auxin was dissolved in ethanol. While these experiments were compared to a control of ethanol added to the NGM plates without auxin, this could introduce a confounding

factor. Therefore, our findings seem to align with previous findings that exposure to auxin or an auxin precursor have variable impacts on longevity.

The AID system has also been used to induce sterility in animals in experiments where fertility would be considered a confounding factor, or in longevity experiments where it is imperative to eliminate contamination from progeny. Kasimatis et al., used AID in *C. elegans* to target the spermatogenesis gene, *spe-44* (238). Other methods to ensure sterility or contamination from progeny during an experiment are labor intensive or cause unwanted side effects. Therefore, the knockdown of *spe-44* using AID was an appealing option. However, Kasimatis et al., found that animals that were exposed to auxin starting in the L4 stage had an extended lifespan (238). Later experiments conducted by Dilberger et al., used this same strain to determine if there were unwanted side effects related to using this strain to induce sterility (239). One of the common methods to induce sterility is exposure to 5-Fluoro-2'-deoxyridine (FUdR). This study compared the *spe-44* AID animals with animals treated with FUdR, on days 2 and 10 of adulthood. They found that while FUdR increased lifespan and healthspan parameters and mitochondrial function, the auxin treated *spe-44* AID strain had similar aging parameters to the control (239). In our experiments, we found that germline specific *sun-1* driven expression of TIR1 increased the lifespan of the animal, while two different experiments found that the expression of TIR1 in the germ line using a different promoter *pie-1* to facilitate protein degradation of SPE-44, both increased lifespan in one experiment and had no impact on lifespan in another experiment (238, 239). Considering that expression of TIR1 in the germ line increased lifespan in two of three independent experiments, there should be caution applied to interpreting longevity data using these AID reagents.

We also observed phenotypes suggesting that the knockdown of target proteins may not have been sustained for the entirety of the animal's lifespan. This was observed in a strain previously generated for auxin induced knockdown of SPO-11, which is required for meiotic recombination (174). Previous experiments have identified that animals with a homozygous mutation in *spo-11* result in embryonic lethality (107, 110). We found that after exposure to auxin, the SPO-11 degraon strain did not have any viable progeny for the first few days of adulthood, but after about 4 days, viable larvae were visible on the plate and they seemed to have resumed reproduction. Also, we used a control strain that had GFP with a degraon tag, and we found while initially there was a lack of GFP signal, after about 8 Days of continuous auxin exposure some GFP signal was visible. More recently, there have been alternative auxins and AID tools developed that minimize these leaky effects and reduction of function. This includes an IAA analogue, 5-Ph-IAA, and mutations made in the auxin binding site of TIR1 to promote higher efficacy, and also to avoid degradation of non-target proteins (237, 240).

5.4 Methods

5.4.1 *Caenorhabditis elegans* maintenance

Strains were maintained at 20 °C on nematode growth media (NGM) plates seeded with *E. coli* strain OP50. Strains used include N2 (WT), and strains obtained from the CGC CA1421 (*meIs8 [pie-1p::GFP::cosa-1+unc-119(+)]II;dsb-2(ie58[dsb-2::AID::3xFLAG] ieSi38 [sun-1p::TIR1::mRuby::sun-1 3'UTR +Cbr-unc-119(+)] IV*, CA1423 (*meIs8 [pie1p::GFP::cosa-1+unc-*

110(+)]III; spo-11(ie59[spo-11::AID::3xFLAG]) ie Si38, [sun-1p::TIR1::mRuby::sun-1 3'UTR +Cbr-unc-119(+)] IV and CA1202 (ieSi57 [eft3p::TIR1::mRuby::unc-54 3'UTR+Cbr-unc119(+)] II; ieSi58 [eft-3p::degron::GFP::unc-54 3'UTR+Cbr-unc-119(+)] IV

5.4.2 Lifespan assays

All lifespan experiments were conducted at 20 °C on *E. coli* OP50 plates unless otherwise noted. Between 20 and 30 L4 hermaphrodites were transferred to 4-5 plates per strain. The plates were observed at 24–48 h intervals to record live, dead or censored (animals that were missing or bagged).

For the auxin lifespan assays, either eggs to larval stage 4 (L4) young adults were placed on auxin (1 mM or 4mM) supplemented or ethanol (2.5%) control added to NGM plates. Indole-3-acetic acid from Alfa Aesar (A#10556) was dissolved in ethanol and filter sterilized before adding to cooled NGM media before plates were poured. The lifespan assays were conducted at 20 °C with L4 stage marked as Day 0. Animals were observed every other day and transferred every other day during the reproductive period unless otherwise noted. Animals were categorized as dead, alive or censored (bagged or missing). The lifespan assays were analyzed using the program Online Application of Survival Analysis (OASIS 2) to calculate P-values (190). GraphPad prism (version 9) was used to graph the results.

6.0 General Discussion

The goal of this research was to determine the causative role of germline integrity in somatic aging. Using *C. elegans* we found that mutations in many aspects of meiosis reduced lifespan and at least three meiotic mutants, *dsb-2*, *spo-11*, and *htp-3*, exhibited an accelerated decline in features of healthspan, especially impairments of protein homeostasis. We used RNAseq to map the transcriptomes of these three mutants and found that at least two of them, *spo-11* and *htp-3*, showed remarkable similarities with the transcriptional profiles of aging wild-type *C. elegans*. Indeed, they also shared significant similarities with the transcriptional profiles associated with human aging tissues. The following sections explore our research in context of existing literature, unanswered questions, and future directions.

6.1 Short lived mutants with reduced fertility

The “Disposable Soma Theory of Aging” predicts that organisms invest resources into either reproduction or somatic maintenance. Application of this theory suggests that an animal with reduced fertility or sterility would live longer. However, evidence in multiple other species shows that the relationship between reproduction and aging is more nuanced than a simple trade-off, as summarized in Chapter 1. Our results add to the evidence that the relationship between reproduction and aging is complex. We tested 38 strains that had at least one mutation in genes involved in meiosis and 31 strains demonstrated a reduction in lifespan at least once. We repeated

these lifespans and identified 13 strains that showed reliable lifespan reduction. Many of the mutants with reduced lifespan also had reduced fertility. While it is not surprising that inactivating genes in an essential germline process impaired fertility, these results were surprising as dogma often associates sterility with longevity. However, in addition to our work, there have been many reports of long-lived mutants, including a specific mutation in *age-1*, which actually have greater reproductive success (241). Conversely, short lived mutants including *mev-1* and *hsf-1* mutants have reduced brood sizes (171, 242). The contradictory evidence is not limited to *C. elegans* studies, in humans, pregnancy can have rejuvenating effects and reduce risk of future disease (243). By specifically inactivating a germline-specific process and demonstrating its impact on overall aging, our study provides direct evidence for the nuanced and highly interlinked relationship between germ line and somatic health.

6.2 Why do mutations in different meiotic genes have different impacts on aging?

We found that some –but not all—of the meiotic mutations reduced lifespan. In part, this could be attributed to redundant functions and genetic compensation for some of the genes where mutations did not impact aging. It would be interesting to ask if, in such cases, double or triple mutants exhibit lifespan reductions. The unique healthspan defects of the mutants that we studied raise the possibility that some meiotic genes' inactivation would only reduce healthspan. If so, our study would not have identified them. Considering recent research indicating genes which have differential effects on healthspan and lifespan (93), it would be interesting to address whether any meiotic genes impact healthspan alone. There are at least 91 identified genes involved in *C. elegans*

meiosis (244). Our study was limited by the number of genes we selected to ask how they impacted lifespan and the three genes we decided to further investigate how they impacted aspects of healthspan. We tried to focus on genes were meiosis specific, while it can be hard to tease apart roles that are specific to the germ line. Recent advances in *C. elegans* research including the development of tools for automated healthspan and lifespan screen, would allow this to be conducted in a high throughput and automatic manner in the future (245).

6.3 Are there sex specific differences in how meiotic gene mutations impact aging?

C. elegans germ cells enter meiosis during the L3 larval stage, first producing sperm and then switching to oocytes (246, 247). Therefore, when we initiated knockdown of *dsb-2*, *htp-3*, or *spo-11* starting during L4, we only affected the production of oocytes. We found that there was only a lifespan reduction when these three genes were knocked down during the entirety of the animal's lifespan. It is possible that beginning gene knockdown during the L4, as the animal is beginning to produce oocytes, did not result in a lifespan reduction because a signal is sent earlier during spermatogenesis or early oogenesis which is important for aging. We studied the impact of meiosis on hermaphrodites alone and do not know if there are sex-specific differences in the aging phenotype. These questions could be addressed using *C. elegans* males or genetically feminized hermaphrodites such as *fog-2* mutants (248). Interestingly, a recent study found that Day 1 adult feminized *fog-2* mutants animals had similar transcriptomic profiles as Day 6 hermaphrodites which were depleted of sperm (249). While that study did not hypothesize a potential mechanism for this aged transcriptome, it is surprising that they found an aging phenotype in the feminized

mutants. While we did not compare the genetic signatures of the meiosis mutants to these *fog-2* mutants, it would be interesting to determine if similar genes are differentially regulated. This could indicate a potential cause for the shortened lifespan, in that an animal with meiosis disrupted may sense the end of reproduction earlier in its life than an animal with meiosis fully intact. Another avenue would be to explore if there are any age-related phenotypes in the *fog-2* mutant or any similar pathways that are regulated in both the meiosis mutants and the *fog-2* mutant.

Recent research has suggested that knockdown of regulatory genes such as *daf-2* later in life, in a post-reproductive animal increases lifespan (250). This suggests that aging can be modulated throughout the lifespan and that interventions do not need to occur early in development or from birth. In addition to our temporally-controlled adult-only RNAi, it would also be interesting to use reversible gene or protein knockdown to ask if restoring meiosis in adulthood could mitigate the longevity phenotypes. We intended to test this question using the AID system, but the confounding impact of Auxins and AID strains on wild-type lifespan, described in Chapter 5, prevented the acquisition of reliable data. But newer developments with this system may resolve some of these side effects (237).

6.4 How is meiotic disruption signaled to the soma to impact aging?

We used both targeted and unbiased techniques to identify the changes that occur in the soma during meiotic disruption. We found that somatic proteostasis declined earlier in *dsb-2*, *htp-3*, and *spo-11* mutants. This data informed our understanding of a potential mechanism through which aging was being impacted. We also were able to identify that overexpression of proteasomal

subunit, RPN-6.1 partially rescued *spo-11* lifespan defects. Disruption of protein homeostasis is a common hallmark of aging and the modulation of protein homeostasis is frequently altered in many longevity pathways (149). While our data point to proteostasis as a downstream mechanism that may be causing the shortened lifespan, the signaling mechanism or molecule involved is unknown. We ruled out that endocytosis between the germ line and the soma is required for lifespan shortening, by observing that knockdown of *cup-4* did not suppress the shortened lifespan of *spo-11* mutants. Somatic regulation of the germ line has been studied extensively in *C. elegans*. This includes communication of environmental conditions to stimulate meiotic progression through DAF-2 and the RAS-ERK pathway (251, 252). In addition, the TGF- β pathway functions in regulating reproductive aging and balances proliferation and differentiation of germ line stem cells based on environmental conditions (252).

Signaling from the germ line also modulates aging and has been studied predominantly in the context of the *glp-1* longevity pathway. This includes DAF-16, which must be dephosphorylated to be translocated to the nucleus (134). But recently these endocrine pathways have also been implicated in regulating reproduction after starvation in worms (253). These studies highlight that some of the signaling pathways function--both from the germ line to the soma, as well as in the opposite direction, from the soma to the germ line. Therefore, it would be interesting to determine if these pathways are altered in the meiosis mutants we identified that shorten lifespan, either by measuring expression levels of genes involved in these pathways or by determining if their knockdown or overexpression altered meiotic mutant lifespan. Similarly, supplementation with signaling molecules such as oleic acid, which has been demonstrated to have protective effects from the increased mortality of mating in *C. elegans*, could be tested for potential protective effects on meiosis mutants (254).

Our RNA sequencing data provided us with an unbiased approach to address the mechanism through which meiotic mutations impacted aging. Further analysis of the transcriptomic data could uncover other signaling pathways that are affected, as well as could determine if previously uncharacterized genes are involved in regulation of aging. We began to uncover this through identification of the anti-longevity targets of *irld-53* and Y19D10A.5 (Section 4.3.2) but considering the number of differentially regulated genes in *spo-11* and *htp-3* mutants, there are many more candidates remaining to be tested. In the future, an RNAi screen knocking down more of the top upregulated targets in *spo-11* and *htp-3* mutants could be conducted to determine other anti-longevity genes and the pathways they function through. We also identified 10 genes that were commonly upregulated in *spo-11* and *htp-3* mutants and published datasets of genes upregulated with age in *C. elegans* and humans (Section 3.2.3). We could verify the upregulation of these genes using qPCR and then can could construct a fluorescent reporter(s) to use as a readout for aging. We could then conduct a genetic screen for genes which reduced the expression of these aging biomarkers. Our screen could include genes upregulated in the meiosis mutants or could also be used to identify more general regulators of aging that had been previously unidentified.

6.5 Using basic research to understand complex relationships

Recently there has been an increased interest in understanding how infertility and reproductive disorders correspond to overall health in humans (243, 255). Women, especially in the United States are delaying childbearing with an increase in women having children in their

30's and 40's (256). There has also been an increase in the number of people using infertility services at older ages (257). Therefore, it is essential and topical to decipher how reproductive health impacts overall health.

Evidence of the close relationship between reproductive and somatic aging in women has accrued. Diminished ovarian reserve has been associated with shortened telomeres, indicating early somatic aging (258). Interestingly, estrogen has been identified as having a neuroprotective effect on women. Bilateral salpingo-oophorectomy, or the removal of ovaries and fallopian tubes, before the onset of menopause has been associated with increased cognitive impairment or dementia in women (259). In contrast, a more recent study found an association between a longer reproductive period and earlier menarche with pre-clinical markers for Alzheimer disease, indicating that longer exposure to endogenous estrogen may also be detrimental (260). There are also primarily reproductive disorders that have systemic implications, such as the association between polycystic ovary syndrome (PCOS) and cardiovascular disease (261). Changes to estrogen and progesterone levels have been implicated in hormone sensitive cancers such as breast, ovarian, and endometrial cancers (243). These correlative observations are not limited to women as there has been data to suggest a link between fertility status and diseases such as testicular cancer in men (262, 263). However, these examples demonstrate the difficulty in teasing apart causation in the relationship between reproduction and longevity. The hormonal changes associated with reproduction complicate interpreting causation. It is difficult to determine if syndromes that manifest primarily in the reproductive system, but have systemic symptoms, such as PCOS, are caused by reproductive dysfunction or caused by other mechanisms.

Through our research that showed meiotic mutants had short lifespan irrespective of their fertility status, we were able to separate the impact of reproduction *per se* on the soma and ask

how germline integrity impacted aging. Our study highlighted the benefits of using a model organism to determine causation. A major benefit of this approach is that many of the genes we studied in *C. elegans* have direct human homologs and roles in mammalian meiosis. Some of these genes were also included in studies in women that identified genetic determinants for age at natural menopause (ANM). Ruth et al., identified 91 genes associated with genetic determinants of ovarian aging (264). The goal of their research was to identify reproductive aging mechanisms and they found that genetic manipulation of these genes in a mouse model extended reproductive span (264). However, it would take years in a mouse model to understand if these manipulations to extend the reproductive span have negative effects on longevity, as some of the correlative data in humans has suggested. Indeed, we found that some of the genes identified as genetic determinants of ANM by Ruth et al., were also included in our list as their *C. elegans* orthologs demonstrated a shortened lifespan in our study (Table 4) (264). Day et al., also had a similar goal and identified similar genes to the Ruth et al., as genetic determinants of ANM (158). Some similarities between these studies including HELQ1, CHEK2, RAD54L, and RAD51, all genes with meiotic functions. Strikingly, we found that mutations in the *C. elegans* orthologs of these genes also had a reduced lifespan (Chapter 2 and Table 5) (158). These discoveries can form the basis for future studies on shared mechanisms for the meiotic control of aging between worms and mammals.

Table 4: Shared genes in ANM genetic variants and our study

Identified ANM variants	Ruth et al., 2021	Day et al., 2016	<i>C. elegans</i> ortholog (OrthoList)	Avg impact on lifespan vs N2
EXO1	✓	✓	<i>exo-1</i>	-21.27%
HELQ	✓	✓	<i>helq-1</i>	-6.85%
CHEK2	✓	✓	<i>chk-2</i>	-21.37%
RAD54L		✓	<i>rad-54</i> , Y116A8C.13	<i>rad-54</i> : -17.1%
MSH5		✓	<i>msh-5</i>	0.88%
RAD51		✓	<i>rad-51</i>	-22.56%
DMC1		✓	<i>rad-51</i>	-22.56%

7.0 Other Contributions

The specific healthspan phenotypes of meiotic mutants described above impelled my interest in the links between lifespan and healthspan and how lifespan-regulatory proteins shaped them. Hence, I participated in projects in our laboratory that focused on two such factors, TCER-1 and NHR-49. Our laboratory recently demonstrated that the pro-longevity factor, TCER-1, represses stress resistance and healthspan. My contribution to this study was elaboration of the healthspan phenotypes of *tcer-1* mutants. While my thesis project focused on how somatic aging was impacted due to the disruption of germline health through mutations in meiosis, the NHR-49 studies focused on its role in the germline-less longevity pathway. I helped enumerate that although NHR-49 promotes both longevity and immune-resistance, it does so through distinct mechanisms. The following sections summarize my involvement in projects directed by other lab members, both published studies where I am a contributing author as well as unpublished projects.

7.1 Transcription elongation factor, TCER-1 impacts longevity, stress resistance and healthspan

The following section highlights my contributions to Amrit, F.R.G., Naim, N., Ratnappan, R. et al. The longevity-promoting factor, TCER-1, widely represses stress resistance and innate immunity. Nat Commun 10, 3042 (2019). <https://doi.org/10.1038/s41467-019-10759-z> Licensed under a Creative Commons Attribution 4.0 International License.

The transcription elongation factor, TCER-1 has been previously identified as essential for longevity in a germline-less animal (133). Often genes that are required for lifespan extension are also required for enhanced stress resistance (265). Surprisingly, our lab discovered that TCER-1 inhibits resistance against both abiotic and biotic stressors.

Considering that *tcer-1* mutants have increased resistance to a variety of stressors, we were curious if *tcer-1* mutants also impacted healthspan. We measured the rate of thrashing in liquid with age, and found *tcer-1* mutants had enhanced stress resistance specifically during the reproductive period. Interestingly, *tcer-1* mutants had increased thrashing rate during day 2 of adulthood compared to wild type (Table S14). By day 5, the *tcer-1* mutants had a similar thrashing rate as wild type (Table S14). During the post reproductive timepoints, Day 7 and Day 9, the *tcer-1* mutants had an impaired thrashing rate compared to wild type (Table S14). Considering the improvement to mobility, we were also curious if the *tcer-1* mutants demonstrated improvements in other aspects of healthspan. Therefore, we utilized a *C. elegans* model of amyloid β ($A\beta$) proteotoxicity, which expressed the human $A\beta_{1-42}$ in the muscle cells, causing the animals to paralyze at 25°C (266). We found that *tcer-1* mutants exhibited a delay in the onset of paralysis. In one trial, 50% of the wild-type animals were paralyzed by 33 hours, and 100% by 50 hours, while the *tcer-1* mutant strain had 50% of the population paralyzed by 95 hours and 100% paralyzed by 125 hours (Table S14). Overall, this data suggested that the TCER-1 may also impact measurements of healthspan in addition to its role in stress resistance. These results also highlight the complexity of the timing of TCER-1 expression in improving healthspan.

7.2 The functional impact of TCER-1 splicing on stress response and healthspan

We continued to examine how the pro-longevity gene, *tcer-1*, impacts healthspan and stress resistance by studying potential mechanisms through which *tcer-1* represses stress resistance. Considering *tcer-1*'s role in alternative splicing, our lab identified several target genes that have either exons skipped or introns retained in the *tcer-1* mutant background. We used a CRISPR generated mutant with an exon deleted in the *dagl-2* gene, which is normally upregulated by *tcer-1*. This mutant mimics the exon skipping event that occurs in *tcer-1* mutants. To determine the functional significance of this event, we used measurements of both healthspan and resistance to both abiotic and biotic stressors to determine the impact of these *dagl-2* Exon 7 mutants. DAGL-2 is a diacylglycerol Lipase homolog with predicted function in the endocannabinoid pathway (267). We determined the resistance to biotic stressors, including two strains of the gram-negative bacteria *Pseudomonas aeruginosa* (PA14 and PA01) and gram-positive bacteria *Enterococcus faecalis*, and an abiotic stressor through oxidative stress. We also investigated how supplementation with various components of the endocannabinoid pathways, including 2-arachidonyl glycerol (2-AG) or arachidonic acid, also influenced the ability to survive pathogen stress (Table S14). Overall, this data contributes towards our understanding of how a specific isoform of *dagl-2* as well as other components of its pathway impact stress resistance and healthspan, in the context of TCER-1.

7.3 Tissue specific immune regulation through NHR-49

The following section highlights my contributions to Naim, N., Amrit, F. R. G., Ratnappan, R., DelBuono, N., Loose, J. A., & Ghazi, A. (2021). Cell nonautonomous roles of NHR-49 in promoting longevity and innate immunity. *Aging Cell*, 20, e13413. <https://doi.org/10.1111/ace1.13413> Licensed under a Creative Commons Attribution 4.0 International License.

Nuclear hormone receptor NHR-49 was previously identified for its essential pro-longevity role in germline-less *C. elegans* (141). Our lab investigated the tissue specific role of NHR-49 in both stress resistance and longevity in the context of a wild-type animal or a germline-less long-lived animal. Other pro-longevity factors, including DAF-16, have been identified for its cell non autonomous role in extended lifespan (268). Our lab previously demonstrated that a gene that promotes longevity can also be detrimental towards stress resistance; therefore, we wanted to understand if NHR-49 contributes toward stress resistance and longevity through a similar site of action (93). We found that NHR-49 is required in the neurons to promote stress resistance (Table S15). Overall, this data contributes towards our understanding of the necessity of NHR-49 in various tissues, based on the context of germline status as well as the type of stress.

Appendix Supplementary Data

Appendix Table 1: Lifespans of all meiosis mutants

Strain	Genotype	mean lifespan (days)	S.E	N2 mean Lifespan (days)	S.E.	P v N2
WS3455	<i>chk-2(gk212)</i>	16	0.73	19.92	0.91	0.0013
		12.91	1.21	16.78	0.33	0.0006
QP1298	<i>rec-8/nT1;coh-3,4</i>	18.55	0.75	17.12	0.62	0.3077
		16.75	0.39	20.32	0.43	<0.0001
		14.37	0.66	15.98	0.57	0.0528
QP0455	<i>htp-1(gsk150)</i>	15.22	1.04	17.12	0.62	0.3543
		15.6	0.63	15.98	0.57	0.5263
	<i>htp-1(gk174);htp-2(tm2543)</i>	15.91	0.83	18.05	0.59	0.0203
	<i>htp-2(tm2543)</i>	14.15	0.43	20.07	0.54	<0.0001
TY4986	<i>htp-3(y428) ccls4251 I/hT2 [bli-4(e937) let-?(q782) als481 (I,III)]</i>	14.2	0.2	21.1	0.2	<0.0001
		16.42	0.81	19.8	0.58	0.0014
		14.06	0.47	16.97	0.61	0.0005
CA1230	<i>htp-3(tm3655)/ht2</i>	15.45	0.64	20.07	0.54	<0.0001
AV307	<i>syp-1(me17)/nT1g</i>	16.4	0.6	19.4	0.6	0.0026
		19.6	0.72	20.7	0.56	0.1724
AC276	<i>syp-2(ok307)/nT1</i>	18.41	0.69	20.32	0.43	0.0158
CV2	<i>syp-3(ok758)/hT2</i>	15.3	0.3	21.1	0.2	<0.0001
CA998	<i>ieDf2/mLs11</i>	22.12	0.76	20.32	0.43	0.0036
CA151	<i>him-8(me4)</i>	15.22	0.72	19.85	0.8	<0.0001
		15.88	0.99	16.78	0.33	0.6769
		13.68	0.62	15.98	0.57	0.0187
RB1183	<i>prom-1(ok1140)</i>	17.25	0.8	16.73	0.4	0.4734
		14.28	0.65	14.9	0.6	0.2866
RB1583	<i>plk-2(ok1936)</i>	18.91	0.62	16.81	0.8	NS
		17.73	0.45	20.32	0.43	0.0002
		20.06	0.57	16.97	0.61	0.0007
AV157	<i>spo-11(me44)/nT1</i>	9.6	0.1	21.1	0.2	<0.0001
		13.8	0.4	19.6	0.7	<0.0001
		14.5	0.15	21.2	0.5	<0.0001
		12.67	0.64	19.55	0.53	<0.0001
		11.8	0.68	16.07	0.83	0.0009
AV106	<i>spo-11(ok79)/nT1</i>	16.33	0.6	19.4	0.6	0.0048
		14.8	0.3	21.2	0.5	<0.0001
RB1562	<i>him-5(ok1896)</i>	11.27	1.13	16.07	0.83	0.0003
		18.8	0.2	21.1	0.2	0.03
CA1117	<i>dsb-1(we11)/nT1g</i>	17.99	0.86	17.12	0.62	NS
		14.76	1.01	19.85	0.8	0.0001
		15.46	0.49	20.32	0.43	<0.0001

Strain	Genotype	mean lifespan (days)	S.E	N2 mean Lifespan (days)	S.E.	P v N2
QP938	<i>dsb-2(me96)</i>	13.6	0.6	19.6	0.7	<0.0001
		18.2	0.5	21.2	0.5	<0.0001
		14.84	0.58	19.55	0.53	<0.0001
		14.93	0.54	19.59	0.64	<0.0001
		14.19	0.64	15.09	0.75	0.483
KR5301	<i>rec-1(h2875)</i>	18	0.6	19.6	0.7	0.5921
		19.6	0.7	21.2	0.5	0.4182
CB5423	<i>him-17(e2707)</i>	14.87	0.98	19.85	0.8	0.0001
		13.1	0.61	20.32	0.43	<0.0001
AV473	<i>rad-50(ok197)</i>	17.73	0.5	19.4	0.6	0.0446
		14.7	0.6	21.2	0.5	<0.0001
SSM72	<i>exo-1(tm1842)</i>	16.8	0.6	19.6	0.7	0.0325
		16.9	0.6	21.2	0.5	0.0006
		13.5	0.48	16.66	0.67	0.0002
		13.91	0.45	19.55	0.53	<0.0001
		13.32	0.54	19.59	0.64	<0.0001
		13.09	0.56	15.09	0.75	0.0207
QP0900	<i>mre-11(iow1)/nTg</i>	17.2	0.3	21.1	0.2	<0.0001
		12.87	0.77	19.89	0.58	<0.0001
		16.77	0.42	20.32	0.43	<0.0001
		14.1	0.47	16.97	0.61	0.004
CA538	<i>rad-51(lg8701)/nTg</i>	15.34	0.6	19.4	0.6	0.0003
		15	0.32	19.8	0.58	<0.0001
	<i>brc-1(tm1842?)</i>	17.47	0.8	19.4	0.6	0.393
RB1279	<i>rfs-1(ok1372)</i>	19.76	0.74	20.24	0.51	0.7792
		17.99	0.77	19.64	0.71	0.1526
VC531	<i>rad-54(ok615)</i>	17.51	0.5	19.4	0.6	0.1193
		15.35	0.5	20.32	0.43	<0.0001
TG1792	<i>helq-1(tm2134)</i>	15.93	0.92	19.8	0.58	0.0032
		17.76	0.82	16.78	0.33	NS
QP1208	<i>sws-1(ea12)</i>	22.06	0.6	20.24	0.51	5.27
	<i>rmh-1(ad92)</i>	15.59	0.79	16.37	0.6	0.3965
		14.69	0.55	16.97	0.61	0.0026
		14.85	0.6	16.78	0.33	0.2431
	<i>him-14(ok230)/mln1</i>	15.09	0.44	16.73	0.4	0.0051
AV115	<i>msh-5(me23)/nT1U</i>	17.27	0.85	17.12	0.62	0.7461
CV98	<i>him-18(tm2181) III/qC1 dpy-19(a1259) gln-</i>	17.5	0.3	21.1	0.2	0.01
		15.27	0.57	16.37	0.6	0.4181
TG1760	<i>mus-81(tm1937)</i>	16.4	0.6	21.1	0.2	0.0004
		15.91	0.78	16.66	0.67	0.4777

Appendix Table 2: Germline specific RNAi lifespans for meiosis gene knockdown

Germline specific lifespan (whole life)					
Trial #1					
Strain	Genotype	RNAi condition	n= obs/tot	Mean (days) ± S.E	P vs DCL569
DCL569	sun-1p::rde-1::sun-1 3'UTR + unc-119(+)	<i>pad-12</i> (control)	71/91	17.85 ± 0.49	
DCL569	sun-1p::rde-1::sun-1 3'UTR + unc-119(+)	<i>spo-11</i>	77/99	14.42 ± 0.52	<0.0001
DCL569	sun-1p::rde-1::sun-1 3'UTR + unc-119(+)	<i>htp-3</i>	59/94	15.55 ± 0.63	0.0247
Trial #2 (shown in Fig 1)					
DCL569	sun-1p::rde-1::sun-1 3'UTR + unc-119(+)	L4440 (control)	75/90	18.94 ± 0.8	
DCL569	sun-1p::rde-1::sun-1 3'UTR + unc-119(+)	<i>dsb-2</i>	86/107	15.36 ± 0.42	<0.0001
DCL569	sun-1p::rde-1::sun-1 3'UTR + unc-119(+)	<i>spo-11</i>	89/107	15.04 ± 0.48	<0.0001
DCL569	sun-1p::rde-1::sun-1 3'UTR + unc-119(+)	<i>htp-3</i>	82/90	15.77 ± 0.45	<0.0001
Germline specific lifespan (adult only)					
DCL569	sun-1p::rde-1::sun-1 3'UTR + unc-119(+)	L4440 (control)	55/62	17.19 ± 0.53	
DCL569	sun-1p::rde-1::sun-1 3'UTR + unc-119(+)	<i>dsb-2</i>	88/97	16.29 ± 0.52	0.8605
DCL569	sun-1p::rde-1::sun-1 3'UTR + unc-119(+)	<i>htp-3</i>	74/106	17.94 ± 0.61	0.0732
DCL569	sun-1p::rde-1::sun-1 3'UTR + unc-119(+)	<i>spo-11</i>	66/107	17.43 ± 0.41	0.0485

Appendix Table 3: Lifespan of AID strains

Whole Life 1 mM auxin exposure							
Trial #1 (shown in figure)							
Strain	Genotype	Plate	Mean + S. E.	n = obs/tot	P vs N2 EtOH	P vs auxin	P vs N2 on auxin
N2		2.5% EtOH	15.25 + 0.58	75/123		0.000017	0.000017
CA1421	<i>dsb-2:degron</i>	2.5% EtOH	18.17 + 0.68	90/125	0.0015	0.2373	0.1415
CA1423	<i>spo-11:degron</i>	2.5% EtOH	17.65 + 0.76	77/124	0.0188	0.7307	0.054
N2		auxin 1 mm	19.64 + 0.81	69/120	0.000017		
CA1421	<i>dsb-2:degron</i>	auxin 1 mm	17.42 + 0.6	93/129	0.0182		0.0152
CA1423	<i>spo-11:degron</i>	auxin 1 mm	18.25 + 0.61	106/122	0.0006		0.0739
Trial #2							
N2		2.5% EtOH	14.87 + 0.5	93/119		2.43E-01	0.2434
CA1421	<i>dsb-2:degron</i>	2.5% EtOH	14.54 + 0.39	104/127	0.3907	0.245	0.7219
CA1423	<i>spo-11:degron</i>	2.5% EtOH	14.79 + 0.4	98/128	9.24E-01	0.683	0.4391
N2		auxin 1 mm	14.39 + 0.39	95/119	2.43E-01		
CA1421	<i>dsb-2:degron</i>	auxin 1 mm	13.96 + 0.32	105/126	0.0625		0.4497
CA1423	<i>spo-11:degron</i>	auxin 1 mm	15.23 + 0.37	111/129	0.976		0.1353
Adult only 1 mM auxin exposure							
Trial #1 (shown in figure)							
Strain	Genotype	Plate	Mean + S. E.	n = obs/tot	P vs N2 EtOH	P vs auxin	P vs N2 on auxin
N2		2.5% EtOH	14.47 + 0.39	91/104		5.03E-02	0.0503
CA1421	<i>dsb-2:degron</i>	2.5% EtOH	13.86 + 0.4	95/118	0.4258	0.1161	0.0169
CA1423	<i>spo-11:degron</i>	2.5% EtOH	14.25 + 0.52	104/124	5.88E-01	0.8986	0.1237
N2		auxin 1 mm	15.55 + 0.6	75/92	5.03E-02		
CA1421	<i>dsb-2:degron</i>	auxin 1 mm	14.64 + 0.45	97/155	0.4259		0.1827
CA1423	<i>spo-11:degron</i>	auxin 1 mm	14.36 + 0.43	112/141	0.6288		0.0928
Trial #2							
N2		2.5% EtOH	13.4 + 0.49	104/118		3.70E-09	3.70E-09
CA1421	<i>dsb-2:degron</i>	2.5% EtOH	16.49 + 0.63	88/115	0.0002	0.5795	0.0096
CA1423	<i>spo-11:degron</i>	2.5% EtOH	17.47 + 0.64	82/119	4.10E-07	0.008	0.2073
N2		auxin 1 mm	18.35 + 0.68	91/125	3.70E-09		
CA1421	<i>dsb-2:degron</i>	auxin 1 mm	16.25 + 0.51	106/124	0.0003		0.0043
CA1423	<i>spo-11:degron</i>	auxin 1 mm	19.07 + 0.67	77/120	0		0.98

Appendix Table 4: Lifespan of meiosis mutants in germline-less background

Strain	Genotype	n=obs/tot	Mean (days) ± S.E.	P vs N2	P vs glp-1
Trial #1					
N2	wildtype	87/111	19.92 ± 0.76		
AV106	<i>spo-11(ok79)/nT1</i>	42/43	15.07 ± 1.08	0.0005	
CF1903	<i>glp-1</i>	48/49	26.53 ± 1.25	<0.0001	
AGP285	<i>spo-11(ok79)/nT1;glp-1</i>	36/52	20.22 ± 1.99	0.4799	
Trial #2					
N2	wildtype	97/123	15.28 ± 0.43		<0.0001
AV106	<i>spo-11(ok79)/nT1</i>	96/102	14.03 ± 0.49	0.057	<0.0001
CF1903	<i>glp-1</i>	115/123	21.53 ± 0.71	<0.0001	
AGP285	<i>spo-11(ok79);glp-1</i>	38/50	16.83 ± 1.35	0.0244	0.0104
Trial #1					
N2	wildtype	73/98	16.56 ± 0.44		<0.0001
AV157	<i>spo-11(me44)/nT1</i>	39/97	13.63 ± 0.7	0.0007	<0.0001
CF1903	<i>glp-1</i>	97/105	27.51 ± 0.65	<0.0001	
AGP310	<i>spo-11(me44);glp-1</i>	21/45	13.59 ± 0.62	0.0012	<0.0001
Trial #2					
N2	wildtype	79/124	16.65 ± 0.47		<0.0001
AV157	<i>spo-11(me44)/nT1</i>	47/62	13.04 ± 0.45	<0.0001	<0.0001
CF1903	<i>glp-1</i>	39/40	20.93 ± 1.03	<0.0001	
AGP310	<i>spo-11(me44);glp-1</i>	38/61	11.05 ± 0.64	<0.0001	<0.0001
Trial #1					
N2	wildtype	78/113	16.5 ± 0.51		<0.0001
AV477	<i>dsb-2(me96)</i>	35/41	9.69 ± 0.71	<0.0001	<0.0001
CF1903	<i>glp-1</i>	94/118	19.87 ± 0.61	<0.0001	
AGP304	<i>dsb-2;glp-1</i>	82/95	18.33 ± 0.67	0.0167	0.1325
Trial #2					
N2	wildtype	113/123	16.29 ± 0.44		<0.0001
CF1903	<i>glp-1</i>	99/120	25.2 ± 0.82	0	0
AV477	<i>dsb-2(me96)</i>	99/120	11.85 ± 0.6	<0.0001	
AGP304	<i>dsb-2;glp-1</i>	100/116	23.26 ± 0.86	0	0
Trial #1					
N2	wildtype	99/118	17.36 ± 0.5		<0.0001
CF1903	<i>glp-1</i>	50/90	29.27 ± 1.25	<0.0001	
AGP322	<i>htp-3;glp-1</i>	117/145	20.92 ± 0.72	<0.0001	<0.0001
TY4986	<i>htp-3(y428)/hT2</i>	82/103	15.77 ± 0.53	0.0534	<0.0001
Trial #2					
N2	wildtype	91/102	14.71 ± 0.52		<0.0001
CF1903	<i>glp-1</i>	117/137	22.13 ± 0.68	<0.0001	
AGP322	<i>htp-3;glp-1</i>	116/121	19.03 ± 0.64	<0.0001	<0.0001
TY4986	<i>htp-3(y428)/hT2</i>	98/110	11.67 ± 0.61	0.0088	<0.0001
Trial #1					
N2	wildtype	60/122	19.93±0.65		0.0625
SS104	<i>glp-4</i>	75/124	17.92±0.66	0.0625	
AV157	<i>spo-11(me44)</i>	57/70	14.66±0.78	<0.0001	0.0013
	<i>spo-11(me44);glp-4</i>	118/125	13.27±0.45	<0.0001	9.30E-09

Appendix Table 5: Thrashing rate of meiosis mutants

Thrashing						
Trial #1						
Strain	Genotype	Age	Thrashes (30 sec)	Strain	Genotype	Thrashes (30 sec)
WT	wildtype	Day 2	92.75	AV106	<i>spo-11(ok79)/nT1</i>	74.2
WT	wildtype	Day 5	94	AV106	<i>spo-11(ok79)/nT1</i>	40.45
WT	wildtype	Day 7	74.75	AV106	<i>spo-11(ok79)/nT1</i>	41.6
WT	wildtype	Day 9	66.38	AV106	<i>spo-11(ok79)/nT1</i>	38.05
Trial #2						
WT	wildtype	Day 2	96.9	AV106	<i>spo-11(ok79)/nT1</i>	80.75
WT	wildtype	Day 5	95.25	AV106	<i>spo-11(ok79)/nT1</i>	63.55
WT	wildtype	Day 7	67.05	AV106	<i>spo-11(ok79)/nT1</i>	29.9
WT	wildtype	Day 9	46.62	AV106	<i>spo-11(ok79)/nT1</i>	22.7
Trial #3						
WT	wildtype	Day 2	89.55	AV106	<i>spo-11(ok79)/nT1</i>	52
WT	wildtype	Day 5	81	AV106	<i>spo-11(ok79)/nT1</i>	44.95
WT	wildtype	Day 7	81.25	AV106	<i>spo-11(ok79)/nT1</i>	53.9
WT	wildtype	Day 9	54.75	AV106	<i>spo-11(ok79)/nT1</i>	29.3
Trial #1						
Strain	Genotype	Age	Thrashes (30 sec)	Strain	Genotype	Thrashes (30 sec)
WT	wildtype	Day 2	95.05	AV477	<i>dsb-2(me96)</i>	53.2
WT	wildtype	Day 5	92.69	AV477	<i>dsb-2(me96)</i>	53.45
WT	wildtype	Day 7	60.88	AV477	<i>dsb-2(me96)</i>	40.67
WT	wildtype	Day 9	43.86	AV477	<i>dsb-2(me96)</i>	17.8
Trial #2						
WT	wildtype	Day 2	83.75	AV477	<i>dsb-2(me96)</i>	46.68
WT	wildtype	Day 5	86	AV477	<i>dsb-2(me96)</i>	39.8
WT	wildtype	Day 7	51.47	AV477	<i>dsb-2(me96)</i>	6.55
WT	wildtype	Day 9	22.5	AV477	<i>dsb-2(me96)</i>	2.82
Trial #3						
WT	wildtype	Day 2	88.75	AV477	<i>dsb-2(me96)</i>	50.4
WT	wildtype	Day 5	87.56	AV477	<i>dsb-2(me96)</i>	56.3
WT	wildtype	Day 7	51	AV477	<i>dsb-2(me96)</i>	39.42
WT	wildtype	Day 9	16.77	AV477	<i>dsb-2(me96)</i>	21.81
Trial #4						
WT	wildtype	Day 2	100	AV477	<i>dsb-2(me96)</i>	45.95
WT	wildtype	Day 5	94.5	AV477	<i>dsb-2(me96)</i>	53.55
WT	wildtype	Day 7	87.65	AV477	<i>dsb-2(me96)</i>	30.8
WT	wildtype	Day 9	58.9	AV477	<i>dsb-2(me96)</i>	28.13
Trial #1						
Strain	Genotype	Age	Thrashes (30 sec)	Strain	Genotype	Thrashes (30 sec)
WT	wildtype	Day 2	88.65	TY4986	<i>htp-3(y428)/hT2</i>	75.25
WT	wildtype	Day 5	83.35	TY4986	<i>htp-3(y428)/hT2</i>	55.65
WT	wildtype	Day 7	67	TY4986	<i>htp-3(y428)/hT2</i>	25.277778
WT	wildtype	Day 9	69.8	TY4986	<i>htp-3(y428)/hT2</i>	18
Trial #2						
WT	wildtype	Day 2	88.75	TY4986	<i>htp-3(y428)/hT2</i>	62.15
WT	wildtype	Day 5	84.2105263	TY4986	<i>htp-3(y428)/hT2</i>	48.95
WT	wildtype	Day 7	67	TY4986	<i>htp-3(y428)/hT2</i>	31.95
WT	wildtype	Day 9	46.55	TY4986	<i>htp-3(y428)/hT2</i>	22.5
Trial #3						
WT	wildtype	Day 2	93.7	TY4986	<i>htp-3(y428)/hT2</i>	71.95
WT	wildtype	Day 5	69.5	TY4986	<i>htp-3(y428)/hT2</i>	69.5
WT	wildtype	Day 7	81.05	TY4986	<i>htp-3(y428)/hT2</i>	51.2631579
WT	wildtype	Day 9	47.1	TY4986	<i>htp-3(v428)/hT2</i>	12.8333333

Appendix Table 6: Pumping rate of meiosis mutants over time

Pumping						
Trial #1						
Strain	Genotype	Age	Pumps (30 sec)	Strain	Genotype	Thrashes (30 sec)
WT	wildtype	Day 2	108.75	AV106	<i>spo-11(ok79)/nT1</i>	96.5
WT	wildtype	Day 5	76.58333333	AV106	<i>spo-11(ok79)/nT1</i>	83.5
WT	wildtype	Day 7	70.5	AV106	<i>spo-11(ok79)/nT1</i>	55.83333333
WT	wildtype	Day 9	26.96078431	AV106	<i>spo-11(ok79)/nT1</i>	28.58333333
Trial #2						
WT	wildtype	Day 2	97.75	AV106	<i>spo-11(ok79)/nT1</i>	95.5
WT	wildtype	Day 5	66.66666667	AV106	<i>spo-11(ok79)/nT1</i>	49.41666667
WT	wildtype	Day 7	58.58333333	AV106	<i>spo-11(ok79)/nT1</i>	36.91666667
WT	wildtype	Day 9	24.83333333	AV106	<i>spo-11(ok79)/nT1</i>	21
Trial #3						
WT	wildtype	Day 2	96.75	AV106	<i>spo-11(ok79)/nT1</i>	88.41666667
WT	wildtype	Day 5	77.91666667	AV106	<i>spo-11(ok79)/nT1</i>	80.16666667
WT	wildtype	Day 7	72.41666667	AV106	<i>spo-11(ok79)/nT1</i>	63
WT	wildtype	Day 9	41.33333333	AV106	<i>spo-11(ok79)/nT1</i>	25.72916667
Trial #1						
Strain	Genotype	Age	Pumps (30 sec)	Strain	Genotype	Thrashes (30 sec)
WT	wildtype	Day 2	134.92	AV477	<i>dsb-2(me96)</i>	135.75
WT	wildtype	Day 5	101.5	AV477	<i>dsb-2(me96)</i>	85.33
WT	wildtype	Day 7	101.25	AV477	<i>dsb-2(me96)</i>	50.38
WT	wildtype	Day 9	21.67	AV477	<i>dsb-2(me96)</i>	15.48
Trial #2						
WT	wildtype	Day 2	140.17	AV477	<i>dsb-2(me96)</i>	118.58
WT	wildtype	Day 5	108.14	AV477	<i>dsb-2(me96)</i>	110.5
WT	wildtype	Day 7	83.44	AV477	<i>dsb-2(me96)</i>	77.92
WT	wildtype	Day 9	57.4	AV477	<i>dsb-2(me96)</i>	40.21
Trial #3						
WT	wildtype	Day 2	116.42	AV477	<i>dsb-2(me96)</i>	108.92
WT	wildtype	Day 5	109.08	AV477	<i>dsb-2(me96)</i>	95.39
WT	wildtype	Day 7	64.83	AV477	<i>dsb-2(me96)</i>	55.73
WT	wildtype	Day 9	39.42	AV477	<i>dsb-2(me96)</i>	24.49
Trial #1						
Strain	Genotype	Age	Pumps (30 sec)	Strain	Genotype	Thrashes (30 sec)
WT	wildtype	Day 2	134.9166667	TY4986	<i>htp-3(y428)/hT2</i>	118.8333333
WT	wildtype	Day 5	101.5	TY4986	<i>htp-3(y428)/hT2</i>	55.58333333
WT	wildtype	Day 7	101.25	TY4986	<i>htp-3(y428)/hT2</i>	48.75
WT	wildtype	Day 9	21.66666667	TY4986	<i>htp-3(y428)/hT2</i>	19.0625
Trial #2						
WT	wildtype	Day 2	108.75	TY4986	<i>htp-3(y428)/hT2</i>	90.25
WT	wildtype	Day 5	76.58333333	TY4986	<i>htp-3(y428)/hT2</i>	54.75
WT	wildtype	Day 7	70.5	TY4986	<i>htp-3(y428)/hT2</i>	41.58333333
WT	wildtype	Day 9	26.96078431	TY4986	<i>htp-3(y428)/hT2</i>	24.1025641
Trial #3						
WT	wildtype	Day 2	97.75	TY4986	<i>htp-3(y428)/hT2</i>	82.41666667
WT	wildtype	Day 5	66.66666667	TY4986	<i>htp-3(y428)/hT2</i>	43.08333333
WT	wildtype	Day 7	58.58333333	TY4986	<i>htp-3(y428)/hT2</i>	25.5
WT	wildtype	Day 9	25.78947368	TY4986	<i>htp-3(y428)/hT2</i>	11.66666667

Appendix Table 7: Learning index of meiosis mutants with age

Learning					
Strain	Genotype	Age	Learning index		
			Trial #1	Trial #2	Trial #3
WT	wildtype	Day 1	0.4952	0.4529	0.4897
		Day 5	0.241	0.2294	0.26429
AV477	<i>dsb-2(me96)</i>	Day 1	0.4869	0.4683	0.49074
		Day 5	-0.0123	0.01136	0.0178
TY4986	<i>htp-3(y428)/hT2</i>	Day 1	0.39	0.3801	0.41897
		Day 5	0.1667	0.1315	0.188
AV106	<i>spo-11(ok79)/nT1</i>	Day 1	0.3977	0.339882	0.3682
		Day 5	0.2	0.166	0.1555

Appendix Table 8: Survival of *dsb-2* mutants upon exposure to PA14

Strain	n= obs/tot	Mean + SE (hours)	P vs N2
Trial #1			
N2	45/79	79.68 + 2.97	
<i>dsb-2</i>	69/91	65.07 + 1.79	0.000023
Trial #2			
N2	95/116	87.31+1.78	
<i>dsb-2</i>	78/95	70.42+1.37	<0.0001
Trial #3 (Figure)			
N2	52/87	83.49 +2.26	
<i>dsb-2</i>	42/58	62.78 +2.06	<0.0001

Appendix Table 9: Aggregation of PAB-1 in meiosis mutant

Percent of animals in each category of aggregation levels over time for each meiosis mutant

WT				
Trial #1				
	low	medium	high	diffuse
Day 2	100	0	0	0
Day 5	95	0	5	0
Day 8	35	25	40	0
Day 10	0	29.412	70.588	0
Day 12	0	0	50	50
Trial #2				
	low	medium	high	diffuse
Day 2	95	5	0	0
Day 5	50	45	5	0
Day 8	10	35	50	5
Day 10	5	35	45	15
Day 12	0	0	93.333	6.667
Trial #3				
	low	medium	high	diffuse
Day 2	100	0	0	0
Day 5	85	15	0	0
Day 8	27.8	50	22.222	0
Day 10	9.52	14.286	76.19	0
Day 12	0	12.5	81.25	6.25

<i>dsb-2</i>				
Trial #1				
low	medium	high	diffuse	
100	0	0	0	
52.63	21.053	26.32	0	
25	25	35	15	
0	21.429	57.14	21.4286	
0	0	72.22	27.7778	
Trial #2				
low	medium	high	diffuse	
90	10	0	0	
80	5	15	0	
5	45	50	0	
0	20	75	5	
0	0	94.12	5.88235	
Trial #3				
low	medium	high	diffuse	
100	0	0	0	
100	0	0	0	
26.32	26.316	47.37	0	
35.29	17.647	47.06	0	
0	0	84.62	15.3846	

<i>htp-3</i>				
Trial #1				
	low	medium	high	diffuse
Day 2	75	25	0	0
Day 5	43.8	31.25	18.75	6.25
Day 8	19	28.571	38.095	14.29
Day 10	0	27.778	33.333	38.89
Day 12	0	0	57.143	42.86
Trial #2				
	low	medium	high	diffuse
Day 2	90	5	0	5
Day 5	75	10	10	5
Day 8	42.1	31.579	21.053	5.263
Day 10	0	38.095	33.333	28.57
Day 12	0	6.25	31.25	62.5
Trial #3				
	low	medium	high	diffuse
Day 2	89.5	10.526	0	0
Day 5	68.4	26.316	0	5.263
Day 8	38.9	50	11.111	0
Day 10	10	5	85	0
Day 12	0	4.7619	23.81	71.43

<i>spo-11</i>				
Trial #1				
low	medium	high	diffuse	
36.84	31.579	10.53	21.0526	
5.263	21.053	36.84	36.8421	
10	0	5	85	
0	0	5	95	
Trial #2				
low	medium	high	diffuse	
25	75	0	0	
5	20	25	50	
0	0	0	100	
0	0	0	100	
Trial #3				
low	medium	high	diffuse	
45	55	0	0	
0	33.333	11.11	55.5556	
0	13.333	0	86.6667	
0	0	6.25	93.75	

Appendix Table 10: Paralysis of *unc-52* animals with meiosis genes knocked down

<i>unc-52</i> paralysis assay					
Trial #1					
Strain	Genotype	RNAi	n = obs/total	Mean (hours) ±	P value vs L4440
HE250	<i>unc-52(e669su250)</i>	L4440	97/103	48.7 ± 1.36	
HE250	<i>unc-52(e669su250)</i>	<i>dsb-2</i>	83/89	43.25 ± 0.95	0.0008
HE250	<i>unc-52(e669su250)</i>	<i>htp-3</i>	94/95	42.84 ± 1.11	0.0013
HE250	<i>unc-52(e669su250)</i>	<i>spo-11</i>	91/95	43.99 ± 1.09	0.0042
Trial #2					
HE250	<i>unc-52(e669su250)</i>	L4440	82/113	49.4 + 1.82	
HE250	<i>unc-52(e669su250)</i>	<i>dsb-2</i>	88/91	43.91 + 1.82	0.0089
HE250	<i>unc-52(e669su250)</i>	<i>htp-3</i>	99/105	45.09 + 1.25	0.0539
HE250	<i>unc-52(e669su250)</i>	<i>spo-11</i>	98/99	45.01 + 0.77	0.1035

Appendix Table 11: Knockdown of *cup-4* in *spo-11* mutants

Trial #1				
Strain/Condition	n= tot/obs	Mean + S.E.	P vs N2 on L440	P vs <i>spo-11(me44)</i> on L440
N2 on L440	92/106	16.01 + 0.53		<0.0001
<i>spo-11(me44)</i> on L440	80/88	11.38 + 0.36	<0.0001	
N2 on <i>cup-4</i>	65/96	13.63 + 0.54	0.0025	0.0003
<i>spo-11(me44)</i> on <i>cup-4</i>	80/90	12.92 + 0.45	0.000011	0.0057
Trial #2 - JL - shown in figure				
Strain/Condition	n= tot/obs	Mean + S.E.	P vs N2 on L440	P vs <i>spo-11(me44)</i> on L440
N2 on L440	80/98	16.59 + 0.4		< 0.0001
<i>spo-11(me44)</i> on L440	43/47	11.01 + 0.46	< 0.0001	
N2 on <i>cup-4</i>	85/91	15.76 + 0.45	0.439	< 0.0001
<i>spo-11(me44)</i> on <i>cup-4</i>	43/45	11.11 + 0.47	< 0.0001	< 0.0001
Trial #3 (Cassandra Rios)				
Strain/Condition	n= tot/obs	Mean + S.E.	P vs N2 on L440	P vs <i>spo-11(me44)</i> on L440
N2 on L440	69/99	17.79 + 0.6		< 0.0001
<i>spo-11(me44)</i> on L440	39/46	9.63 + 0.59	< 0.0001	
N2 on <i>cup-4</i>	66/91	16.5 + 0.6	0.118	< 0.0001
<i>spo-11(me44)</i> on <i>cup-4</i>	44/61	9.5 + 0.48	< 0.0001	0.8814

Appendix Table 12: Wnt ligand knockdown in *spo-11* and *htp-3* mutants

Trial #1 - shown in figure					
Strain	RNAi	n = obs/tot	mean (days) ± S.E.	P vs N2 L4440	P vs L4440
N2	L4440	55/93	15.88 ± 0.53		
N2	<i>cwn-2</i>	84/113	16.52 ± 0.36	0.4299	0.4299
N2	<i>egl-20</i>	52/111	15.79 ± 0.67	0.9184	0.9184
<i>spo-11</i>	L4440	51/78	11.63 ± 0.42	1.60E-08	
<i>spo-11</i>	<i>cwn-2</i>	38/89	12.04 ± 0.35	5.20E-07	0.3516
<i>spo-11</i>	<i>egl-20</i>	50/78	13.04 ± 0.42	0.0001	0.0352
<i>htp-3</i>	L4440	20/46	17.84 ± 0.99	0.0658	
<i>htp-3</i>	<i>cwn-2</i>	19/33	19.51 ± 0.74	0.0007	0.2223
<i>htp-3</i>	<i>egl-20</i>	17/43	14.79 ± 0.45	0.1861	0.5898
Strain	RNAi	n = obs/tot	mean (days) ± S.E.	P vs N2 L4440	P vs L4440
N2	L4440	82/103	14.31 ± 0.43		
N2	<i>cwn-1</i>	87/100	15.7 ± 0.35	0.0704	0.0704
<i>htp-3</i>	L4440	100/128	15.7 ± 0.53	0.0012	
<i>htp-3</i>	<i>cwn-1</i>	67/88	15.75 ± 0.57	0.0036	0.5972
<i>spo-11</i>	L4440	65/76	11.59 ± 0.37	<0.0001	
<i>spo-11</i>	<i>cwn-1</i>	89/100	10.06 ± 0.3	<0.0001	0.003
Trial #2					
Strain	RNAi	n = obs/tot	mean (days) ± S.E.	P vs N2 L4440	P vs L4440
N2	L4440	103/123	15.26 ± 0.39		
N2	<i>cwn-2</i>	70/111	16.08 ± 0.57	0.05	0.05
N2	<i>egl-20</i>	97/135	17.58 ± 0.44	0.000015	0.000015
N2	<i>lin-44</i>	119/136	13.64 ± 0.41	0.0461	0.0461
<i>htp-3</i>	L4440	97/112	15.77 ± 0.63	0.0175	
<i>htp-3</i>	<i>cwn-2</i>	93/108	14.6 ± 0.68	0.4516	0.3933
<i>htp-3</i>	<i>egl-20</i>	77/89	15.41 ± 0.7	0.0988	0.5787
<i>htp-3</i>	<i>lin-44</i>	84/92	14.89 ± 0.7	0.2481	0.4292
<i>spo-11</i>	L4440	50/71	11.35 ± 0.47	6.80E-09	
<i>spo-11</i>	<i>cwn-2</i>	60/73	11.58 ± 0.35	<0.0001	0.8307
<i>spo-11</i>	<i>egl-20</i>	42/63	10.57 ± 0.48	<0.0001	0.2693
<i>spo-11</i>	<i>lin-44</i>	86/93	10.28 ± 0.36	<0.0001	0.0788
Trial #3					
Strain	RNAi	n = obs/tot	mean (days) ± S.E.	P vs N2 L4440	
N2	L4440	73/88	16.82 ± 0.49		
N2	<i>egl-20</i>	59/117	17.16 ± 0.42	0.013	
<i>spo-11</i>	L4440	77/113	12.3 ± 0.46		
<i>spo-11</i>	<i>egl-20</i>	66/76	12.5 ± 0.55	<0.0001	

Appendix Table 13: Knockdown of upregulated genes in *dsb-2*, *htp-3*, and *spo-11* mutants

Trial #1 - Whole life				
Strain	RNAi	n = obs/tot	Mean \pm S.E.	P vs L4440
N2	L4440	104/132	16.49 \pm 0.43	
N2	<i>ketn-1</i>	100/119	13.27 \pm 0.41	5.50E-07
N2	<i>him-4</i>	88/91	3.18 \pm 0.3	0
N2	<i>mua-3</i>	88/118	16.27 \pm 0.53	0.8699
N2	F39C12.1	96/118	13.24 \pm 0.4	5.60E-07
N2	<i>unc-2</i>	95/121	15.8 \pm 0.51	0.6618
N2	F45D3.4	107/128	16.02 \pm 0.35	0.1366
N2	C01B4.7	99/121	18.24 \pm 0.5	0.0047
N2	<i>sma-1</i>	110/128	11.39 \pm 0.38	0
N2	<i>dig-1</i>	107/130	13.9 \pm 0.39	0.000033
N2	<i>lrp-2</i>	96/127	17.1 \pm 0.45	0.4871
N2	Y19D10A.5	109/131	18.05 \pm 0.4	0.0275
Trial #2 - Whole life				
Strain	RNAi	n = obs/tot	Mean \pm S.E.	P vs L4440
N2	L4440	70/108	15.65 \pm 0.51	
N2	C01B4.7	97/114	15.48 \pm 0.39	0.6533
N2	<i>irld-53</i>	87/130	17.21 \pm 0.46	0.0277
N2	Y19D10A.5	72/101	15.95 \pm 0.52	0.6448
Trial #3 - Whole life - in figure				
Strain	RNAi	n = obs/total	Mean \pm S.E.	P vs L4440
N2	L4440	92/120	14.83 \pm 0.47	
N2	C01B4.7	57/97	15.23 \pm 0.67	0.4343
N2	Y19D10A.5	76/116	17.85 \pm 0.6	0.0001
N2	<i>irld-53</i>	59/95	17.97 \pm 0.62	<0.0001
Trial #1 Adult only				
Strain	RNAi	n=obs/tot	Mean (days)	P vs L4440
N2	L4440	44/86	19.33 \pm 0.71	
N2	<i>unc-2</i>	39/76	18.28 \pm 0.72	0.312
N2	F39C12.1	35/72	18.08 \pm 0.77	0.3423
N2	Y19D10A.5	54/93	19.58 \pm 0.55	0.8287
N2	<i>sma-1</i>	55/84	16.28 \pm 0.58	0.0004
N2	<i>mua-3</i>	52/91	17.59 \pm 0.49	0.1233
N2	C01B4.7	42/68	19.68 \pm 0.83	0.5526
N2	<i>irld-53</i>	57/97	18.07 \pm 0.6	0.1469
N2	F45D3.4	60/89	18.28 \pm 0.61	0.2353
N2	<i>ketn-1</i>	44/70	16.65 \pm 0.56	0.0029
N2	<i>dig-1</i>	48/98	17.82 \pm 0.54	0.041
N2	<i>him-4</i>	34/96	15.09 \pm 0.83	0.0001
N2	<i>lrp-2</i>	32/82	20.07 \pm 0.72	0.3772

Appendix Table 14: Lifespans of RPN-6.1, CCT-2, or CCT-8 overexpression strains with *spo-11* or *htp-3*

knocked down

Trial #1						P value	
Strain	genotype	RNAi	n=obs/tot	mean (days)	S.E.	vs <i>myo-3p::GFP</i>	vs <i>myo-3p::GFP</i> on L4440
AGD597	<i>sur-5p::rpn-6</i>	L4440	68/75	14.73	0.47	0.0051	
AGD598	<i>sur-5p::rpn-6</i>	L4440	77/99	15.7	0.41	0.0345	
AGD614	<i>myo-3p::GFP</i>	L4440	43/48	16.69	0.86		
AGD597	<i>sur-5p::rpn-6</i>	<i>htp-3</i>	88/104	14.99	0.47	0.8271	0.0203
AGD598	<i>sur-5p::rpn-6</i>	<i>htp-3</i>	113/138	15.66	0.4	0.3772	0.0751
AGD614	<i>myo-3p::GFP</i>	<i>htp-3</i>	33/39	14.8	0.79		0.0358
AGD597	<i>sur-5p::rpn-6</i>	<i>spo-11</i>	71/94	14.78	0.46	0.306	0.0081
AGD598	<i>sur-5p::rpn-6</i>	<i>spo-11</i>	87/117	16.25	0.5	0.0084	0.2816
AGD614	<i>myo-3p::GFP</i>	<i>spo-11</i>	31/66	12.27	0.34		0.0074
Trial #2 - in figure						P value	
Strain	Genotype	RNAi	n=obs/tot	mean (days)	S.E.	vs <i>myo-3p::GFP</i>	vs <i>myo-3p::GFP</i> on L4440
AGD597	<i>sur-5p::rpn-6</i>	L4440	73/89	16.68	0.47	0.2074	0.2074
AGD597	<i>sur-5p::rpn-6</i>	<i>spo-11</i>	67/78	16.87	0.57	0.000035	0.1642
AGD614	<i>myo-3p::GFP</i>	L4440	54/80	14.49	0.6		
AGD614	<i>myo-3p::GFP</i>	<i>spo-11</i>	38/59	12.75	0.64		0.0403

Trial #1						P value	
Strain	genotype	RNAi	n=obs/tot	mean (days)	S.E.	vs <i>myo3p::GFP</i>	vs L4440
DVG9	<i>ocbEx9[myo3p::GFP]</i>	L4440	40/50	12.39	0.65		
DVG9	<i>ocbEx9[myo3p::GFP]</i>	<i>spo-11</i>	42/43	11.95	0.5	0.3896	0.3896
DVG47	<i>ocbEx47[psur5::cct-2, pmyo3::GFP]</i>	L4440	104/140	12.96	0.29	0.6817	
DVG47	<i>ocbEx47[psur5::cct-2, pmyo3::GFP]</i>	<i>spo-11</i>	77/110	12.35	0.26	0.3688	0.1434
DVG48	<i>ocbEx48[psur5::cct-8, pmyo3::GFP]</i>	L4440	89/109	11.55	0.32	0.3772	
DVG48	<i>ocbEx48[psur5::cct-8, pmyo3::GFP]</i>	<i>spo-11</i>	95/143	12.4	0.32	0.7183	0.0127

Appendix Table 15: Primers

Primer	Sequence
ins-7_FWD	AGAACCAGAAGAGTCCCTG
ins-7_REV	TGCGAATCGAATACTGAAGT
dsb-2_clone_FWD	GCA CGT GGC CTG AAA GTT GAG
dsb-2_clone_REV	CGT GTT GCT CAA GCT GTG GTT G
spo-11_FWD	CGTTGACTTTGAGAATATCGAC
spo-11_REV	GACAGTGCAAATCTCTATCCA
hsp-6_FWD	TCTTCGTGTCATCAACGAG
hsp-6_REV	ACAGCGATGATCTTATCTCC
hsp-4_FWD	GGAGGATCAACCAGAATTCC
hsp-4_REV	GGTTGATTCCACGAGATGG
hsp-16.2_FWD	ATATGGCTCTGATGGAACG
hsp-16.2_REV	CAT TGT TAA CAA TCT CAG AAG AC

Bibliography

1. Niccoli T, Partridge L. Ageing as a risk factor for disease. *Curr Biol*. 2012;22(17):R741-52. Epub 2012/09/15. doi: 10.1016/j.cub.2012.07.024. PubMed PMID: 22975005.
2. World Population Ageing. United Nations, Department of Economic and Social Affairs, Population Division, 2015.
3. Gavrilov LA, Gavrilova NS. Evolutionary theories of aging and longevity. *ScientificWorldJournal*. 2002;2:339-56. Epub 2002/02/07. doi: 10.1100/tsw.2002.96. PubMed PMID: 12806021; PMCID: PMC6009642.
4. Bjorksten J, Tenhu H. The crosslinking theory of aging--added evidence. *Exp Gerontol*. 1990;25(2):91-5. Epub 1990/01/01. doi: 10.1016/0531-5565(90)90039-5. PubMed PMID: 2115005.
5. Harman D. Aging: a theory based on free radical and radiation chemistry. *J Gerontol*. 1956;11(3):298-300. Epub 1956/07/01. doi: 10.1093/geronj/11.3.298. PubMed PMID: 13332224.
6. Harman D. The biologic clock: the mitochondria? *J Am Geriatr Soc*. 1972;20(4):145-7. Epub 1972/04/01. doi: 10.1111/j.1532-5415.1972.tb00787.x. PubMed PMID: 5016631.
7. Williams GC. Pleiotropy, Natural Selection, and the Evolution of Senescence. *Evolution* 1957. p. 398-411.
8. Kirkwood TB, Holliday R. The evolution of ageing and longevity. *Proc R Soc Lond B Biol Sci*. 1979;205(1161):531-46. Epub 1979/09/21. PubMed PMID: 42059.
9. Westendorp RG, Kirkwood TB. Human longevity at the cost of reproductive success. *Nature*. 1998;396(6713):743-6. doi: 10.1038/25519. PubMed PMID: 9874369.
10. Le Bourg E. Does reproduction decrease longevity in human beings? *Ageing Res Rev*. 2007;6(2):141-9. Epub 2007/05/01. doi: 10.1016/j.arr.2007.04.002. PubMed PMID: 17532269.
11. Hurt LS, Ronsmans C, Thomas SL. The effect of number of births on women's mortality: systematic review of the evidence for women who have completed their childbearing. *Popul Stud (Camb)*. 2006;60(1):55-71. doi: 10.1080/00324720500436011. PubMed PMID: 16464775.
12. Gagnon A, Smith KR, Tremblay M, Vézina H, Paré PP, Desjardins B. Is there a trade-off between fertility and longevity? A comparative study of women from three large historical

- databases accounting for mortality selection. *Am J Hum Biol.* 2009;21(4):533-40. doi: 10.1002/ajhb.20893. PubMed PMID: 19298004; PMCID: PMC6121733.
13. Min KJ, Lee CK, Park HN. The lifespan of Korean eunuchs. *Curr Biol.* 2012;22(18):R792-3. doi: 10.1016/j.cub.2012.06.036. PubMed PMID: 23017989.
 14. Doblhammer G. Reproductive history and mortality later in life: a comparative study of England and Wales and Austria. *Popul Stud (Camb).* 2000;54(2):169-76. doi: 10.1080/713779087. PubMed PMID: 11624633.
 15. Grundy E, Tomassini C. Fertility history and health in later life: a record linkage study in England and Wales. *Soc Sci Med.* 2005;61(1):217-28. doi: 10.1016/j.socscimed.2004.11.046. PubMed PMID: 15847974.
 16. Gagnon A. Natural fertility and longevity. *Fertil Steril.* 2015;103(5):1109-16. doi: 10.1016/j.fertnstert.2015.03.030. PubMed PMID: 25934597.
 17. Ricklefs RE, Cadena CD. Lifespan is unrelated to investment in reproduction in populations of mammals and birds in captivity. *Ecol Lett.* 2007;10(10):867-72. doi: 10.1111/j.1461-0248.2007.01085.x. PubMed PMID: 17845285.
 18. Jones OR, Gaillard JM, Tuljapurkar S, Alho JS, Armitage KB, Becker PH, Bize P, Brommer J, Charmantier A, Charpentier M, Clutton-Brock T, Dobson FS, Festa-Bianchet M, Gustafsson L, Jensen H, Jones CG, Lillandt BG, McCleery R, Merilä J, Neuhaus P, Nicoll MA, Norris K, Oli MK, Pemberton J, Pietiäinen H, Ringsby TH, Roulin A, Saether BE, Setchell JM, Sheldon BC, Thompson PM, Weimerskirch H, Jean Wickings E, Coulson T. Senescence rates are determined by ranking on the fast-slow life-history continuum. *Ecol Lett.* 2008;11(7):664-73. Epub 2008/04/28. doi: 10.1111/j.1461-0248.2008.01187.x. PubMed PMID: 18445028.
 19. Lund E, Arnesen E, Borgan JK. Pattern of childbearing and mortality in married women--a national prospective study from Norway. *J Epidemiol Community Health.* 1990;44(3):237-40. doi: 10.1136/jech.44.3.237. PubMed PMID: 2273363; PMCID: PMC1060649.
 20. Mirowsky J. Age at first birth, health, and mortality. *J Health Soc Behav.* 2005;46(1):32-50. doi: 10.1177/002214650504600104. PubMed PMID: 15869119.
 21. Helle S, Lummaa V, Jokela J. Are reproductive and somatic senescence coupled in humans? Late, but not early, reproduction correlated with longevity in historical Sami women. *Proc Biol Sci.* 2005;272(1558):29-37. doi: 10.1098/rspb.2004.2944. PubMed PMID: 15875567; PMCID: PMC1634941.
 22. Tabatabaie V, Atzmon G, Rajpathak SN, Freeman R, Barzilai N, Crandall J. Exceptional longevity is associated with decreased reproduction. *Aging (Albany NY).*

- 2011;3(12):1202-5. doi: 10.18632/aging.100415. PubMed PMID: 22199025; PMCID: PMC3273900.
23. Perls TT, Alpert L, Fretts RC. Middle-aged mothers live longer. *Nature*. 1997;389(6647):133. doi: 10.1038/38148. PubMed PMID: 9296486.
 24. Sun F, Sebastiani P, Schupf N, Bae H, Andersen SL, McIntosh A, Abel H, Elo IT, Perls TT. Extended maternal age at birth of last child and women's longevity in the Long Life Family Study. *Menopause*. 2015;22(1):26-31. doi: 10.1097/GME.0000000000000276. PubMed PMID: 24977462; PMCID: PMC4270889.
 25. Grundy E. Women's fertility and mortality in late mid life: A comparison of three contemporary populations. *Am J Hum Biol*. 2009;21(4):541-7. doi: 10.1002/ajhb.20953. PubMed PMID: 19418527.
 26. Egan KM, Giovannucci E, Titus-Ernstoff L, Newcomb P, Stampfer M. Mixed blessings for middle-aged mothers. *Nature*. 1997;389(6654):922. doi: 10.1038/40042. PubMed PMID: 9353115.
 27. Zwaan B, Bijlsma R, Hoekstra RF. Artificial Selection for Developmental Time in *Drosophila Melanogaster* in Relation to the Evolution of Aging: Direct and Correlated Responses. *Evolution*. 1995;49(4):635-48. Epub 1995/08/01. doi: 10.1111/j.1558-5646.1995.tb02300.x. PubMed PMID: 28565147.
 28. Hughes SE, Evason K, Xiong C, Kornfeld K. Genetic and pharmacological factors that influence reproductive aging in nematodes. *PLoS Genet*. 2007;3(2):e25. Epub 2007/02/20. doi: 10.1371/journal.pgen.0030025. PubMed PMID: 17305431; PMCID: PMC1797816.
 29. Snowdon DA, Kane RL, Beeson WL, Burke GL, Sprafka JM, Potter J, Iso H, Jacobs DR, Phillips RL. Is early natural menopause a biologic marker of health and aging? *Am J Public Health*. 1989;79(6):709-14. doi: 10.2105/ajph.79.6.709. PubMed PMID: 2729468; PMCID: PMC1349628.
 30. Wu X, Cai H, Kallianpur A, Gao YT, Yang G, Chow WH, Li HL, Zheng W, Shu XO. Age at menarche and natural menopause and number of reproductive years in association with mortality: results from a median follow-up of 11.2 years among 31,955 naturally menopausal Chinese women. *PLoS One*. 2014;9(8):e103673. Epub 2014/08/04. doi: 10.1371/journal.pone.0103673. PubMed PMID: 25090234; PMCID: PMC4121137.
 31. Jacobsen BK, Heuch I, Kvåle G. Age at natural menopause and all-cause mortality: a 37-year follow-up of 19,731 Norwegian women. *Am J Epidemiol*. 2003;157(10):923-9. doi: 10.1093/aje/kwg066. PubMed PMID: 12746245.
 32. Ossewaarde ME, Bots ML, Verbeek AL, Peeters PH, van der Graaf Y, Grobbee DE, van der Schouw YT. Age at menopause, cause-specific mortality and total life expectancy.

- Epidemiology. 2005;16(4):556-62. Epub 2005/06/14. doi: 10.1097/01.ede.0000165392.35273.d4. PubMed PMID: 15951675.
33. Mondul AM, Rodriguez C, Jacobs EJ, Calle EE. Age at natural menopause and cause-specific mortality. *Am J Epidemiol*. 2005;162(11):1089-97. Epub 2005/10/12. doi: 10.1093/aje/kwi324. PubMed PMID: 16221806.
 34. Podfigurna-Stopa A, Czyzyk A, Grymowicz M, Smolarczyk R, Katulski K, Czajkowski K, Meczekalski B. Premature ovarian insufficiency: the context of long-term effects. *J Endocrinol Invest*. 2016;39(9):983-90. Epub 2016/04/20. doi: 10.1007/s40618-016-0467-z. PubMed PMID: 27091671; PMCID: PMC4987394.
 35. Levine ME, Lu AT, Chen BH, Hernandez DG, Singleton AB, Ferrucci L, Bandinelli S, Salfati E, Manson JE, Quach A, Kusters CDJ, Kuh D, Wong A, Teschendorff AE, Widschwendter M, Ritz BR, Absher D, Assimes TL, Horvath S. Menopause accelerates biological aging. *Proceedings of the National Academy of Sciences of the United States of America*. 2016;113(33):9327-32. doi: 10.1073/pnas.1604558113. PubMed PMID: PMC4995944.
 36. Giller A, Andrawus M, Gutman D, Atzmon G. Pregnancy as a model for aging. *Ageing Res Rev*. 2020;62:101093. Epub 2020/06/06. doi: 10.1016/j.arr.2020.101093. PubMed PMID: 32502628.
 37. Finkel T. Oxygen radicals and signaling. *Curr Opin Cell Biol*. 1998;10(2):248-53. Epub 1998/04/30. doi: 10.1016/s0955-0674(98)80147-6. PubMed PMID: 9561849.
 38. Naim N, Amrit FRG, McClendon TB, Yanowitz JL, Ghazi A. The molecular tug of war between immunity and fertility: Emergence of conserved signaling pathways and regulatory mechanisms. *Bioessays*. 2020;42(12):e2000103. Epub 2020/11/11. doi: 10.1002/bies.202000103. PubMed PMID: 33169418; PMCID: PMC8219210.
 39. Ryan CP, Hayes MG, Lee NR, McDade TW, Jones MJ, Kobor MS, Kuzawa CW, Eisenberg DTA. Reproduction predicts shorter telomeres and epigenetic age acceleration among young adult women. *Sci Rep*. 2018;8(1):11100. Epub 2018/07/25. doi: 10.1038/s41598-018-29486-4. PubMed PMID: 30038336; PMCID: PMC6056536.
 40. Garratt M, Kee AJ, Palme R, Brooks RC. Male Presence can Increase Body Mass and Induce a Stress-Response in Female Mice Independent of Costs of Offspring Production. *Sci Rep*. 2016;6:23538. Epub 2016/03/23. doi: 10.1038/srep23538. PubMed PMID: 27004919; PMCID: PMC4804214.
 41. Flanagan KA, Webb W, Stowers L. Analysis of male pheromones that accelerate female reproductive organ development. *PLoS One*. 2011;6(2):e16660. Epub 2011/02/08. doi: 10.1371/journal.pone.0016660. PubMed PMID: 21347429; PMCID: PMC3035649.

42. Chapman T, Liddle LF, Kalb JM, Wolfner MF, Partridge L. Cost of mating in *Drosophila melanogaster* females is mediated by male accessory gland products. *Nature*. 1995;373(6511):241-4. doi: 10.1038/373241a0. PubMed PMID: 7816137.
43. Maures TJ, Booth LN, Benayoun BA, Izrayelit Y, Schroeder FC, Brunet A. Males shorten the life span of *C. elegans* hermaphrodites via secreted compounds. *Science*. 2014;343(6170):541-4. Epub 2013/11/29. doi: 10.1126/science.1244160. PubMed PMID: 24292626; PMCID: PMC4126796.
44. Shi C, Murphy CT. Mating induces shrinking and death in *Caenorhabditis* mothers. *Science*. 2014;343(6170):536-40. Epub 2013/12/19. doi: 10.1126/science.1242958. PubMed PMID: 24356112; PMCID: PMC6719292.
45. Booth LN, Maures TJ, Yeo RW, Tantilert C, Brunet A. Self-sperm induce resistance to the detrimental effects of sexual encounters with males in hermaphroditic nematodes. *Elife*. 2019;8. Epub 2019/07/08. doi: 10.7554/eLife.46418. PubMed PMID: 31282863; PMCID: PMC6697445.
46. Ludewig AH, Artyukhin AB, Aprison EZ, Rodrigues PR, Pulido DC, Burkhardt RN, Panda O, Zhang YK, Gudibanda P, Ruvinsky I, Schroeder FC. An excreted small molecule promotes *C. elegans* reproductive development and aging. *Nat Chem Biol*. 2019;15(8):838-45. Epub 2019/07/20. doi: 10.1038/s41589-019-0321-7. PubMed PMID: 31320757; PMCID: PMC6650165.
47. Meslin C, Cherwin TS, Plakke MS, Hill J, Small BS, Goetz BJ, Wheat CW, Morehouse NI, Clark NL. Structural complexity and molecular heterogeneity of a butterfly ejaculate reflect a complex history of selection. *Proc Natl Acad Sci U S A*. 2017;114(27):E5406-E13. Epub 2017/06/19. doi: 10.1073/pnas.1707680114. PubMed PMID: 28630352; PMCID: PMC5502654.
48. Gwynne DT. Sexual conflict over nuptial gifts in insects. *Annu Rev Entomol*. 2008;53:83-101. doi: 10.1146/annurev.ento.53.103106.093423. PubMed PMID: 17680720.
49. Negroni MA, Macit MN, Stoldt M, Feldmeyer B, Foitzik S. Molecular regulation of lifespan extension in fertile ant workers. *Philos Trans R Soc Lond B Biol Sci*. 2021;376(1823):20190736. Epub 2021/03/09. doi: 10.1098/rstb.2019.0736. PubMed PMID: 33678017; PMCID: PMC7938160.
50. Sahm A, Platzer M, Koch P, Henning Y, Bens M, Groth M, Burda H, Begall S, Ting S, Goetz M, Van Daele P, Staniszevska M, Klose JM, Costa PF, Hoffmann S, Szafranski K, Dammann P. Increased longevity due to sexual activity in mole-rats is associated with transcriptional changes in the HPA stress axis. *Elife*. 2021;10. Epub 2021/03/17. doi: 10.7554/eLife.57843. PubMed PMID: 33724179; PMCID: PMC8012063.
51. Johns ME, Warzybok P, Bradley RW, Jahncke J, Lindberg M, Breed GA. Increased reproductive investment associated with greater survival and longevity in Cassin's auklets.

- Proc Biol Sci. 2018;285(1885). Epub 2018/08/31. doi: 10.1098/rspb.2018.1464. PubMed PMID: 30158312; PMCID: PMC6125915.
52. te Velde ER, Pearson PL. The variability of female reproductive ageing. *Hum Reprod Update*. 2002;8(2):141-54. Epub 2002/07/09. PubMed PMID: 12099629.
 53. Practice ACoOaGCoG, Medicine PCotASfR. Female age-related fertility decline. Committee Opinion No. 589. *Obstet Gynecol*. 2014;123(3):719-21. doi: 10.1097/01.AOG.0000444440.96486.61. PubMed PMID: 24553169.
 54. Hassold T, Hunt P. Maternal age and chromosomally abnormal pregnancies: what we know and what we wish we knew. *Curr Opin Pediatr*. 2009;21(6):703-8. Epub 2009/11/03. doi: 10.1097/MOP.0b013e328332c6ab. PubMed PMID: 19881348; PMCID: PMC2894811.
 55. Luo S, Murphy CT. *Caenorhabditis elegans* reproductive aging: Regulation and underlying mechanisms. *Genesis*. 2011;49(2):53-65. Epub 2010/11/26. doi: 10.1002/dvg.20694. PubMed PMID: 21105070.
 56. Andux S, Ellis RE. Apoptosis maintains oocyte quality in aging *Caenorhabditis elegans* females. *PLoS Genet*. 2008;4(12):e1000295. Epub 2008/12/05. doi: 10.1371/journal.pgen.1000295. PubMed PMID: 19057674; PMCID: PMC2585808.
 57. Luo S, Kleemann GA, Ashraf JM, Shaw WM, Murphy CT. TGF-beta and insulin signaling regulate reproductive aging via oocyte and germline quality maintenance. *Cell*. 2010;143(2):299-312. Epub 2010/10/16. doi: 10.1016/j.cell.2010.09.013. PubMed PMID: 20946987; PMCID: PMC2955983.
 58. Quesada-Candela C, Loose J, Ghazi A, Yanowitz JL. Molecular basis of reproductive senescence: insights from model organisms. *J Assist Reprod Genet*. 2021;38(1):17-32. Epub 2020/10/03. doi: 10.1007/s10815-020-01959-4. PubMed PMID: 33006069; PMCID: PMC7822982.
 59. David DC, Ollikainen N, Trinidad JC, Cary MP, Burlingame AL, Kenyon C. Widespread protein aggregation as an inherent part of aging in *C. elegans*. *PLoS Biol*. 2010;8(8):e1000450. Epub 2010/08/17. doi: 10.1371/journal.pbio.1000450. PubMed PMID: 20711477; PMCID: PMC2919420.
 60. Templeman NM, Murphy CT. Regulation of reproduction and longevity by nutrient-sensing pathways. *J Cell Biol*. 2018;217(1):93-106. Epub 2017/10/26. doi: 10.1083/jcb.201707168. PubMed PMID: 29074705; PMCID: PMC5748989.
 61. Gumienny TL, Savage-Dunn C. TGF- β signaling in *C. elegans*. *WormBook*. 2013:1-34. Epub 2013/07/10. doi: 10.1895/wormbook.1.22.2. PubMed PMID: 23908056; PMCID: PMC5081272.
 62. Luo S, Shaw WM, Ashraf J, Murphy CT. TGF-beta Sma/Mab signaling mutations uncouple reproductive aging from somatic aging. *PLoS Genet*. 2009;5(12):e1000789.

- Epub 2009/12/24. doi: 10.1371/journal.pgen.1000789. PubMed PMID: 20041217; PMCID: PMC2791159.
63. Templeman NM, Cota V, Keyes W, Kaletsky R, Murphy CT. CREB Non-autonomously Controls Reproductive Aging through Hedgehog/Patched Signaling. *Dev Cell*. 2020. Epub 2020/06/05. doi: 10.1016/j.devcel.2020.05.023. PubMed PMID: 32544391.
 64. Luo S, Kleemann GA, Ashraf JM, Shaw WM, Murphy CT. TGF- β and insulin signaling regulate reproductive aging via oocyte and germline quality maintenance. *Cell*. 2010;143(2):299-312. doi: 10.1016/j.cell.2010.09.013. PubMed PMID: 20946987; PMCID: PMC2955983.
 65. Gems D, Sutton AJ, Sundermeyer ML, Albert PS, King KV, Edgley ML, Larsen PL, Riddle DL. Two pleiotropic classes of *daf-2* mutation affect larval arrest, adult behavior, reproduction and longevity in *Caenorhabditis elegans*. *Genetics*. 1998;150(1):129-55. Epub 1998/09/02. doi: 10.1093/genetics/150.1.129. PubMed PMID: 9725835; PMCID: PMC1460297.
 66. Cassada RC, Russell RL. The dauerlarva, a post-embryonic developmental variant of the nematode *Caenorhabditis elegans*. *Dev Biol*. 1975;46(2):326-42. Epub 1975/10/01. doi: 10.1016/0012-1606(75)90109-8. PubMed PMID: 1183723.
 67. Lai CH, Chou CY, Ch'ang LY, Liu CS, Lin W. Identification of novel human genes evolutionarily conserved in *Caenorhabditis elegans* by comparative proteomics. *Genome Res*. 2000;10(5):703-13. Epub 2000/05/16. PubMed PMID: 10810093; PMCID: PMC310876.
 68. Nance J, Frøkjær-Jensen C. The *Caenorhabditis elegans* transgenic toolbox. *Genetics*. 2019;212(4):959-90. doi: 10.1534/genetics.119.301506. PubMed PMID: 31405997; PMCID: PMC6707460.
 69. Kamath RS, Fraser AG, Dong Y, Poulin G, Durbin R, Gotta M, Kanapin A, Le Bot N, Moreno S, Sohrmann M, Welchman DP, Zipperlen P, Ahringer J. Systematic functional analysis of the *Caenorhabditis elegans* genome using RNAi. *Nature*. 2003;421(6920):231-7. Epub 2003/01/17. doi: 10.1038/nature01278. PubMed PMID: 12529635.
 70. Rual JF, Ceron J, Koreth J, Hao T, Nicot AS, Hirozane-Kishikawa T, Vandenhaute J, Orkin SH, Hill DE, van den Heuvel S, Vidal M. Toward improving *Caenorhabditis elegans* phenome mapping with an ORFeome-based RNAi library. *Genome Res*. 2004;14(10B):2162-8. Epub 2004/10/19. doi: 10.1101/gr.2505604. PubMed PMID: 15489339; PMCID: PMC528933.
 71. Keith SA, Amrit FR, Ratnappan R, Ghazi A. The *C. elegans* healthspan and stress-resistance assay toolkit. *Methods*. 2014;68(3):476-86. Epub 2014/04/15. doi: 10.1016/j.ymeth.2014.04.003. PubMed PMID: 24727065.

72. Garigan D, Hsu AL, Fraser AG, Kamath RS, Ahringer J, Kenyon C. Genetic analysis of tissue aging in *Caenorhabditis elegans*: a role for heat-shock factor and bacterial proliferation. *Genetics*. 2002;161(3):1101-12. Epub 2002/07/24. PubMed PMID: 12136014; PMCID: PMC1462187.
73. Son HG, Altintas O, Kim EJE, Kwon S, Lee SV. Age-dependent changes and biomarkers of aging in *Caenorhabditis elegans*. *Aging Cell*. 2019;18(2):e12853. Epub 2019/02/09. doi: 10.1111/accel.12853. PubMed PMID: 30734981; PMCID: PMC6413654.
74. Herndon LA, Schmeissner PJ, Dudaronek JM, Brown PA, Listner KM, Sakano Y, Paupard MC, Hall DH, Driscoll M. Stochastic and genetic factors influence tissue-specific decline in ageing *C. elegans*. *Nature*. 2002;419(6909):808-14. Epub 2002/10/25. doi: 10.1038/nature01135. PubMed PMID: 12397350.
75. Collins JJ, Huang C, Hughes S, Kornfeld K. The measurement and analysis of age-related changes in *Caenorhabditis elegans*. *WormBook*. 2008:1-21. Epub 2008/04/03. doi: 10.1895/wormbook.1.137.1. PubMed PMID: 18381800; PMCID: PMC4781475.
76. Kenyon CJ. The genetics of ageing. *Nature*. 2010;464(7288):504-12. Epub 2010/03/26. doi: 10.1038/nature08980. PubMed PMID: 20336132.
77. Klass MR. A method for the isolation of longevity mutants in the nematode *Caenorhabditis elegans* and initial results. *Mech Ageing Dev*. 1983;22(3-4):279-86. Epub 1983/07/01. doi: 10.1016/0047-6374(83)90082-9. PubMed PMID: 6632998.
78. Friedman DB, Johnson TE. Three mutants that extend both mean and maximum life span of the nematode, *Caenorhabditis elegans*, define the age-1 gene. *J Gerontol*. 1988;43(4):B102-9. Epub 1988/07/01. doi: 10.1093/geronj/43.4.b102. PubMed PMID: 3385139.
79. Kenyon C. The plasticity of aging: insights from long-lived mutants. *Cell*. 2005;120(4):449-60. Epub 2005/03/01. doi: 10.1016/j.cell.2005.02.002. PubMed PMID: 15734678.
80. Green CL, Lamming DW, Fontana L. Molecular mechanisms of dietary restriction promoting health and longevity. *Nat Rev Mol Cell Biol*. 2022;23(1):56-73. Epub 2021/09/15. doi: 10.1038/s41580-021-00411-4. PubMed PMID: 34518687; PMCID: PMC8692439.
81. Kapahi P, Kaeberlein M, Hansen M. Dietary restriction and lifespan: Lessons from invertebrate models. *Ageing Res Rev*. 2017;39:3-14. Epub 2016/12/23. doi: 10.1016/j.arr.2016.12.005. PubMed PMID: 28007498; PMCID: PMC5476520.
82. Kenyon C, Chang J, Gensch E, Rudner A, Tabtiang R. A *C. elegans* mutant that lives twice as long as wild type. *Nature*. 1993;366(6454):461-4. doi: 10.1038/366461a0. PubMed PMID: 8247153.

83. Sheaffer KL, Updike DL, Mango SE. The Target of Rapamycin pathway antagonizes pha-4/FoxA to control development and aging. *Curr Biol.* 2008;18(18):1355-64. Epub 2008/09/23. doi: 10.1016/j.cub.2008.07.097. PubMed PMID: 18804378; PMCID: PMC2615410.
84. Apfeld J, O'Connor G, McDonagh T, DiStefano PS, Curtis R. The AMP-activated protein kinase AAK-2 links energy levels and insulin-like signals to lifespan in *C. elegans*. *Genes Dev.* 2004;18(24):3004-9. Epub 2004/12/03. doi: 10.1101/gad.1255404. PubMed PMID: 15574588; PMCID: PMC535911.
85. Martin-Montalvo A, Mercken EM, Mitchell SJ, Palacios HH, Mote PL, Scheibye-Knudsen M, Gomes AP, Ward TM, Minor RK, Blouin MJ, Schwab M, Pollak M, Zhang Y, Yu Y, Becker KG, Bohr VA, Ingram DK, Sinclair DA, Wolf NS, Spindler SR, Bernier M, de Cabo R. Metformin improves healthspan and lifespan in mice. *Nat Commun.* 2013;4:2192. Epub 2013/08/01. doi: 10.1038/ncomms3192. PubMed PMID: 23900241; PMCID: PMC3736576.
86. Berdichevsky A, Viswanathan M, Horvitz HR, Guarente L. *C. elegans* SIR-2.1 interacts with 14-3-3 proteins to activate DAF-16 and extend life span. *Cell.* 2006;125(6):1165-77. Epub 2006/06/17. doi: 10.1016/j.cell.2006.04.036. PubMed PMID: 16777605.
87. Dues DJ, Andrews EK, Schaar CE, Bergsma AL, Senchuk MM, Van Raamsdonk JM. Aging causes decreased resistance to multiple stresses and a failure to activate specific stress response pathways. *Aging (Albany NY).* 2016;8(4):777-95. Epub 2016/04/08. doi: 10.18632/aging.100939. PubMed PMID: 27053445; PMCID: PMC4925828.
88. Huang C, Xiong C, Kornfeld K. Measurements of age-related changes of physiological processes that predict lifespan of *Caenorhabditis elegans*. *Proc Natl Acad Sci U S A.* 2004;101(21):8084-9. Epub 2004/05/14. doi: 10.1073/pnas.0400848101. PubMed PMID: 15141086; PMCID: PMC419561.
89. Huang C, Xiong C, Kornfeld K. Measurements of age-related changes of physiological processes that predict lifespan of *Caenorhabditis elegans*. *Proceedings of the National Academy of Sciences of the United States of America.* 2004;101(21):8084-9. doi: 10.1073/pnas.0400848101.
90. Bansal A, Zhu LJ, Yen K, Tissenbaum HA. Uncoupling lifespan and healthspan in *Caenorhabditis elegans* longevity mutants. *Proc Natl Acad Sci U S A.* 2015;112(3):E277-86. Epub 2015/01/07. doi: 10.1073/pnas.1412192112. PubMed PMID: 25561524; PMCID: PMC4311797.
91. Rollins JA, Howard AC, Dobbins SK, Washburn EH, Rogers AN. Assessing Health Span in *Caenorhabditis elegans*: Lessons From Short-Lived Mutants. *J Gerontol A Biol Sci Med Sci.* 2017;72(4):473-80. Epub 2017/02/06. doi: 10.1093/gerona/glw248. PubMed PMID: 28158466; PMCID: PMC6075462.

92. Iwasa H, Yu S, Xue J, Driscoll M. Novel EGF pathway regulators modulate *C. elegans* healthspan and lifespan via EGF receptor, PLC-gamma, and IP3R activation. *Aging Cell*. 2010;9(4):490-505. Epub 2010/05/26. doi: 10.1111/j.1474-9726.2010.00575.x. PubMed PMID: 20497132; PMCID: PMC5859306.
93. Amrit FRG, Naim N, Ratnappan R, Loose J, Mason C, Steenberge L, McClendon BT, Wang G, Driscoll M, Yanowitz JL, Ghazi A. The longevity-promoting factor, TCER-1, widely represses stress resistance and innate immunity. *Nat Commun*. 2019;10(1):3042. Epub 2019/07/17. doi: 10.1038/s41467-019-10759-z. PubMed PMID: 31316054; PMCID: PMC6637209.
94. Hubbard EJ, Greenstein D. Introduction to the germ line. *WormBook*. 2005:1-4. Epub 2005/09/01. doi: 10.1895/wormbook.1.18.1. PubMed PMID: 18050415; PMCID: PMC4781435.
95. Severson AF, Meyer BJ. Divergent kleisin subunits of cohesin specify mechanisms to tether and release meiotic chromosomes. *Elife*. 2014;3:e03467. Epub 2014/08/31. doi: 10.7554/eLife.03467. PubMed PMID: 25171895; PMCID: PMC4174578.
96. Phillips CM, Dernburg AF. A family of zinc-finger proteins is required for chromosome-specific pairing and synapsis during meiosis in *C. elegans*. *Dev Cell*. 2006;11(6):817-29. Epub 2006/12/05. doi: 10.1016/j.devcel.2006.09.020. PubMed PMID: 17141157.
97. Harper NC, Rillo R, Jover-Gil S, Assaf ZJ, Bhalla N, Dernburg AF. Pairing centers recruit a Polo-like kinase to orchestrate meiotic chromosome dynamics in *C. elegans*. *Dev Cell*. 2011;21(5):934-47. Epub 2011/10/25. doi: 10.1016/j.devcel.2011.09.001. PubMed PMID: 22018922; PMCID: PMC4343031.
98. Penkner AM, Fridkin A, Gloggnitzer J, Baudrimont A, Machacek T, Woglar A, Csaszar E, Pasierbek P, Ammerer G, Gruenbaum Y, Jantsch V. Meiotic chromosome homology search involves modifications of the nuclear envelope protein Matefin/SUN-1. *Cell*. 2009;139(5):920-33. Epub 2009/11/17. doi: 10.1016/j.cell.2009.10.045. PubMed PMID: 19913286.
99. Malone CJ, Misner L, Le Bot N, Tsai MC, Campbell JM, Ahringer J, White JG. The *C. elegans* hook protein, ZYG-12, mediates the essential attachment between the centrosome and nucleus. *Cell*. 2003;115(7):825-36. Epub 2003/12/31. PubMed PMID: 14697201.
100. Sato A, Isaac B, Phillips CM, Rillo R, Carlton PM, Wynne DJ, Kasad RA, Dernburg AF. Cytoskeletal forces span the nuclear envelope to coordinate meiotic chromosome pairing and synapsis. *Cell*. 2009;139(5):907-19. Epub 2009/11/17. doi: 10.1016/j.cell.2009.10.039. PubMed PMID: 19913287; PMCID: PMC2825574.
101. Kim Y, Rosenberg SC, Kugel CL, Kostow N, Rog O, Davydov V, Su TY, Dernburg AF, Corbett KD. The chromosome axis controls meiotic events through a hierarchical assembly

- of HORMA domain proteins. *Dev Cell*. 2014;31(4):487-502. Epub 2014/12/03. doi: 10.1016/j.devcel.2014.09.013. PubMed PMID: 25446517; PMCID: PMC4254552.
102. Smolikov S, Schild-Prufert K, Colaiacovo MP. A yeast two-hybrid screen for SYP-3 interactors identifies SYP-4, a component required for synaptonemal complex assembly and chiasma formation in *Caenorhabditis elegans* meiosis. *PLoS Genet*. 2009;5(10):e1000669. Epub 2009/10/03. doi: 10.1371/journal.pgen.1000669. PubMed PMID: 19798442; PMCID: PMC2742731.
 103. Smolikov S, Eizinger A, Schild-Prufert K, Hurlburt A, McDonald K, Engebrecht J, Villeneuve AM, Colaiacovo MP. SYP-3 restricts synaptonemal complex assembly to bridge paired chromosome axes during meiosis in *Caenorhabditis elegans*. *Genetics*. 2007;176(4):2015-25. Epub 2007/06/15. doi: 10.1534/genetics.107.072413. PubMed PMID: 17565948; PMCID: PMC1950610.
 104. Colaiacovo MP, MacQueen AJ, Martinez-Perez E, McDonald K, Adamo A, La Volpe A, Villeneuve AM. Synaptonemal complex assembly in *C. elegans* is dispensable for loading strand-exchange proteins but critical for proper completion of recombination. *Dev Cell*. 2003;5(3):463-74. Epub 2003/09/12. PubMed PMID: 12967565.
 105. MacQueen AJ, Colaiacovo MP, McDonald K, Villeneuve AM. Synapsis-dependent and -independent mechanisms stabilize homolog pairing during meiotic prophase in *C. elegans*. *Genes Dev*. 2002;16(18):2428-42. Epub 2002/09/17. doi: 10.1101/gad.1011602. PubMed PMID: 12231631; PMCID: PMC187442.
 106. Hurlock ME, Cavka I, Kursel LE, Haversat J, Wooten M, Nizami Z, Turniansky R, Hoess P, Ries J, Gall JG, Rog O, Kohler S, Kim Y. Identification of novel synaptonemal complex components in *C. elegans*. *J Cell Biol*. 2020;219(5). Epub 2020/03/27. doi: 10.1083/jcb.201910043. PubMed PMID: 32211899; PMCID: PMC7199856.
 107. Dernburg AF, McDonald K, Moulder G, Barstead R, Dresser M, Villeneuve AM. Meiotic recombination in *C. elegans* initiates by a conserved mechanism and is dispensable for homologous chromosome synapsis. *Cell*. 1998;94(3):387-98. Epub 1998/08/26. PubMed PMID: 9708740.
 108. Reddy KC, Villeneuve AM. *C. elegans* HIM-17 links chromatin modification and competence for initiation of meiotic recombination. *Cell*. 2004;118(4):439-52. Epub 2004/08/19. doi: 10.1016/j.cell.2004.07.026. PubMed PMID: 15315757.
 109. Stamper EL, Rodenbusch SE, Rosu S, Ahringer J, Villeneuve AM, Dernburg AF. Identification of DSB-1, a protein required for initiation of meiotic recombination in *Caenorhabditis elegans*, illuminates a crossover assurance checkpoint. *PLoS Genet*. 2013;9(8):e1003679. Epub 2013/08/31. doi: 10.1371/journal.pgen.1003679. PubMed PMID: 23990794; PMCID: PMC3749324.

110. Rosu S, Zawadzki KA, Stamper EL, Libuda DE, Reese AL, Dernburg AF, Villeneuve AM. The *C. elegans* DSB-2 protein reveals a regulatory network that controls competence for meiotic DSB formation and promotes crossover assurance. *PLoS Genet.* 2013;9(8):e1003674. Epub 2013/08/08. doi: 10.1371/journal.pgen.1003674. PubMed PMID: 23950729; PMCID: PMC3738457.
111. Meneely PM, McGovern OL, Heinis FI, Yanowitz JL. Crossover distribution and frequency are regulated by *him-5* in *Caenorhabditis elegans*. *Genetics.* 2012;190(4):1251-66. Epub 2012/01/24. doi: 10.1534/genetics.111.137463. PubMed PMID: 22267496; PMCID: PMC3316641.
112. Wagner CR, Kuervers L, Baillie DL, Yanowitz JL. *xnd-1* regulates the global recombination landscape in *Caenorhabditis elegans*. *Nature.* 2010;467(7317):839-43. Epub 2010/10/15. doi: 10.1038/nature09429. PubMed PMID: 20944745; PMCID: PMC3045774.
113. Yin Y, Smolikove S. Impaired resection of meiotic double-strand breaks channels repair to nonhomologous end joining in *Caenorhabditis elegans*. *Mol Cell Biol.* 2013;33(14):2732-47. Epub 2013/05/15. doi: 10.1128/MCB.00055-13. PubMed PMID: 23671188; PMCID: PMC3700128.
114. Lemmens BB, Johnson NM, Tijsterman M. COM-1 promotes homologous recombination during *Caenorhabditis elegans* meiosis by antagonizing Ku-mediated non-homologous end joining. *PLoS Genet.* 2013;9(2):e1003276. Epub 2013/02/15. doi: 10.1371/journal.pgen.1003276. PubMed PMID: 23408909; PMCID: PMC3567172.
115. Garcia V, Phelps SE, Gray S, Neale MJ. Bidirectional resection of DNA double-strand breaks by Mre11 and Exo1. *Nature.* 2011;479(7372):241-4. Epub 2011/10/18. doi: 10.1038/nature10515. PubMed PMID: 22002605; PMCID: PMC3214165.
116. Petalcorin MI, Galkin VE, Yu X, Egelman EH, Boulton SJ. Stabilization of RAD-51-DNA filaments via an interaction domain in *Caenorhabditis elegans* BRCA2. *Proc Natl Acad Sci U S A.* 2007;104(20):8299-304. Epub 2007/05/08. doi: 10.1073/pnas.0702805104. PubMed PMID: 17483448; PMCID: PMC1895944.
117. Mets DG, Meyer BJ. Condensins regulate meiotic DNA break distribution, thus crossover frequency, by controlling chromosome structure. *Cell.* 2009;139(1):73-86. Epub 2009/09/29. doi: 10.1016/j.cell.2009.07.035. PubMed PMID: 19781752; PMCID: PMC2785808.
118. Ward JD, Muzzini DM, Petalcorin MI, Martinez-Perez E, Martin JS, Plevani P, Cassata G, Marini F, Boulton SJ. Overlapping mechanisms promote postsynaptic RAD-51 filament disassembly during meiotic double-strand break repair. *Mol Cell.* 2010;37(2):259-72. Epub 2010/02/04. doi: 10.1016/j.molcel.2009.12.026. PubMed PMID: 20122407.

119. Kelly KO, Dernburg AF, Stanfield GM, Villeneuve AM. *Caenorhabditis elegans* msh-5 is required for both normal and radiation-induced meiotic crossing over but not for completion of meiosis. *Genetics*. 2000;156(2):617-30. Epub 2000/10/03. doi: 10.1093/genetics/156.2.617. PubMed PMID: 11014811; PMCID: PMC1461284.
120. Zalevsky J, MacQueen AJ, Duffy JB, Kempthues KJ, Villeneuve AM. Crossing over during *Caenorhabditis elegans* meiosis requires a conserved MutS-based pathway that is partially dispensable in budding yeast. *Genetics*. 1999;153(3):1271-83. Epub 1999/11/05. doi: 10.1093/genetics/153.3.1271. PubMed PMID: 10545458; PMCID: PMC1460811.
121. Saito TT, Lui DY, Kim HM, Meyer K, Colaiacovo MP. Interplay between structure-specific endonucleases for crossover control during *Caenorhabditis elegans* meiosis. *PLoS Genet*. 2013;9(7):e1003586. Epub 2013/07/23. doi: 10.1371/journal.pgen.1003586. PubMed PMID: 23874210; PMCID: PMC3715419.
122. Youds JL, Mets DG, McIlwraith MJ, Martin JS, Ward JD, NJ ON, Rose AM, West SC, Meyer BJ, Boulton SJ. RTEL-1 enforces meiotic crossover interference and homeostasis. *Science*. 2010;327(5970):1254-8. Epub 2010/03/06. doi: 10.1126/science.1183112. PubMed PMID: 20203049; PMCID: PMC4770885.
123. Hong Y, Sonnevile R, Agostinho A, Meier B, Wang B, Blow JJ, Gartner A. The SMC-5/6 Complex and the HIM-6 (BLM) Helicase Synergistically Promote Meiotic Recombination Intermediate Processing and Chromosome Maturation during *Caenorhabditis elegans* Meiosis. *PLoS Genet*. 2016;12(3):e1005872. Epub 2016/03/25. doi: 10.1371/journal.pgen.1005872. PubMed PMID: 27010650; PMCID: PMC4807058.
124. Martinez-Perez E, Villeneuve AM. HTP-1-dependent constraints coordinate homolog pairing and synapsis and promote chiasma formation during *C. elegans* meiosis. *Genes Dev*. 2005;19(22):2727-43. Epub 2005/11/18. doi: 10.1101/gad.1338505. PubMed PMID: 16291646; PMCID: PMC1283965.
125. Hillers KJ, Jantsch V, Martinez-Perez E, Yanowitz JL. Meiosis. *WormBook*. 2017:1-43. Epub 2015/12/24. doi: 10.1895/wormbook.1.178.1. PubMed PMID: 26694509; PMCID: PMC5215044.
126. Hillers KJ, Jantsch V, Martinez-Perez E, Yanowitz JLx. Meiosis. *Wormbook*. 2015:1551-8507. doi: 10.1895/wormbook.1.178.1.
127. Hodgkin J, Horvitz HR, Brenner S. Nondisjunction Mutants of the Nematode CAENORHABDITIS ELEGANS. *Genetics*. 1979;91(1):67-94. Epub 1979/01/01. PubMed PMID: 17248881; PMCID: PMC1213932.
128. Hsin H, Kenyon C. Signals from the reproductive system regulate the lifespan of *C. elegans*. *Nature*. 1999;399(6734):362-6. Epub 1999/06/09. doi: 10.1038/20694. PubMed PMID: 10360574.

129. Flatt T, Min KJ, D'Alterio C, Villa-Cuesta E, Cumbers J, Lehmann R, Jones DL, Tatar M. *Drosophila* germ-line modulation of insulin signaling and lifespan. *Proc Natl Acad Sci U S A*. 2008;105(17):6368-73. Epub 2008/04/23. doi: 10.1073/pnas.0709128105. PubMed PMID: 18434551; PMCID: PMC2359818.
130. Arantes-Oliveira N, Apfeld J, Dillin A, Kenyon C. Regulation of life-span by germ-line stem cells in *Caenorhabditis elegans*. *Science*. 2002;295(5554):502-5. doi: 10.1126/science.1065768. PubMed PMID: 11799246.
131. Panowski SH, Dillin A. Signals of youth: endocrine regulation of aging in *Caenorhabditis elegans*. *Trends Endocrinol Metab*. 2009;20(6):259-64. Epub 2009/07/29. doi: 10.1016/j.tem.2009.03.006. PubMed PMID: 19646896.
132. Berman JR, Kenyon C. Germ-cell loss extends *C. elegans* life span through regulation of DAF-16 by *kri-1* and lipophilic-hormone signaling. *Cell*. 2006;124(5):1055-68. doi: 10.1016/j.cell.2006.01.039. PubMed PMID: 16530050.
133. Ghazi A, Henis-Korenblit S, Kenyon C. A transcription elongation factor that links signals from the reproductive system to lifespan extension in *Caenorhabditis elegans*. *PLoS Genet*. 2009;5(9):e1000639. Epub 2009/09/11. doi: 10.1371/journal.pgen.1000639. PubMed PMID: 19749979; PMCID: PMC2729384.
134. Antebi A. Regulation of longevity by the reproductive system. *Exp Gerontol*. 2013;48(7):596-602. Epub 2012/10/11. doi: 10.1016/j.exger.2012.09.009. PubMed PMID: 23063987; PMCID: PMC3593982.
135. Gerisch B, Rottiers V, Li D, Motola DL, Cummins CL, Lehrach H, Mangelsdorf DJ, Antebi A. A bile acid-like steroid modulates *Caenorhabditis elegans* lifespan through nuclear receptor signaling. *Proc Natl Acad Sci U S A*. 2007;104(12):5014-9. Epub 2007/03/14. doi: 10.1073/pnas.0700847104. PubMed PMID: 17360327; PMCID: PMC1821127.
136. Shen Y, Wollam J, Magner D, Karalay O, Antebi A. A steroid receptor-microRNA switch regulates life span in response to signals from the gonad. *Science*. 2012;338(6113):1472-6. doi: 10.1126/science.1228967. PubMed PMID: 23239738; PMCID: PMC3909774.
137. Boulias K, Horvitz HR. The *C. elegans* microRNA *mir-71* acts in neurons to promote germline-mediated longevity through regulation of DAF-16/FOXO. *Cell Metab*. 2012;15(4):439-50. doi: 10.1016/j.cmet.2012.02.014. PubMed PMID: 22482727; PMCID: PMC3344382.
138. Amrit FRG, Ghazi A. Influences of Germline Cells on Organismal Lifespan and Healthspan. *Ageing: Lessons from C elegans*2017. p. 109-35.
139. Amrit FR, Steenkiste EM, Ratnappan R, Chen SW, McClendon TB, Kostka D, Yanowitz J, Olsen CP, Ghazi A. DAF-16 and TCER-1 Facilitate Adaptation to Germline Loss by Restoring Lipid Homeostasis and Repressing Reproductive Physiology in *C. elegans*. *PLoS*

- Genet. 2016;12(2):e1005788. Epub 2016/02/11. doi: 10.1371/journal.pgen.1005788. PubMed PMID: 26862916; PMCID: PMC4749232.
140. Goudeau J, Bellemin S, Toselli-Mollereau E, Shamalnasab M, Chen Y, Aguilaniu H. Fatty acid desaturation links germ cell loss to longevity through NHR-80/HNF4 in *C. elegans*. PLoS Biol. 2011;9(3):e1000599. Epub 2011/03/15. doi: 10.1371/journal.pbio.1000599. PubMed PMID: 21423649; PMCID: PMC3057950.
 141. Ratnappan R, Amrit FR, Chen SW, Gill H, Holden K, Ward J, Yamamoto KR, Olsen CP, Ghazi A. Germline signals deploy NHR-49 to modulate fatty-acid β -oxidation and desaturation in somatic tissues of *C. elegans*. PLoS Genet. 2014;10(12):e1004829. Epub 2014/12/04. doi: 10.1371/journal.pgen.1004829. PubMed PMID: 25474470; PMCID: PMC4256272.
 142. Lapierre LR, Gelino S, Meléndez A, Hansen M. Autophagy and lipid metabolism coordinately modulate life span in germline-less *C. elegans*. Curr Biol. 2011;21(18):1507-14. Epub 2011/09/08. doi: 10.1016/j.cub.2011.07.042. PubMed PMID: 21906946; PMCID: PMC3191188.
 143. Nakamura S, Yoshimori T. Autophagy and Longevity. Mol Cells. 2018;41(1):65-72. Epub 2018/01/23. doi: 10.14348/molcells.2018.2333. PubMed PMID: 29370695; PMCID: PMC5792715.
 144. Lapierre LR, De Magalhaes Filho CD, McQuary PR, Chu CC, Visvikis O, Chang JT, Gelino S, Ong B, Davis AE, Irazoqui JE, Dillin A, Hansen M. The TFEB orthologue HLH-30 regulates autophagy and modulates longevity in *Caenorhabditis elegans*. Nat Commun. 2013;4:2267. doi: 10.1038/ncomms3267. PubMed PMID: 23925298; PMCID: PMC3866206.
 145. Nakamura S, Karalay Ö, Jäger PS, Horikawa M, Klein C, Nakamura K, Latza C, Templer SE, Dieterich C, Antebi A. Mondo complexes regulate TFEB via TOR inhibition to promote longevity in response to gonadal signals. Nat Commun. 2016;7:10944. Epub 2016/03/22. doi: 10.1038/ncomms10944. PubMed PMID: 27001890; PMCID: PMC4804169.
 146. Steinbaugh MJ, Narasimhan SD, Robida-Stubbs S, Moronetti Mazzeo LE, Dreyfuss JM, Hourihan JM, Raghavan P, Operaña TN, Esmailie R, Blackwell TK. Lipid-mediated regulation of SKN-1/Nrf in response to germ cell absence. Elife. 2015;4. Epub 2015/08/24. doi: 10.7554/eLife.07836. PubMed PMID: 26196144; PMCID: PMC4541496.
 147. Hansen M, Hsu AL, Dillin A, Kenyon C. New genes tied to endocrine, metabolic, and dietary regulation of lifespan from a *Caenorhabditis elegans* genomic RNAi screen. PLoS Genet. 2005;1(1):119-28. Epub 2005/08/17. doi: 10.1371/journal.pgen.0010017. PubMed PMID: 16103914; PMCID: PMC1183531.

148. Vilchez D, Morantte I, Liu Z, Douglas PM, Merkwirth C, Rodrigues AP, Manning G, Dillin A. RPN-6 determines *C. elegans* longevity under proteotoxic stress conditions. *Nature*. 2012;489(7415):263-8. doi: 10.1038/nature11315. PubMed PMID: 22922647.
149. Lopez-Otin C, Blasco MA, Partridge L, Serrano M, Kroemer G. The hallmarks of aging. *Cell*. 2013;153(6):1194-217. Epub 2013/06/12. doi: 10.1016/j.cell.2013.05.039. PubMed PMID: 23746838; PMCID: PMC3836174.
150. Shemesh N, Shai N, Ben-Zvi A. Germline stem cell arrest inhibits the collapse of somatic proteostasis early in *Caenorhabditis elegans* adulthood. *Aging Cell*. 2013;12(5):814-22. Epub 2013/06/06. doi: 10.1111/accel.12110. PubMed PMID: 23734734.
151. Vilchez D, Boyer L, Morantte I, Lutz M, Merkwirth C, Joyce D, Spencer B, Page L, Masliah E, Berggren WT, Gage FH, Dillin A. Increased proteasome activity in human embryonic stem cells is regulated by PSMD11. *Nature*. 2012;489(7415):304-8. Epub 2012/09/14. doi: 10.1038/nature11468. PubMed PMID: 22972301; PMCID: PMC5215918.
152. Goudeau J, Aguilaniu H. Carbonylated proteins are eliminated during reproduction in *C. elegans*. *Aging Cell*. 2010;9(6):991-1003. Epub 2010/10/29. doi: 10.1111/j.1474-9726.2010.00625.x. PubMed PMID: 21040398.
153. Bohnert KA, Kenyon C. A Lysosomal Switch Triggers Proteostasis Renewal in the Immortal *C. Elegans* Germ Lineage. *Nature*. 2017;551(7682):629-63.
154. Samaddar M, Goudeau J, Sanchez M, Hall DH, Bohnert KA, Ingaramo M, Kenyon C. A genetic screen identifies new steps in oocyte maturation that enhance proteostasis in the immortal germ lineage. *Elife*. 2021;10. Epub 2021/04/14. doi: 10.7554/eLife.62653. PubMed PMID: 33848238; PMCID: PMC8043744.
155. Jaul E, Barron J. Age-Related Diseases and Clinical and Public Health Implications for the 85 Years Old and Over Population. *Front Public Health*. 2017;5:335. Epub 2018/01/10. doi: 10.3389/fpubh.2017.00335. PubMed PMID: 29312916; PMCID: PMC5732407.
156. Mason JB, Cargill SL, Anderson GB, Carey JR. Transplantation of young ovaries to old mice increased life span in transplant recipients. *J Gerontol A Biol Sci Med Sci*. 2009;64(12):1207-11. Epub 2009/09/23. doi: 10.1093/gerona/glp134. PubMed PMID: 19776215; PMCID: PMC2773817.
157. O'Neil N, Rose A. DNA repair. *WormBook*. 2006:1-12. Epub 2007/12/01. doi: 10.1895/wormbook.1.54.1. PubMed PMID: 18050489; PMCID: PMC4781471.
158. Day FR, Ruth KS, Thompson DJ, Lunetta KL, Pervjakova N, Chasman DI, Stolk L, Finucane HK, Sulem P, Bulik-Sullivan B, Esko T, Johnson AD, Elks CE, Franceschini N, He C, Altmaier E, Brody JA, Franke LL, Huffman JE, Keller MF, McArdle PF, Nutile T, Porcu E, Robino A, Rose LM, Schick UM, Smith JA, Teumer A, Traglia M, Vuckovic D,

Yao J, Zhao W, Albrecht E, Amin N, Corre T, Hottenga J-J, Mangino M, Smith AV, Tanaka T, Abecasis GR, Andrulis IL, Anton-Culver H, Antoniou AC, Arndt V, Arnold AM, Barbieri C, Beckmann MW, Beeghly-Fadiel A, Benitez J, Bernstein L, Bielinski SJ, Blomqvist C, Boerwinkle E, Bogdanova NV, Bojesen SE, Bolla MK, Borresen-Dale A-L, Boutin TS, Brauch H, Brenner H, Bruning T, Burwinkel B, Campbell A, Campbell H, Chanock SJ, Chapman JR, Chen Y-DI, Chenevix-Trench G, Couch FJ, Coviello AD, Cox A, Czene K, Darabi H, De Vivo I, Demerath EW, Dennis J, Devilee P, Dork T, dos-Santos-Silva I, Dunning AM, Eicher JD, Fasching PA, Faul JD, Figueroa J, Flesch-Janys D, Gandin I, Garcia ME, Garcia-Closas M, Giles GG, Girotto GG, Goldberg MS, Gonzalez-Neira A, Goodarzi MO, Grove ML, Gudbjartsson DF, Guenel P, Guo X, Haiman CA, Hall P, Hamann U, Henderson BE, Hocking LJ, Hofman A, Homuth G, Hooning MJ, Hopper JL, Hu FB, Huang J, Humphreys K, Hunter DJ, Jakubowska A, Jones SE, Kabisch M, Karasik D, Knight JA, Kolcic I, Kooperberg C, Kosma V-M, Kriebel J, Kristensen V, Lambrechts D, Langenberg C, Li J, Li X, Lindstrom S, Liu Y, Luan Ja, Lubinski J, Magi R, Mannermaa A, Manz J, Margolin S, Marten J, Martin NG, Masciullo C, Meindl A, Michailidou K, Mihailov E, Milani L, Milne RL, Muller-Nurasyid M, Nalls M, Neale BM, Nevanlinna H, Neven P, Newman AB, Nordestgaard BG, Olson JE, Padmanabhan S, Peterlongo P, Peters U, Petersmann A, Peto J, Pharoah PDP, Pirastu NN, Pirie A, Pistis G, Polasek O, Porteous D, Psaty BM, Pylkas K, Radice P, Raffel LJ, Rivadeneira F, Rudan I, Rudolph A, Ruggiero D, Sala CF, Sanna S, Sawyer EJ, Schlessinger D, Schmidt MK, Schmidt F, Schmutzler RK, Schoemaker MJ, Scott RA, Seynaeve CM, Simard J, Sorice R, Southey MC, Stockl D, Strauch K, Swerdlow A, Taylor KD, Thorsteinsdottir U, Toland AE, Tomlinson I, Truong T, Tryggvadottir L, Turner ST, Vozzi D, Wang Q, Wellons M, Willemsen G, Wilson JF, Winqvist R, Wolffenbuttel BBHR, Wright AF, Yannoukakos D, Zemunik T, Zheng W, Zygmont M, Bergmann S, Boomsma DI, Buring JE, Ferrucci L, Montgomery GW, Gudnason V, Spector TD, van Duijn CM, Alizadeh BZ, Ciullo M, Crisponi L, Easton DF, Gasparini PP, Gieger C, Harris TB, Hayward C, Kardia SLR, Kraft P, McKnight B, Metspalu A, Morrison AC, Reiner AP, Ridker PM, Rotter JI, Toniolo D, Uitterlinden AG, Ulivi S, Volzke H, Wareham NJ, Weir DR, Yerges-Armstrong LM, The PC, kConFab I, Investigators A, Generation S, Consortium EP-I, LifeLines Cohort S, Price AL, Stefansson K, Visser JA, Ong KK, Chang-Claude J, Murabito JM, Perry JRB, Murray A. Large-scale genomic analyses link reproductive aging to hypothalamic signaling, breast cancer susceptibility and BRCA1-mediated DNA repair. *Nat Genet.* 2015;47(11):1294-303. doi: 10.1038/ng.3412

<http://www.nature.com/ng/journal/v47/n11/abs/ng.3412.html#supplementary-information>.

159. Ben-Zvi A, Miller EA, Morimoto RI. Collapse of proteostasis represents an early molecular event in *Caenorhabditis elegans* aging. *Proc Natl Acad Sci U S A.* 2009;106(35):14914-9. Epub 2009/08/27. doi: 10.1073/pnas.0902882106. PubMed PMID: 19706382; PMCID: PMC2736453.
160. Stergiou L, Doukometzidis K, Sandoel A, Hengartner MO. The nucleotide excision repair pathway is required for UV-C-induced apoptosis in *Caenorhabditis elegans*. *Cell Death*

- Differ. 2007;14(6):1129-38. Epub 2007/03/10. doi: 10.1038/sj.cdd.4402115. PubMed PMID: 17347667.
161. Severson AF, Ling L, van Zuylen V, Meyer BJ. The axial element protein HTP-3 promotes cohesin loading and meiotic axis assembly in *C. elegans* to implement the meiotic program of chromosome segregation. *Genes Dev.* 2009;23(15):1763-78. Epub 2009/07/04. doi: 10.1101/gad.1808809. PubMed PMID: 19574299; PMCID: PMC2720254.
 162. Phillips CM, Wong C, Bhalla N, Carlton PM, Weiser P, Meneely PM, Dernburg AF. HIM-8 binds to the X chromosome pairing center and mediates chromosome-specific meiotic synapsis. *Cell.* 2005;123(6):1051-63. Epub 2005/12/20. doi: 10.1016/j.cell.2005.09.035. PubMed PMID: 16360035; PMCID: PMC4435792.
 163. Hayashi M, Chin GM, Villeneuve AM. *C. elegans* germ cells switch between distinct modes of double-strand break repair during meiotic prophase progression. *PLoS Genet.* 2007;3(11):e191. Epub 2007/11/07. doi: 10.1371/journal.pgen.0030191. PubMed PMID: 17983271; PMCID: PMC2048528.
 164. Adamo A, Montemauri P, Silva N, Ward JD, Boulton SJ, La Volpe A. BRC-1 acts in the inter-sister pathway of meiotic double-strand break repair. *EMBO Rep.* 2008;9(3):287-92. Epub 2008/01/26. doi: 10.1038/sj.embor.7401167. PubMed PMID: 18219312; PMCID: PMC2267377.
 165. O'Neil NJ, Martin JS, Youds JL, Ward JD, Petalcorin MI, Rose AM, Boulton SJ. Joint molecule resolution requires the redundant activities of MUS-81 and XPF-1 during *Caenorhabditis elegans* meiosis. *PLoS Genet.* 2013;9(7):e1003582. Epub 2013/07/23. doi: 10.1371/journal.pgen.1003582. PubMed PMID: 23874209; PMCID: PMC3715453.
 166. Martin JS, Winkelmann N, Petalcorin MI, McIlwraith MJ, Boulton SJ. RAD-51-dependent and -independent roles of a *Caenorhabditis elegans* BRCA2-related protein during DNA double-strand break repair. *Mol Cell Biol.* 2005;25(8):3127-39. Epub 2005/03/31. doi: 10.1128/MCB.25.8.3127-3139.2005. PubMed PMID: 15798199; PMCID: PMC1069622.
 167. Saito TT, Mohideen F, Meyer K, Harper JW, Colaiacovo MP. SLX-1 is required for maintaining genomic integrity and promoting meiotic noncrossovers in the *Caenorhabditis elegans* germline. *PLoS Genet.* 2012;8(8):e1002888. Epub 2012/08/29. doi: 10.1371/journal.pgen.1002888. PubMed PMID: 22927825; PMCID: PMC3426554.
 168. Sgro CM, Partridge L. A delayed wave of death from reproduction in *Drosophila*. *Science.* 1999;286(5449):2521-4. Epub 2000/01/05. doi: 10.1126/science.286.5449.2521. PubMed PMID: 10617470.
 169. Marchal L, Hamsanathan S, Karthikappallil R, Han S, Shinglot H, Gurkar AU. Analysis of representative mutants for key DNA repair pathways on healthspan in *Caenorhabditis elegans*. *Mech Ageing Dev.* 2021;200:111573. Epub 2021/09/26. doi: 10.1016/j.mad.2021.111573. PubMed PMID: 34562508; PMCID: PMC8627479.

170. Zou L, Wu D, Zang X, Wang Z, Wu Z, Chen D. Construction of a germline-specific RNAi tool in *C. elegans*. *Sci Rep.* 2019;9(1):2354. Epub 2019/02/23. doi: 10.1038/s41598-019-38950-8. PubMed PMID: 30787374; PMCID: PMC6382888.
171. Edwards SL, Erdenebat P, Morphis AC, Kumar L, Wang L, Chamera T, Georgescu C, Wren JD, Li J. Insulin/IGF-1 signaling and heat stress differentially regulate HSF1 activities in germline development. *Cell Rep.* 2021;36(9):109623. Epub 2021/09/02. doi: 10.1016/j.celrep.2021.109623. PubMed PMID: 34469721; PMCID: PMC8442575.
172. Das S, Min S, Prahlad V. Gene bookmarking by the heat shock transcription factor programs the insulin-like signaling pathway. *Mol Cell.* 2021;81(23):4843-60 e8. Epub 2021/10/15. doi: 10.1016/j.molcel.2021.09.022. PubMed PMID: 34648748; PMCID: PMC8642288.
173. Curran SP, Wu X, Riedel CG, Ruvkun G. A soma-to-germline transformation in long-lived *Caenorhabditis elegans* mutants. *Nature.* 2009;459(7250):1079-84. Epub 2009/06/10. doi: 10.1038/nature08106. PubMed PMID: 19506556; PMCID: PMC2716045.
174. Zhang L, Köhler S, Rillo-Bohn R, Dernburg AF. A compartmentalized signaling network mediates crossover control in meiosis. *Elife.* 2018;7. Epub 2018/03/09. doi: 10.7554/eLife.30789. PubMed PMID: 29521627; PMCID: PMC5906097.
175. Glenn CF, Chow DK, David L, Cooke CA, Gami MS, Iser WB, Hanselman KB, Goldberg IG, Wolkow CA. Behavioral deficits during early stages of aging in *Caenorhabditis elegans* result from locomotory deficits possibly linked to muscle frailty. *J Gerontol A Biol Sci Med Sci.* 2004;59(12):1251-60. Epub 2005/02/09. doi: 10.1093/gerona/59.12.1251. PubMed PMID: 15699524; PMCID: PMC1458366.
176. Kauffman AL, Ashraf JM, Corces-Zimmerman MR, Landis JN, Murphy CT. Insulin signaling and dietary restriction differentially influence the decline of learning and memory with age. *PLoS Biol.* 2010;8(5):e1000372. Epub 2010/05/18. doi: 10.1371/journal.pbio.1000372. PubMed PMID: 20502519; PMCID: PMC2872642.
177. Youngman MJ, Rogers ZN, Kim DH. A decline in p38 MAPK signaling underlies immunosenescence in *Caenorhabditis elegans*. *PLoS Genet.* 2011;7(5):e1002082. Epub 2011/06/01. doi: 10.1371/journal.pgen.1002082. PubMed PMID: 21625567; PMCID: PMC3098197.
178. Sutphin GL, Backer G, Sheehan S, Bean S, Corban C, Liu T, Peters MJ, van Meurs JBJ, Murabito JM, Johnson AD, Korstanje R, Cohorts for H, Aging Research in Genomic Epidemiology Consortium Gene Expression Working G. *Caenorhabditis elegans* orthologs of human genes differentially expressed with age are enriched for determinants of longevity. *Aging Cell.* 2017;16(4):672-82. Epub 2017/04/13. doi: 10.1111/ace1.12595. PubMed PMID: 28401650; PMCID: PMC5506438.

179. Lund J, Tedesco P, Duke K, Wang J, Kim SK, Johnson TE. Transcriptional profile of aging in *C. elegans*. *Curr Biol*. 2002;12(18):1566-73. Epub 2002/10/10. doi: 10.1016/s0960-9822(02)01146-6. PubMed PMID: 12372248.
180. Golden TR, Melov S. Microarray analysis of gene expression with age in individual nematodes. *Aging Cell*. 2004;3(3):111-24. Epub 2004/05/22. doi: 10.1111/j.1474-9728.2004.00095.x. PubMed PMID: 15153179.
181. Hoppe T, Cohen E. Organismal Protein Homeostasis Mechanisms. *Genetics*. 2020;215(4):889-901. Epub 2020/08/08. doi: 10.1534/genetics.120.301283. PubMed PMID: 32759342; PMCID: PMC7404231.
182. O'Rourke EJ, Kuballa P, Xavier R, Ruvkun G. omega-6 Polyunsaturated fatty acids extend life span through the activation of autophagy. *Genes Dev*. 2013;27(4):429-40. Epub 2013/02/09. doi: 10.1101/gad.205294.112. PubMed PMID: 23392608; PMCID: PMC3589559.
183. Walker GA, Lithgow GJ. Lifespan extension in *C. elegans* by a molecular chaperone dependent upon insulin-like signals. *Aging Cell*. 2003;2(2):131-9. Epub 2003/07/29. doi: 10.1046/j.1474-9728.2003.00045.x. PubMed PMID: 12882326.
184. Lechler MC, Crawford ED, Groh N, Widmaier K, Jung R, Kirstein J, Trinidad JC, Burlingame AL, David DC. Reduced Insulin/IGF-1 Signaling Restores the Dynamic Properties of Key Stress Granule Proteins during Aging. *Cell Rep*. 2017;18(2):454-67. Epub 2017/01/12. doi: 10.1016/j.celrep.2016.12.033. PubMed PMID: 28076789; PMCID: PMC5263236.
185. Morley JF, Brignull HR, Weyers JJ, Morimoto RI. The threshold for polyglutamine-expansion protein aggregation and cellular toxicity is dynamic and influenced by aging in *Caenorhabditis elegans*. *Proc Natl Acad Sci U S A*. 2002;99(16):10417-22. Epub 2002/07/18. doi: 10.1073/pnas.152161099. PubMed PMID: 12122205; PMCID: PMC124929.
186. Li ST, Zhao HQ, Zhang P, Liang CY, Zhang YP, Hsu AL, Dong MQ. DAF-16 stabilizes the aging transcriptome and is activated in mid-aged *Caenorhabditis elegans* to cope with internal stress. *Aging Cell*. 2019;18(3):e12896. Epub 2019/02/19. doi: 10.1111/ace1.12896. PubMed PMID: 30773782; PMCID: PMC6516157.
187. Drori D, Folman Y. Environmental effects on longevity in the male rat: exercise, mating, castration and restricted feeding. *Exp Gerontol*. 1976;11(1-2):25-32. Epub 1976/01/01. doi: 10.1016/0531-5565(76)90007-3. PubMed PMID: 1278267.
188. Kato Y, Moriwaki T, Funakoshi M, Zhang-Akiyama QM. *Caenorhabditis elegans* EXO-3 contributes to longevity and reproduction: differential roles in somatic cells and germ cells. *Mutat Res*. 2015;772:46-54. Epub 2015/03/17. doi: 10.1016/j.mrfmmm.2015.01.001. PubMed PMID: 25772110.

189. Ermolaeva MA, Segref A, Dakhovnik A, Ou HL, Schneider JI, Utermohlen O, Hoppe T, Schumacher B. DNA damage in germ cells induces an innate immune response that triggers systemic stress resistance. *Nature*. 2013;501(7467):416-20. Epub 2013/08/27. doi: 10.1038/nature12452. PubMed PMID: 23975097; PMCID: PMC4120807.
190. Han SK, Lee D, Lee H, Kim D, Son HG, Yang JS, Lee SV, Kim S. OASIS 2: online application for survival analysis 2 with features for the analysis of maximal lifespan and healthspan in aging research. *Oncotarget*. 2016;7(35):56147-52. Epub 2016/08/17. doi: 10.18632/oncotarget.11269. PubMed PMID: 27528229; PMCID: PMC5302902.
191. Rudich P, Watkins S, Lamitina T. PolyQ-independent toxicity associated with novel translational products from CAG repeat expansions. *PLoS One*. 2020;15(4):e0227464. Epub 2020/04/03. doi: 10.1371/journal.pone.0227464. PubMed PMID: 32240172; PMCID: PMC7117740.
192. Green MR, Sambrook J. Total RNA Extraction from *Caenorhabditis elegans*. *Cold Spring Harb Protoc*. 2020;2020(9):101683. Epub 2020/09/03. doi: 10.1101/pdb.prot101683. PubMed PMID: 32873731.
193. Golden TR, Hubbard A, Dando C, Herren MA, Melov S. Age-related behaviors have distinct transcriptional profiles in *Caenorhabditis elegans*. *Aging Cell*. 2008;7(6):850-65. Epub 2008/09/10. doi: 10.1111/j.1474-9726.2008.00433.x. PubMed PMID: 18778409; PMCID: PMC2613281.
194. Amrit FRG, Ghazi A. Transcriptomic Analysis of *C. elegans* RNA Sequencing Data Through the Tuxedo Suite on the Galaxy Project. *J Vis Exp*. 2017(122). Epub 2017/04/28. doi: 10.3791/55473. PubMed PMID: 28448031; PMCID: PMC5564484.
195. Naim N, Amrit FRG, Ratnappan R, DelBuono N, Loose JA, Ghazi A. Cell nonautonomous roles of NHR-49 in promoting longevity and innate immunity. *Aging Cell*. 2021;20(7):e13413. Epub 2021/06/23. doi: 10.1111/accel.13413. PubMed PMID: 34156142; PMCID: PMC8282243.
196. Rangaraju S, Solis GM, Thompson RC, Gomez-Amaro RL, Kurian L, Encalada SE, Niculescu AB, 3rd, Salomon DR, Petrascheck M. Suppression of transcriptional drift extends *C. elegans* lifespan by postponing the onset of mortality. *Elife*. 2015;4:e08833. Epub 2015/12/02. doi: 10.7554/eLife.08833. PubMed PMID: 26623667; PMCID: PMC4720515.
197. Peters MJ, Joehanes R, Pilling LC, Schurmann C, Conneely KN, Powell J, Reinmaa E, Sutphin GL, Zhernakova A, Schramm K, Wilson YA, Kobes S, Tukiainen T, Consortium NU, Ramos YF, Goring HH, Fornage M, Liu Y, Gharib SA, Stranger BE, De Jager PL, Aviv A, Levy D, Murabito JM, Munson PJ, Huan T, Hofman A, Uitterlinden AG, Rivadeneira F, van Rooij J, Stolk L, Broer L, Verbiest MM, Jhamai M, Arp P, Metspalu A, Tserel L, Milani L, Samani NJ, Peterson P, Kasela S, Codd V, Peters A, Ward-Caviness CK, Herder C, Waldenberger M, Roden M, Singmann P, Zeilinger S, Illig T, Homuth G,

- Grabe HJ, Volzke H, Steil L, Kocher T, Murray A, Melzer D, Yaghootkar H, Bandinelli S, Moses EK, Kent JW, Curran JE, Johnson MP, Williams-Blangero S, Westra HJ, McRae AF, Smith JA, Kardia SL, Hovatta I, Perola M, Ripatti S, Salomaa V, Henders AK, Martin NG, Smith AK, Mehta D, Binder EB, Nylocks KM, Kennedy EM, Klengel T, Ding J, Suchy-Dacey AM, Enquobahrie DA, Brody J, Rotter JI, Chen YD, Houwing-Duistermaat J, Kloppenburg M, Slagboom PE, Helmer Q, den Hollander W, Bean S, Raj T, Bakhshi N, Wang QP, Oyston LJ, Psaty BM, Tracy RP, Montgomery GW, Turner ST, Blangero J, Meulenbelt I, Ressler KJ, Yang J, Franke L, Kettunen J, Visscher PM, Neely GG, Korstanje R, Hanson RL, Prokisch H, Ferrucci L, Esko T, Teumer A, van Meurs JB, Johnson AD. The transcriptional landscape of age in human peripheral blood. *Nat Commun.* 2015;6:8570. Epub 2015/10/23. doi: 10.1038/ncomms9570. PubMed PMID: 26490707; PMCID: PMC4639797.
198. Shaye DD, Greenwald I. OrthoList: a compendium of *C. elegans* genes with human orthologs. *PLoS One.* 2011;6(5):e20085. Epub 2011/06/08. doi: 10.1371/journal.pone.0020085. PubMed PMID: 21647448; PMCID: PMC3102077.
 199. Chatsirisupachai K, Palmer D, Ferreira S, de Magalhaes JP. A human tissue-specific transcriptomic analysis reveals a complex relationship between aging, cancer, and cellular senescence. *Aging Cell.* 2019;18(6):e13041. Epub 2019/09/29. doi: 10.1111/accel.13041. PubMed PMID: 31560156; PMCID: PMC6826163.
 200. Statzer C, Jongsma E, Liu SX, Dakhovnik A, Wandrey F, Mozharovskiy P, Zulli F, Ewald CY. Youthful and age-related matreotypes predict drugs promoting longevity. *Aging Cell.* 2021;20(9):e13441. Epub 2021/08/05. doi: 10.1111/accel.13441. PubMed PMID: 34346557; PMCID: PMC8441316.
 201. Lapierre LR, Hansen M. Lessons from *C. elegans*: signaling pathways for longevity. *Trends Endocrinol Metab.* 2012;23(12):637-44. Epub 2012/09/04. doi: 10.1016/j.tem.2012.07.007. PubMed PMID: 22939742; PMCID: PMC3502657.
 202. Landis G, Shen J, Tower J. Gene expression changes in response to aging compared to heat stress, oxidative stress and ionizing radiation in *Drosophila melanogaster*. *Aging (Albany NY).* 2012;4(11):768-89. Epub 2012/12/06. doi: 10.18632/aging.100499. PubMed PMID: 23211361; PMCID: PMC3560439.
 203. Zhang MJ, Pisco AO, Darmanis S, Zou J. Mouse aging cell atlas analysis reveals global and cell type-specific aging signatures. *Elife.* 2021;10. Epub 2021/04/14. doi: 10.7554/eLife.62293. PubMed PMID: 33847263; PMCID: PMC8046488.
 204. Golden TR, Melov S. Gene expression changes associated with aging in *C. elegans*. *WormBook.* 2007:1-12. Epub 2007/12/01. doi: 10.1895/wormbook.1.127.2. PubMed PMID: 18050504; PMCID: PMC4781587.
 205. Ewald CY. The Matrisome during Aging and Longevity: A Systems-Level Approach toward Defining Matreotypes Promoting Healthy Aging. *Gerontology.* 2020;66(3):266-74.

- Epub 2019/12/16. doi: 10.1159/000504295. PubMed PMID: 31838471; PMCID: PMC7214094.
206. Wu J, Jiang X, Li Y, Zhu T, Zhang J, Zhang Z, Zhang L, Zhang Y, Wang Y, Zou X, Liang B. PHA-4/FoxA senses nucleolar stress to regulate lipid accumulation in *Caenorhabditis elegans*. *Nat Commun*. 2018;9(1):1195. Epub 2018/03/24. doi: 10.1038/s41467-018-03531-2. PubMed PMID: 29567958; PMCID: PMC5864837.
 207. Hardy J, Selkoe DJ. The amyloid hypothesis of Alzheimer's disease: progress and problems on the road to therapeutics. *Science*. 2002;297(5580):353-6. Epub 2002/07/20. doi: 10.1126/science.1072994. PubMed PMID: 12130773.
 208. Li J, Brown G, Ailion M, Lee S, Thomas JH. NCR-1 and NCR-2, the *C. elegans* homologs of the human Niemann-Pick type C1 disease protein, function upstream of DAF-9 in the dauer formation pathways. *Development*. 2004;131(22):5741-52. Epub 2004/10/29. doi: 10.1242/dev.01408. PubMed PMID: 15509773.
 209. Guerrero GA, Derisbourg MJ, Mayr FA, Wester LE, Giorda M, Dinort JE, Hartman MD, Schilling K, Alonso-De Gennaro MJ, Lu RJ, Benayoun BA, Denzel MS. NHR-8 and P-glycoproteins uncouple xenobiotic resistance from longevity in chemosensory *C. elegans* mutants. *Elife*. 2021;10. Epub 2021/08/28. doi: 10.7554/eLife.53174. PubMed PMID: 34448454; PMCID: PMC8460253.
 210. Kim W, Underwood RS, Greenwald I, Shaye DD. OrthoList 2: A New Comparative Genomic Analysis of Human and *Caenorhabditis elegans* Genes. *Genetics*. 2018;210(2):445-61. Epub 2018/08/19. doi: 10.1534/genetics.118.301307. PubMed PMID: 30120140; PMCID: PMC6216590.
 211. Lan J, Rollins JA, Zang X, Wu D, Zou L, Wang Z, Ye C, Wu Z, Kapahi P, Rogers AN, Chen D. Translational Regulation of Non-autonomous Mitochondrial Stress Response Promotes Longevity. *Cell Rep*. 2019;28(4):1050-62 e6. Epub 2019/07/25. doi: 10.1016/j.celrep.2019.06.078. PubMed PMID: 31340143; PMCID: PMC6684276.
 212. Calculli G, Lee HJ, Shen K, Pham U, Herholz M, Trifunovic A, Dillin A, Vilchez D. Systemic regulation of mitochondria by germline proteostasis prevents protein aggregation in the soma of *C. elegans*. *Sci Adv*. 2021;7(26). Epub 2021/06/27. doi: 10.1126/sciadv.abg3012. PubMed PMID: 34172445; PMCID: PMC8232903.
 213. Fares H, Greenwald I. Genetic analysis of endocytosis in *Caenorhabditis elegans*: coelomocyte uptake defective mutants. *Genetics*. 2001;159(1):133-45. Epub 2001/09/19. doi: 10.1093/genetics/159.1.133. PubMed PMID: 11560892; PMCID: PMC1461804.
 214. Patton A, Knuth S, Schaheen B, Dang H, Greenwald I, Fares H. Endocytosis function of a ligand-gated ion channel homolog in *Caenorhabditis elegans*. *Curr Biol*. 2005;15(11):1045-50. Epub 2005/06/07. doi: 10.1016/j.cub.2005.04.057. PubMed PMID: 15936276.

215. Mikels AJ, Nusse R. Wnts as ligands: processing, secretion and reception. *Oncogene*. 2006;25(57):7461-8. Epub 2006/12/05. doi: 10.1038/sj.onc.1210053. PubMed PMID: 17143290.
216. Noormohammadi A, Khodakarami A, Gutierrez-Garcia R, Lee HJ, Koyuncu S, Konig T, Schindler C, Saez I, Fatima A, Dieterich C, Vilchez D. Somatic increase of CCT8 mimics proteostasis of human pluripotent stem cells and extends *C. elegans* lifespan. *Nat Commun*. 2016;7:13649. Epub 2016/11/29. doi: 10.1038/ncomms13649. PubMed PMID: 27892468; PMCID: PMC5133698.
217. Sawa H, Korswagen HC. Wnt signaling in *C. elegans*. *WormBook*. 2013:1-30. Epub 2013/01/01. doi: 10.1895/wormbook.1.7.2. PubMed PMID: 25263666; PMCID: PMC5402212.
218. Lezzerini M, Budovskaya Y. A dual role of the Wnt signaling pathway during aging in *Caenorhabditis elegans*. *Aging Cell*. 2014;13(1):8-18. Epub 2013/07/25. doi: 10.1111/accel.12141. PubMed PMID: 23879250; PMCID: PMC4326866.
219. Hardin J, King RS. The long and the short of Wnt signaling in *C. elegans*. *Curr Opin Genet Dev*. 2008;18(4):362-7. Epub 2008/07/16. doi: 10.1016/j.gde.2008.06.006. PubMed PMID: 18625312; PMCID: PMC4523225.
220. Zhang Q, Wu X, Chen P, Liu L, Xin N, Tian Y, Dillin A. The Mitochondrial Unfolded Protein Response Is Mediated Cell-Non-autonomously by Retromer-Dependent Wnt Signaling. *Cell*. 2018;174(4):870-83 e17. Epub 2018/07/31. doi: 10.1016/j.cell.2018.06.029. PubMed PMID: 30057120; PMCID: PMC6086732.
221. Baird NA, Douglas PM, Simic MS, Grant AR, Moresco JJ, Wolff SC, Yates JR, 3rd, Manning G, Dillin A. HSF-1-mediated cytoskeletal integrity determines thermotolerance and life span. *Science*. 2014;346(6207):360-3. Epub 2014/10/18. doi: 10.1126/science.1253168. PubMed PMID: 25324391; PMCID: PMC4403873.
222. Kumsta C, Ching TT, Nishimura M, Davis AE, Gelino S, Catan HH, Yu X, Chu CC, Ong B, Panowski SH, Baird N, Bodmer R, Hsu AL, Hansen M. Integrin-linked kinase modulates longevity and thermotolerance in *C. elegans* through neuronal control of HSF-1. *Aging Cell*. 2014;13(3):419-30. Epub 2013/12/10. doi: 10.1111/accel.12189. PubMed PMID: 24314125; PMCID: PMC4059541.
223. Von Stetina SE, Watson JD, Fox RM, Olszewski KL, Spencer WC, Roy PJ, Miller DM, 3rd. Cell-specific microarray profiling experiments reveal a comprehensive picture of gene expression in the *C. elegans* nervous system. *Genome Biol*. 2007;8(7):R135. Epub 2007/07/07. doi: 10.1186/gb-2007-8-7-r135. PubMed PMID: 17612406; PMCID: PMC2323220.

224. Shostak Y, Van Gilst MR, Antebi A, Yamamoto KR. Identification of *C. elegans* DAF-12-binding sites, response elements, and target genes. *Genes Dev.* 2004;18(20):2529-44. Epub 2004/10/19. doi: 10.1101/gad.1218504. PubMed PMID: 15489294; PMCID: PMC529540.
225. Larsen PL, Albert PS, Riddle DL. Genes that regulate both development and longevity in *Caenorhabditis elegans*. *Genetics.* 1995;139(4):1567-83. Epub 1995/04/01. doi: 10.1093/genetics/139.4.1567. PubMed PMID: 7789761; PMCID: PMC1206485.
226. Murphy CT, Lee SJ, Kenyon C. Tissue entrainment by feedback regulation of insulin gene expression in the endoderm of *Caenorhabditis elegans*. *Proc Natl Acad Sci U S A.* 2007;104(48):19046-50. Epub 2007/11/21. doi: 10.1073/pnas.0709613104. PubMed PMID: 18025456; PMCID: PMC2141905.
227. Ahringer J. Reverse genetics. *WormBook2006.*
228. Kamath RS, Ahringer J. Genome-wide RNAi screening in *Caenorhabditis elegans*. *Methods.* 2003;30(4):313-21. Epub 2003/06/28. PubMed PMID: 12828945.
229. Kumsta C, Hansen M. *C. elegans* rrf-1 mutations maintain RNAi efficiency in the soma in addition to the germline. *PLoS One.* 2012;7(5):e35428. Epub 2012/05/11. doi: 10.1371/journal.pone.0035428. PubMed PMID: 22574120; PMCID: PMC3344830.
230. Rual JF, Klitgord N, Achaz G. Novel insights into RNAi off-target effects using *C. elegans* paralogs. *BMC Genomics.* 2007;8:106. Epub 2007/04/21. doi: 10.1186/1471-2164-8-106. PubMed PMID: 17445269; PMCID: PMC1868761.
231. Parrish S, Fleenor J, Xu S, Mello C, Fire A. Functional anatomy of a dsRNA trigger: differential requirement for the two trigger strands in RNA interference. *Mol Cell.* 2000;6(5):1077-87. Epub 2000/12/07. doi: 10.1016/s1097-2765(00)00106-4. PubMed PMID: 11106747.
232. Zhang L, Ward JD, Cheng Z, Dernburg AF. The auxin-inducible degradation (AID) system enables versatile conditional protein depletion in *C. elegans*. *Development.* 2015;142(24):4374-84. Epub 2015/11/09. doi: 10.1242/dev.129635. PubMed PMID: 26552885; PMCID: PMC4689222.
233. Teale WD, Paponov IA, Palme K. Auxin in action: signalling, transport and the control of plant growth and development. *Nat Rev Mol Cell Biol.* 2006;7(11):847-59. Epub 2006/09/20. doi: 10.1038/nrm2020. PubMed PMID: 16990790.
234. Sonowal R, Swimm A, Sahoo A, Luo L, Matsunaga Y, Wu Z, Bhingarde JA, Ejzak EA, Ranawade A, Qadota H, Powell DN, Capaldo CT, Flacker JM, Jones RM, Benian GM, Kalman D. Indoles from commensal bacteria extend healthspan. *Proc Natl Acad Sci U S A.* 2017;114(36):E7506-E15. Epub 2017/08/21. doi: 10.1073/pnas.1706464114. PubMed PMID: 28827345; PMCID: PMC5594673.

235. Lee JH, Kim YG, Kim M, Kim E, Choi H, Kim Y, Lee J. Indole-associated predator-prey interactions between the nematode *Caenorhabditis elegans* and bacteria. *Environ Microbiol.* 2017;19(5):1776-90. Epub 2017/02/03. doi: 10.1111/1462-2920.13649. PubMed PMID: 28028877.
236. Bhoi A, Palladino F, Fabrizio P. Auxin confers protection against ER stress in *Caenorhabditis elegans*. *Biol Open.* 2021;10(2). Epub 2021/02/03. doi: 10.1242/bio.057992. PubMed PMID: 33495210; PMCID: PMC7875485.
237. Hills-Muckey K, Martinez MAQ, Stec N, Hebbar S, Saldanha J, Medwig-Kinney TN, Moore FEQ, Ivanova M, Morao A, Ward JD, Moss EG, Ercan S, Zinovyeva AY, Matus DQ, Hammell CM. An engineered, orthogonal auxin analog/AtTIR1(F79G) pairing improves both specificity and efficacy of the auxin degradation system in *Caenorhabditis elegans*. *Genetics.* 2021. Epub 2021/11/06. doi: 10.1093/genetics/iyab174. PubMed PMID: 34739048.
238. Kasimatis KR, Moerdyk-Schauwecker MJ, Phillips PC. Auxin-Mediated Sterility Induction System for Longevity and Mating Studies in *Caenorhabditis elegans*. *G3 (Bethesda).* 2018;8(8):2655-62. Epub 2018/07/31. doi: 10.1534/g3.118.200278. PubMed PMID: 29880556; PMCID: PMC6071612.
239. Dilberger B, Baumanns S, Spieth ST, Wenzel U, Eckert GP. Infertility induced by auxin in PX627 *Caenorhabditis elegans* does not affect mitochondrial function and aging parameters. *Aging (Albany NY).* 2020;12(12):12268-84. Epub 2020/06/08. doi: 10.18632/aging.103413. PubMed PMID: 32516128; PMCID: PMC7343439.
240. Yesbolatova A, Saito Y, Kitamoto N, Makino-Itou H, Ajima R, Nakano R, Nakaoka H, Fukui K, Gamo K, Tominari Y, Takeuchi H, Saga Y, Hayashi KI, Kanemaki MT. The auxin-inducible degron 2 technology provides sharp degradation control in yeast, mammalian cells, and mice. *Nat Commun.* 2020;11(1):5701. Epub 2020/11/11. doi: 10.1038/s41467-020-19532-z. PubMed PMID: 33177522; PMCID: PMC7659001.
241. Maklakov AA, Carlsson H, Denbaum P, Lind MI, Mautz B, Hinas A, Immler S. Antagonistically pleiotropic allele increases lifespan and late-life reproduction at the cost of early-life reproduction and individual fitness. *Proc Biol Sci.* 2017;284(1856). Epub 2017/06/16. doi: 10.1098/rspb.2017.0376. PubMed PMID: 28615498; PMCID: PMC5474071.
242. Ishii N, Takahashi K, Tomita S, Keino T, Honda S, Yoshino K, Suzuki K. A methyl viologen-sensitive mutant of the nematode *Caenorhabditis elegans*. *Mutat Res.* 1990;237(3-4):165-71. Epub 1990/05/01. doi: 10.1016/0921-8734(90)90022-j. PubMed PMID: 2233820.
243. Senapati S. Infertility: a marker of future health risk in women? *Fertil Steril.* 2018;110(5):783-9. Epub 2018/10/15. doi: 10.1016/j.fertnstert.2018.08.058. PubMed PMID: 30316412.

244. Hillers KJ, Jantsch V, Martinez-Perez E, Yanowitz JL. Meiosis. *Wormbook*. 2015:1551-8507. doi: 10.1895/wormbook.1.178.1.
245. Le KN, Zhan M, Cho Y, Wan J, Patel DS, Lu H. An automated platform to monitor long-term behavior and healthspan in *Caenorhabditis elegans* under precise environmental control. *Commun Biol*. 2020;3(1):297. Epub 2020/06/12. doi: 10.1038/s42003-020-1013-2. PubMed PMID: 32523044; PMCID: PMC7287092.
246. Kimble JE, White JG. On the control of germ cell development in *Caenorhabditis elegans*. *Dev Biol*. 1981;81(2):208-19. Epub 1981/01/30. doi: 10.1016/0012-1606(81)90284-0. PubMed PMID: 7202837.
247. Hansen D, Wilson-Berry L, Dang T, Schedl T. Control of the proliferation versus meiotic development decision in the *C. elegans* germline through regulation of GLD-1 protein accumulation. *Development*. 2004;131(1):93-104. Epub 2003/12/09. doi: 10.1242/dev.00916. PubMed PMID: 14660440.
248. Schedl T, Kimble J. *fog-2*, a germ-line-specific sex determination gene required for hermaphrodite spermatogenesis in *Caenorhabditis elegans*. *Genetics*. 1988;119(1):43-61. Epub 1988/05/01. PubMed PMID: 3396865; PMCID: PMC1203344.
249. Angeles-Albores D, Leighton DHW, Tsou T, Khaw TH, Antoshechkin I, Sternberg PW. The *Caenorhabditis elegans* Female-Like State: Decoupling the Transcriptomic Effects of Aging and Sperm Status. *G3 (Bethesda)*. 2017;7(9):2969-77. Epub 2017/07/29. doi: 10.1534/g3.117.300080. PubMed PMID: 28751504; PMCID: PMC5592924.
250. Venz R, Pekec T, Katic I, Ciosk R, Ewald CY. End-of-life targeted degradation of DAF-2 insulin/IGF-1 receptor promotes longevity free from growth-related pathologies. *Elife*. 2021;10. Epub 2021/09/11. doi: 10.7554/eLife.71335. PubMed PMID: 34505574; PMCID: PMC8492056.
251. Lopez AL, 3rd, Chen J, Joo HJ, Drake M, Shidate M, Kseib C, Arur S. DAF-2 and ERK couple nutrient availability to meiotic progression during *Caenorhabditis elegans* oogenesis. *Dev Cell*. 2013;27(2):227-40. Epub 2013/10/15. doi: 10.1016/j.devcel.2013.09.008. PubMed PMID: 24120884; PMCID: PMC3829605.
252. Dalfo D, Michaelson D, Hubbard EJ. Sensory regulation of the *C. elegans* germline through TGF-beta-dependent signaling in the niche. *Curr Biol*. 2012;22(8):712-9. Epub 2012/04/10. doi: 10.1016/j.cub.2012.02.064. PubMed PMID: 22483938; PMCID: PMC3633564.
253. Ow MC, Nichitean AM, Hall SE. Somatic aging pathways regulate reproductive plasticity in *Caenorhabditis elegans*. *Elife*. 2021;10. Epub 2021/07/09. doi: 10.7554/eLife.61459. PubMed PMID: 34236316; PMCID: PMC8291976.

254. Choi LS, Shi C, Ashraf J, Sohrabi S, Murphy CT. Oleic Acid Protects *Caenorhabditis* Mothers From Mating-Induced Death and the Cost of Reproduction. *Front Cell Dev Biol.* 2021;9:690373. Epub 2021/06/29. doi: 10.3389/fcell.2021.690373. PubMed PMID: 34179018; PMCID: PMC8226236.
255. Cedars MI, Taymans SE, DePaolo LV, Warner L, Moss SB, Eisenberg ML. The sixth vital sign: what reproduction tells us about overall health. Proceedings from a NICHD/CDC workshop. *Hum Reprod Open.* 2017;2017(2):hox008. Epub 2017/07/12. doi: 10.1093/hropen/hox008. PubMed PMID: 30895226; PMCID: PMC6276647.
256. Martin JA, Hamilton BE, Osterman MJ, Driscoll AK, Mathews TJ. Births: Final Data for 2015. *Natl Vital Stat Rep.* 2017;66(1):1. Epub 2017/01/31. PubMed PMID: 28135188.
257. Chandra A, Copen CE, Stephen EH. Infertility service use in the United States: data from the National Survey of Family Growth, 1982-2010. *Natl Health Stat Report.* 2014(73):1-21. Epub 2014/01/29. PubMed PMID: 24467919.
258. Butts S, Riethman H, Ratcliffe S, Shaunik A, Coutifaris C, Barnhart K. Correlation of telomere length and telomerase activity with occult ovarian insufficiency. *J Clin Endocrinol Metab.* 2009;94(12):4835-43. Epub 2009/10/30. doi: 10.1210/jc.2008-2269. PubMed PMID: 19864453; PMCID: PMC2795650.
259. Rocca WA, Bower JH, Maraganore DM, Ahlskog JE, Grossardt BR, de Andrade M, Melton LJ, 3rd. Increased risk of cognitive impairment or dementia in women who underwent oophorectomy before menopause. *Neurology.* 2007;69(11):1074-83. Epub 2007/09/01. doi: 10.1212/01.wnl.0000276984.19542.e6. PubMed PMID: 17761551.
260. Najar J, Hallstrom T, Zettergren A, Johansson L, Joas E, Fassberg MM, Zetterberg H, Blennow K, Kern S, Skoog I. Reproductive period and preclinical cerebrospinal fluid markers for Alzheimer disease: a 25-year study. *Menopause.* 2021;28(10):1099-107. Epub 2021/07/06. doi: 10.1097/GME.0000000000001816. PubMed PMID: 34225325; PMCID: PMC8462446.
261. Fauser BC, Tarlatzis BC, Rebar RW, Legro RS, Balen AH, Lobo R, Carmina E, Chang J, Yildiz BO, Laven JS, Boivin J, Petraglia F, Wijeyeratne CN, Norman RJ, Dunaif A, Franks S, Wild RA, Dumesic D, Barnhart K. Consensus on women's health aspects of polycystic ovary syndrome (PCOS): the Amsterdam ESHRE/ASRM-Sponsored 3rd PCOS Consensus Workshop Group. *Fertil Steril.* 2012;97(1):28-38 e25. Epub 2011/12/14. doi: 10.1016/j.fertnstert.2011.09.024. PubMed PMID: 22153789.
262. Hotaling JM, Walsh TJ. Male infertility: a risk factor for testicular cancer. *Nat Rev Urol.* 2009;6(10):550-6. Epub 2009/09/03. doi: 10.1038/nrurol.2009.179. PubMed PMID: 19724246.
263. Eisenberg ML, Li S, Behr B, Cullen MR, Galusha D, Lamb DJ, Lipshultz LI. Semen quality, infertility and mortality in the USA. *Hum Reprod.* 2014;29(7):1567-74. Epub

2014/05/20. doi: 10.1093/humrep/deu106. PubMed PMID: 24838701; PMCID: PMC4059337.

264. Ruth KS, Day FR, Hussain J, Martinez-Marchal A, Aiken CE, Azad A, Thompson DJ, Knoblochova L, Abe H, Tarry-Adkins JL, Gonzalez JM, Fontanillas P, Claringbould A, Bakker OB, Sulem P, Walters RG, Terao C, Turon S, Horikoshi M, Lin K, Onland-Moret NC, Sankar A, Hertz EPT, Timshel PN, Shukla V, Borup R, Olsen KW, Aguilera P, Ferrer-Roda M, Huang Y, Stankovic S, Timmers P, Ahearn TU, Alizadeh BZ, Naderi E, Andrulis IL, Arnold AM, Aronson KJ, Augustinsson A, Bandinelli S, Barbieri CM, Beaumont RN, Becher H, Beckmann MW, Benonisdottir S, Bergmann S, Bochud M, Boerwinkle E, Bojesen SE, Bolla MK, Boomsma DI, Bowker N, Brody JA, Broer L, Buring JE, Campbell A, Campbell H, Castela JE, Catamo E, Chanock SJ, Chenevix-Trench G, Ciullo M, Corre T, Couch FJ, Cox A, Crisponi L, Cross SS, Cucca F, Czene K, Smith GD, de Geus E, de Mutsert R, De Vivo I, Demerath EW, Dennis J, Dunning AM, Dwek M, Eriksson M, Esko T, Fasching PA, Faul JD, Ferrucci L, Franceschini N, Frayling TM, Gago-Dominguez M, Mezzavilla M, Garcia-Closas M, Gieger C, Giles GG, Grallert H, Gudbjartsson DF, Gudnason V, Guenel P, Haiman CA, Hakansson N, Hall P, Hayward C, He C, He W, Heiss G, Hoffding MK, Hopper JL, Hottenga JJ, Hu F, Hunter D, Ikram MA, Jackson RD, Joaquim MDR, John EM, Joshi PK, Karasik D, Kardia SLR, Kartsonaki C, Karlsson R, Kitahara CM, Kolcic I, Kooperberg C, Kraft P, Kurian AW, Kutalik Z, La Bianca M, LaChance G, Langenberg C, Launer LJ, Laven JSE, Lawlor DA, Le Marchand L, Li J, Lindblom A, Lindstrom S, Lindstrom T, Linet M, Liu Y, Liu S, Luan J, Magi R, Magnusson PKE, Mangino M, Mannermaa A, Marco B, Marten J, Martin NG, Mbarek H, McKnight B, Medland SE, Meisinger C, Meitinger T, Menni C, Metspalu A, Milani L, Milne RL, Montgomery GW, Mook-Kanamori DO, Mulas A, Mulligan AM, Murray A, Nalls MA, Newman A, Noordam R, Nutile T, Nyholt DR, Olshan AF, Olsson H, Painter JN, Patel AV, Pedersen NL, Perjakova N, Peters A, Peters U, Pharoah PDP, Polasek O, Porcu E, Psaty BM, Rahman I, Rennert G, Rennert HS, Ridker PM, Ring SM, Robino A, Rose LM, Rosendaal FR, Rossouw J, Rudan I, Rueedi R, Ruggiero D, Sala CF, Saloustros E, Sandler DP, Sanna S, Sawyer EJ, Sarnowski C, Schlessinger D, Schmidt MK, Schoemaker MJ, Schraut KE, Scott C, Shekari S, Shrikhande A, Smith AV, Smith BH, Smith JA, Sorice R, Southey MC, Spector TD, Spinelli JJ, Stampfer M, Stockl D, van Meurs JBJ, Strauch K, Stykarsdottir U, Swerdlow AJ, Tanaka T, Teras LR, Teumer A, Thornorsteinsdottir U, Timpson NJ, Toniolo D, Traglia M, Troester MA, Truong T, Tyrrell J, Uitterlinden AG, Ulivi S, Vachon CM, Vitart V, Volker U, Vollenweider P, Volzke H, Wang Q, Wareham NJ, Weinberg CR, Weir DR, Wilcox AN, van Dijk KW, Willemsen G, Wilson JF, Wolffenbuttel BHR, Wolk A, Wood AR, Zhao W, Zygmont M, Biobank-based Integrative Omics Study C, e QC, Biobank Japan P, China Kadoorie Biobank Collaborative G, kConFab I, LifeLines Cohort S, InterAct c, and Me Research T, Chen Z, Li L, Franke L, Burgess S, Deelen P, Pers TH, Grondahl ML, Andersen CY, Pujol A, Lopez-Contreras AJ, Daniel JA, Stefansson K, Chang-Claude J, van der Schouw YT, Lunetta KL, Chasman DI, Easton DF, Visser JA, Ozanne SE, Namekawa SH, Solc P, Murabito JM, Ong KK, Hoffmann ER, Murray A, Roig I, Perry JRB. Genetic insights into biological mechanisms governing human ovarian ageing. *Nature*. 2021;596(7872):393-7. Epub 2021/08/06. doi: 10.1038/s41586-021-03779-7. PubMed PMID: 34349265; PMCID: PMC7611832.

265. Zhou KI, Pincus Z, Slack FJ. Longevity and stress in *Caenorhabditis elegans*. *Aging* (Albany NY). 2011;3(8):733-53. doi: 10.18632/aging.100367. PubMed PMID: 21937765; PMCID: PMC3184976.
266. McColl G, Roberts BR, Pukala TL, Kenche VB, Roberts CM, Link CD, Ryan TM, Masters CL, Barnham KJ, Bush AI, Cherny RA. Utility of an improved model of amyloid-beta (A β (1-42)) toxicity in *Caenorhabditis elegans* for drug screening for Alzheimer's disease. *Mol Neurodegener*. 2012;7:57. Epub 2012/11/23. doi: 10.1186/1750-1326-7-57. PubMed PMID: 23171715; PMCID: PMC3519830.
267. Estrada-Valencia R, de Lima ME, Colonnello A, Rangel-Lopez E, Saraiva NR, de Avila DS, Aschner M, Santamaria A. The Endocannabinoid System in *Caenorhabditis elegans*. *Rev Physiol Biochem Pharmacol*. 2021. Epub 2021/08/18. doi: 10.1007/112_2021_64. PubMed PMID: 34401955.
268. Libina N, Berman JR, Kenyon C. Tissue-specific activities of *C. elegans* DAF-16 in the regulation of lifespan. *Cell*. 2003;115(4):489-502. Epub 2003/11/19. doi: 10.1016/s0092-8674(03)00889-4. PubMed PMID: 14622602.